

CANNABINOID 2 RECEPTOR SIGNALLING IN ENDOTOXIN-INDUCED UVEITIS

by

Richard Frederick Porter IV

Submitted in partial fulfilment of the requirements  
for the degree of Master of Science

at

Dalhousie University  
Halifax, Nova Scotia  
August 2017

© Copyright by Richard Frederick Porter IV, 2017

## DEDICATION PAGE

This thesis is dedicated to my colleague, Dr. Anna-Maria Szczesniak, who has helped me throughout the years. I thank you for your mentorship and friendship.

## Table of Contents

<b>List of Tables</b> .....	<b>v</b>
<b>List of Figures</b> .....	<b>vi</b>
<b>Abstract</b> .....	<b>viii</b>
<b>List of Abbreviations Used</b> .....	<b>ix</b>
<b>Acknowledgments</b> .....	<b>xvi</b>
<b>Chapter I: Introduction</b> .....	<b>1</b>
1.1 Uveitis .....	1
1.1.1 <i>Definition and epidemiology of uveitis</i> .....	1
1.1.2 <i>Current therapies for uveitis</i> .....	1
1.1.3 <i>Experimental models of uveitis</i> .....	4
1.2 The immune response .....	8
1.2.1 <i>Leukocyte recruitment and transmigration</i> .....	8
1.2.2 <i>Resident ocular immune cells and ocular immune response</i> .....	12
1.3 The Endocannabinoid System.....	15
1.3.1 <i>ECS ligands</i> .....	19
1.3.2 <i>CB<sub>2</sub>R signalling pathways</i> .....	30
1.3.3 <i>CB<sub>2</sub>R distribution and expression</i> .....	35
1.3.4 <i>CB<sub>2</sub>R and the immune system</i> .....	36
1.3.5 <i>CB<sub>2</sub>R and macrophages</i> .....	37
1.3.6 <i>CB<sub>2</sub>R involvement in the ocular immune response</i> .....	39
1.4 Novel selective CB <sub>2</sub> R ligands .....	40
1.4.1 <i>Currently used CB<sub>2</sub>R agonists and their pharmacokinetics (PK) and pharmacodynamics (PD)</i> .....	40
1.4.2 <i>High-throughput screen and lead optimization</i> .....	41
1.4.3 <i>Physico-chemical properties: PK and ADME</i> .....	42
1.4.4 <i>Affinity and selectivity in the CBR binding studies</i> .....	43
1.4.5 <i>Activity of CBR signaling pathways and selectivity in the CBR binding studies</i> .....	43
1.4.6 <i>Clinical advantage of improved drug-likeness</i> .....	44

1.5 Hypothesis and objectives.....	44
<b>Chapter II: Methods and Materials .....</b>	<b>46</b>
2.1 Animals .....	46
2.2 Genotyping CB <sub>2</sub> R <sup>-/-</sup> animals .....	46
2.3 Induction of endotoxin-induced uveitis (EIU).....	47
2.4 Intravital microscopy .....	47
2.5 Isolation of murine bone marrow cell neutrophils .....	49
2.6 Neutrophil migration assay .....	49
2.7 Neutrophil-depletion and adoptive transfer .....	50
2.8 Peripheral blood leukocyte isolation.....	51
2.9 Antibodies and flow cytometry.....	51
2.10 Pharmacological treatments.....	52
2.11 Statistical analysis .....	53
<b>Chapter III: Results.....</b>	<b>60</b>
3.1 Intravital microscopy .....	60
3.1.1 <i>CB<sub>2</sub>R activation decreases leukocyte-endothelial interactions in the iridial microcirculation</i> .....	60
3.1.2 <i>Comparison of CB<sub>2</sub>R agonist to a clinically used anti-inflammatory drug used to treat uveitis</i> .....	67
3.1.3 <i>Determining the therapeutic time window for treatment with the CB<sub>2</sub>R agonist to modulate leukocyte adhesion during EIU</i> .....	72
3.1.4 <i>The effects of CB<sub>2</sub>R genetic deletion (CB<sub>2</sub>R<sup>-/-</sup>) or decrease in constitutive CB<sub>2</sub>R activity on leukocyte-endothelial interactions in the iridial microcirculation during EIU</i> .....	72
3.2 Neutrophil migration.....	79
3.2.1 <i>CB<sub>2</sub>R activation decreases neutrophil migration in-vitro</i> .....	79
3.2.2 <i>Loss of constitutive activity of CB<sub>2</sub>R activation does not affect neutrophil migration in-vitro</i> .....	80
3.2.3 <i>RO6871304 and RO6851228 do not affect cell viability</i> .....	80

3.3 Adoptive transfer .....	85
3.3.1 <i>CB<sub>2</sub>R activation on resident ocular immune cells mediates CB<sub>2</sub>R leukocyte-adherence effects</i> .....	85
<b>Chapter IV: Discussion.....</b>	<b>93</b>
4.1.1 <i>Effect of CB<sub>2</sub>R activation on leukocyte-endothelial interactions</i> .....	93
4.1.2 <i>Effect of pharmacological block of CB<sub>2</sub>R activity, using an inverse agonist, or genetic loss of CB<sub>2</sub>R, on leukocyte-endothelial interactions</i> .....	95
4.1.3 <i>Comparison of CB<sub>2</sub>R agonist to the effect of a clinical steroid treatment on leukocyte-endothelial interactions</i> .....	96
4.1.4 <i>Therapeutic time window for CB<sub>2</sub>R treatment</i> .....	96
4.1.5 <i>Effect of CB<sub>2</sub>R modulation on neutrophil migration in vitro</i> .....	97
4.1.6 <i>Cell type(s) responsible for the CB<sub>2</sub>R mediated anti-inflammatory effects</i> ..	98
4.2 Comparisons of our findings to other studies in the field .....	99
4.2.1 <i>ECS and the eye</i> .....	99
4.2.2 <i>ECS and immune cell migration</i> .....	101
4.2.3 <i>ECS and other inflammatory diseases</i> .....	102
4.3 Limitations .....	103
4.3.1 <i>Other models of ocular inflammation</i> .....	103
4.3.2 <i>Markers of inflammation and ocular function</i> .....	104
4.3.3 <i>CB<sub>2</sub>R expression</i> .....	105
4.3.4 <i>Optimizing neutrophil depletion</i> .....	106
4.4 Proposed CB <sub>2</sub> R anti-inflammatory signalling mechanism .....	107
4.5 Conclusion .....	110
4.6 Future directions .....	110
4.6.1 <i>Markers of inflammation</i> .....	111
4.6.2 <i>Retinal pathology</i> .....	111
4.6.3 <i>PK and systemic effects</i> .....	112
<b>References .....</b>	<b>113</b>

## **List of Tables**

Table 1. Binding and biased selectivity for cannabinoids .....	26
Table 2. Chemical structures, physicochemical properties, binding affinity and selectivity of human and mouse cannabinoid receptors for a novel series of CB <sub>2</sub> R ligands .....	28
Table 3. Leukocyte-endothelial rolling during EIU .....	63

## List of Figures

Figure 1. TLR4 activation signalling pathway .....	5
Figure 2. Leukocyte recruitment cascade .....	10
Figure 3. Synthesis and degradation of endocannabinoids .....	17
Figure 4. Change in receptor activity after agonist, antagonist, inverse agonist .....	20
Figure 5. Structures of different classical and non-classical cannabinoid ligands .....	23
Figure 6. CB <sub>2</sub> R activation signalling pathway.....	31
Figure 7. Signalling bias for cannabinoid ligands .....	33
Figure 8. Experimental timeline for EIU studies in mice .....	54
Figure 9. Experimental timeline for EIU studies with treatment at 3 h.....	56
Figure 10. Experimental timeline for EIU adoptive transfer studies .....	58
Figure 11. Selective CB <sub>2</sub> R agonists effects on leukocyte-adhesion during EIU .....	61
Figure 12. Dose response for the CB <sub>2</sub> R agonist, HU910.....	65
Figure 13. Dose response for the CB <sub>2</sub> R agonist, HU308 .....	68
Figure 14. Effects of dexamethasone on leukocyte-adhesion during EIU .....	70
Figure 15. Determining the therapeutic time window for CB <sub>2</sub> R agonist treatment during EIU.....	73
Figure 16. RO6871304 exerts its anti-inflammatory effects through CB <sub>2</sub> R .....	75
Figure 17. The CB <sub>2</sub> R inverse agonist, RO6851228 increases leukocyte adhesion in the iridial microcirculation during EIU .....	77
Figure 18. CB <sub>2</sub> R activation reduces neutrophil migration towards chemoattractant ..	81
Figure 19. IC <sub>50</sub> of RO6871304 effect on neutrophil migration towards chemoattractant .....	83
Figure 20. Gr-1 antibody depletes neutrophils in the peripheral blood after 24 h .....	87

Figure 21. Neutrophil depletion abolishes leukocyte adhesion to iridial microvasculature at 6 h post-EIU induction .....	89
Figure 22. CB <sub>2</sub> R activation in neutrophil-depleted EIU mice with accompanying leukocyte adoptive transfer reduces leukocyte-adhesion in the iridial microcirculation .....	91
Figure 23. Proposed CB <sub>2</sub> R activation pathway that modulates EIU-induced ocular inflammation .....	108

## Abstract

Activation of the cannabinoid 2 receptor (CB<sub>2</sub>R) is anti-inflammatory in models of ocular inflammation. The objective of this study was to examine the anti-inflammatory actions of the novel highly potent and selective CB<sub>2</sub>R agonists, RO6871304 and RO6871085, that originate from two chemically diverse series, as well as a novel structurally related CB<sub>2</sub>R inverse agonist, RO6851228, in a model of experimental endotoxin-induced uveitis (EIU). We used the CB<sub>2</sub>R agonists, HU308 and HU910, for comparison. Both of these cannabinoids are based on the structure of the classical cannabinoid,  $\Delta^9$ -tetrahydrocannabinol (THC). EIU was induced by intravitreal injection of lipopolysaccharide (LPS) into wild-type (WT) and CB<sub>2</sub>R genetic knockout mice. Leukocyte-endothelial adhesion in the iris microvasculature was studied 6 h after LPS injection using intravital microscopy. Topical treatment with the CB<sub>2</sub>R agonists, RO6871304, RO6871085, and HU910, significantly decreased LPS-induced leukocyte-endothelial adhesion compared to vehicle. Conversely, treatment with the CB<sub>2</sub>R inverse agonist, RO6851228, increased LPS-induced leukocyte-endothelial adhesion. Consistent with *in vivo* inhibition of leukocyte adhesion, the CB<sub>2</sub>R agonist, RO6871304, significantly decreased neutrophil migration *in vitro* compared to vehicle. Topical treatment with RO6871304 in neutrophil-depleted mice 5 h prior to leukocyte adoptive transfer, significantly decreased LPS-induced adhesion of adoptively-transferred leukocytes compared to vehicle; this suggests that the effect of CB<sub>2</sub>R agonists on leukocyte adhesion is likely mediated by a reduction in activation of resident ocular immune cells. Taken together, these data demonstrate an anti-inflammatory role for CB<sub>2</sub>R in the eye and suggest that drugs targeting the endocannabinoid system may be useful therapeutics for ocular inflammatory disease.

## List of Abbreviations Used

$\Delta^9$ -THC	$\Delta^9$ -tetrahydrocannabinol
2-AG	2-arachidonoyl glycerol
5-HT	5-hydroxytryptamine
AA	arachidonic acid
AC	adenylate/adenylyl cyclase
Abs	antibodies
AD	Alzheimer's disease
ADME	absorption, distribution, metabolism and excretion
ACAID	anterior chamber-associated immune deviation
AEA	arachidonoyl ethanolamide or anandamide
Ag	antigen
Akt	protein kinase B
AM841	hexahydrocannabinol
AM11542	tetrahydrocannabinol
AMP	adenosine monophosphate
ANOVA	analysis of variance
AP-1	activating protein-1
APC	antigen presenting cell
BSA	bovine serum albumin
bp	base pairs
BRB	blood retinal barrier
CACF	Carleton Animal Care Facility

CAM	cellular adhesion molecule
cAMP	cyclic adenosine monophosphate
CASP	colon ascendens stent peritonitis
CB <sub>1</sub> R	cannabinoid 1 receptor
CB <sub>2</sub> R	cannabinoid 2 receptor
CB <sub>2</sub> R <sup>-/-</sup>	cannabinoid 2 receptor knock-out
CBR	cannabinoid receptor
CCL	CC chemokine ligand
CCR	CC chemokine receptor
CD	cluster of differentiation
CBD	cannabidiol
CHO	Chinese hamster ovary
CNS	central nervous system
COX	cyoclooxygenase
CREB	cAMP responsive element-binding protein
CXCL	CXC chemokine ligand
CXCR	CXC chemokine receptor
CYP	cytochrome P450
DAG	diacylglycerol
DAGL	diacylglycerol lipase
DC	dendritic cell
DEX	dexamethasone
DMSO	dimethyl sulfoxide

DNA	deoxyribonucleic acid
EAE	experimental autoimmune encephalitis
EAU	experimental autoimmune uveoretinitis/uveitis
ECS	endocannabinoid system
EDTA	ethylene diamine triacetic acid
EIU	endotoxin-induced uveitis
ERG	electroretinography
ERK	extracellular signaling regulated kinases
FAAH	fatty acid amide hydrolase
FACS	fluorescence activated cell sorting
FBS	fetal bovine serum
FITC	fluorescein isothiocyanate
fu	fraction unbound
GFAP	glial fibrillary acidic protein
GFP	green fluorescent protein
GIRK	G-protein-coupled inward rectifying K <sup>+</sup>
GlyCAM-1	glycosylatotin dependent cell adhesion molecule-1
GMCSF	granulocyte macrophage colony-stimulation factor
GPCR	G-protein coupled receptor
HD	Huntington's disease
i.p.	intraperitoneal
i.v.	intravenous
Iba-1	ionized calcium-binding adapter molecule 1

ICAM	intracellular adhesion molecule;
IFN	interferon
Ig	immunoglobulin
IKK	inhibitor of NF- $\kappa$ B
IL	interleukin
iNOS	inducible nitric oxide synthase
IOP	intraocular pressure
IRAK	IL-1 receptor associated kinases
IRBP	interphotoreceptor binding protein
IRF	interferon regulatory factor
IVM	intravital microscopy
JNK	c-Jun NH <sub>2</sub> -terminal kinase
JWH133	3-(1'-dimethylbutyl)-1-deoxy- $\Delta^8$ -THC
LDF	laser Doppler flowmetry
LFA-1	lymphocyte functional associated antigen-1
logD	distribution coefficient
LPS	lipopolysaccharide
LRR	leucine rich repeat
Lysa	aqueous solubility
MAC-1	macrophage-1 antigen
MAdCAM-1	mucosal vascular adhesion cell adhesion molecule 1
MAGL	monoacylglycerol lipase
MAPK	mitogen activated protein kinase

MCP	monocyte chemotactic protein
MHC	major histocompatibility complex
Mic. CL	microsomal stability assess by clearance
MIP	macrophage inflammatory protein
MS	multiple schlerosis
MSH	melanocyte stimulating hormone
MyD88	myeloid differentiation primary-response protein 88
NAPE	N-arachidonoyl phosphatidylethanolamide
NF- $\kappa$ B	nuclear factor kappa B
NK	natural killer cell
NO	nitric oxide
NSAIDS	non-steroidal anti-inflammatory drugs
p38	p38 mitogen activated protein kinase
PAMP	pathogen associated molecular patter
PAMPA`	parallel artificial membrane permeability
PBMCs	peripheral-blood mononuclear cells
PCR	polymerase chain reaction
PD	pharmacodynamics
PECAM	platelet endothelial cell adhesion molecule
Peff	permeation coefficient
pERK	phosphorylated extracellular signal-regulated kinase
PFA	paraformaldehyde
PI3K	phosphatidyl inositol 3 kinase

pJNK	phosphorylated c-Jun-N-terminal kinase
PK	pharmacokinetics
PKA	protein kinase A
PLA <sub>2</sub>	phospholipase A 2
PLC	phospholipase C
PMN	polymorphonuclear leukocytes
PNS	peripheral nervous system
pp38	phosphorylated p38 mitogen activated protein kinase
PPAR $\gamma$	peroxisome proliferator-activated receptor gamma
PRR	pathogen-associated molecular patterns
PSGL-1	P-selectin glycoprotein ligand
PVR	proliferative vitreoretinopathy
qRT-PCR	quantitative reverse transcriptase polymerase chain reaction
RANTES	regulated on activation, normal T cell expressed and secreted
RPE	retinal pigmented epithelium
RPMI	Roswell Park Memorial Institute medium
SAR	structure-activity based relationship
SD	standard deviation
TCR	T-cell receptor
TEM	transendothelial migration
TGF- $\beta$	transforming growth factor beta
TIR	Toll-interleukin 1 receptor
TLR	toll-like receptor

TNF- $\alpha$	tumor necrosis factor alpha
TRAF	TNF-receptor associated factor
TRAM	TRIF related adapter protein,
TRIF	TIR-domain-containing adapter-inducing interferon- $\beta$
TRPV1	transient receptor potential vanilloid type 1 receptor
VCAM	vascular cell adhesion molecule
VEGF	vascular endothelial growth factor
VLA-4	very late antigen-4
V <sub>ss</sub>	volume of distribution
WT	wild type

## **Acknowledgements**

First and foremost, I would like to thank my supervisor, Dr. Melanie Kelly, for your guidance and mentorship. I am extremely fortunate to have been a member of your lab and can never thank you enough.

I am also very fortunate to have worked with an extraordinary group of colleagues in the Retina and Optic Nerve Lab, the Microcirculation Lab, the Department of Pharmacology, and Hoffmann-La Roche Pharmaceuticals. It has been a pleasure working with all of you.

Most importantly, I would like to also like express my gratitude towards Drs. Anna-Maria Szczesniak, Tom Toguri, Karim Wafa and Christian Lehmann, and Elizabeth Cairns, Simon Gebremeskel, and Dinesh Thapa, all of whom have helped me throughout the entire course of this project.

I am also grateful to the members of my advisory and examining committees, Drs. Jana Sawynok, Morgan Langille, Kishore Pasumarthi, David Hoskin, and Christian Lehmann. Thank you for your input in developing my thesis.

An important thank you to Luisa Vaughan, Sandi Leaf, and Cheryl Bailey for all their hard work in the departmental administrative office. I would also like to thank everyone in the Department of Pharmacology for an incredible experience. I am so lucky to have shared the last few years with you all. Lastly, thank you to my family and Amy Pike whom have always supported me.

## **Chapter I: Introduction**

### ***1.1 Uveitis***

#### ***1.1.1 Definition and epidemiology of uveitis***

A common cause of visual impairment is uveitis, a form of intraocular inflammation of tissues of the uveal tract including: iris, ciliary body, and choroid. This disorder accounts for up to 10% of preventable blindness in developed countries (Smith et al., 1998). Uveitis is usually classified according to the anatomical location it affects and can be referred to as anterior, posterior or pan-uveitis, which encompasses the whole eye (Forrester et al., 2013). Anterior uveitis is the most commonly diagnosed form of uveitis (Allensworth et al., 2011). Patients usually present with pain, red eye, photophobia, miosis (contraction of the pupil) and decreased vision. There are many causes of uveitis which can be attributed to both infectious or non-infectious causes, including autoimmunity. For 50% of patients, however, the etiology of the disease is idiopathic (Fraunfelder and Rosenbaum, 1997). When an infection is the underlying cause antimicrobial therapy (antibiotics, antivirals and/or antifungals) is needed against the causative agent, in addition to immunosuppression. Control of intraocular inflammation is paramount for preserving the delicate ocular structures and maintaining vision.

#### ***1.1.2 Current therapies for uveitis***

The current pharmacological treatments for uveitis are corticosteroids (namely dexamethasone and prednisolone), non-steroidal anti-inflammatory drugs (NSAIDs; bromfenac and nepafenac), immunosuppressive agents (antimetabolites, cell inhibitors, alkylating agents) and newer biologics (anti-TNF- $\alpha$  [tumor necrosis factor- $\alpha$ ], anti-

interleukin-2 [IL-2] receptor alpha therapies, anti-vascular endothelial growth factor [VEGF]) (Babu and Mahendradas, 2013; Cairns et al., 2016). Topical corticosteroids are the mainstay treatments and are effective for infectious and non-infectious uveitis, but in severe cases peri-ocular or systemic corticosteroids are also indicated (Martin et al., 2002; Smith et al., 1998).

The mechanism of action for corticosteroids involves binding of the drug to cytosolic glucocorticoid receptor which forms a complex that can bind to glucocorticoid response elements on DNA. This controls the transcription of many genes including modulating activity of transcription factors nuclear factor kappa-light-chain enhancer of activated B cells (NF- $\kappa$ B) and activator protein-1 (AP-1). These effects control inflammation by upregulating anti-inflammatory cytokines and decreasing pro-inflammatory cytokines (van der Velden, 1998). It is well established that use of corticosteroids can lead to severe adverse ocular or systemic effects (Kersey and Broadway, 2006). Adverse effects include increasing intraocular pressure (IOP), risk of developing cataracts (opacification of the lens), glaucoma (visual field defects due to increased IOP-induced optic nerve damage), susceptibility to infection, hypertension, impaired wound healing, corneal and scleral thinning, osteoporosis and hyperglycemia (Smith et al., 1998).

NSAIDs block the COX pathway, which is anti-inflammatory but use of these agents is usually not sufficient to control severe sight-threatening ocular inflammation. One of the advantages of the use of NSAIDs is that they have less side-effects than steroids and are commonly used as a prophylactic treatment during cataract surgery to minimize postoperative inflammation complications (Saban, 2012). Immunosuppressive agents like

the T-cell inhibitor, cyclosporine, generates its effects by binding to cyclophilin in T-cells. This complex inhibits calcineurin (serine/threonine phosphatase) and prevents T cell receptor (TCR)-induced activation of T-cells, which decreases the production of inflammatory cytokines IL-4 and IL-2 (Matsuda and Koyasu, 2000). Cyclosporine, however, suffers from a number of adverse effects including producing hypertension and nephrotoxicity (Mérida et al., 2015).

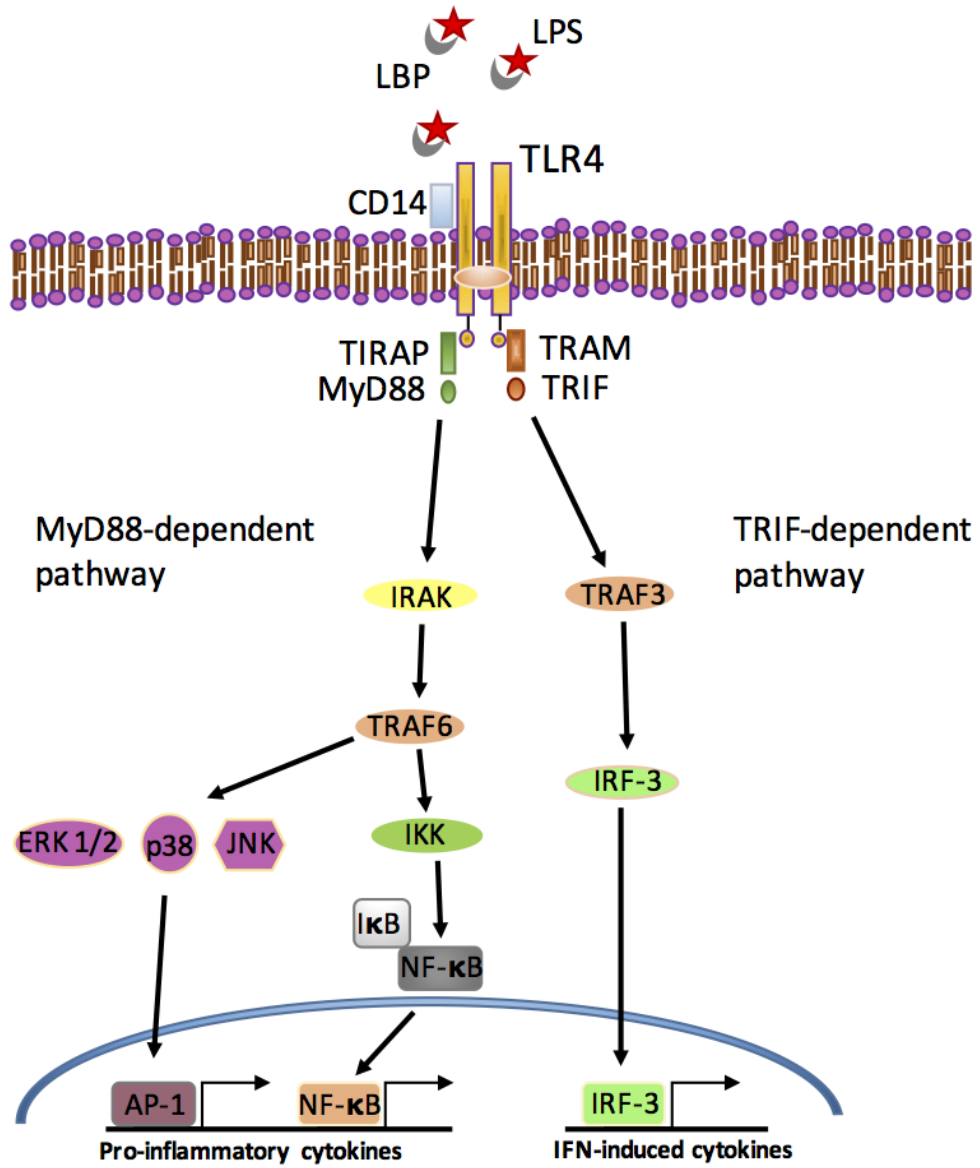
Biologics on the other hand target inflammatory cytokines involved in the pathogenesis of uveitis. The different biologics are monoclonal antibodies, soluble receptors, cytokines themselves, and cytokine antagonists. Biologics are not a first line-therapy for uveitis due to their potentially serious adverse effects including thromboembolism, susceptibility to infection, lupus-like syndrome, malignancy, congestive heart failure and hypertension (Pasadhika and Rosenbaum, 2014). Biologics, however, are indicated in cases where conventional steroids or immunosuppressive drugs are ineffective, or when there is a concomitant systemic inflammatory disease, such as rheumatoid arthritis, inflammatory bowel disease, or juvenile idiopathic arthritis. Patients therefore will require therapeutic monitoring by an ophthalmologist which is associated with high costs (Mérida et al., 2015). Identification of new drug targets for ocular inflammation is critical, especially in cases of relapsing disease, since current clinical treatments can be ineffective and are associated with, in some instances, serious adverse effects (Kersey and Broadway, 2006).

### *1.1.3 Experimental models of uveitis*

Research into new therapeutics for uveitis takes advantage of two established experimental animal models of uveitis: 1) endotoxin-induced uveitis (EIU), induced by systemic or intravitreal injection of bacterial endotoxin, (2) experimental autoimmune uveitis (EAU), induced by immunization with interphotoreceptor binding protein (IRBP) derived peptide, which is a retinal antigen (Smith et al., 1998). EAU is a model of uveoretinitis (posterior uveitis) and is a chronic autoimmune T cell-mediated disease. In my thesis, I used a model of EIU adapted for mice. Intravitreal injection of lipopolysaccharide (LPS) into the posterior chamber of the globe in mice generates a model of acute pan-uveitis with resultant inflammation within uveal tissues as well as retina (Rosenbaum et al., 1980). LPS is an endotoxin derived from the cell wall of Gram-negative bacteria, and is a pathogen associated molecular pattern (PAMP), which activates Toll-like 4 receptor (TLR4) on uveal microglia, macrophages and dendritic cells (DCs). EIU is a well-established experimental model of uveitis with many publications documenting the molecular signalling pathways contributing to LPS-induced ocular inflammation (Allensworth et al., 2011; Kezic et al., 2011).

In the eye, TLR4s are located on a variety of cells including, antigen presenting cells (APCs; microglia, macrophages, and DCs), neutrophils, eosinophils, basophils, T cells, B cells, endothelial and epithelial cells (Kezic et al., 2011). TLR4 is a transmembrane bound receptor, characterized by an extracellular leucine-rich repeat (LRR) domain involved in PAMP recognition and an intracellular toll/interleukin 1 (IL-1) receptor-like (TIR) domain which permits downstream signal transduction (Kawasaki and Kawai, 2014).

**Figure 1:** TLR4 activation signalling pathway. Lipopolysaccharide (LPS), LPS binding protein (LBP), cluster of differentiation 14 (CD14), TIR-domain-containing adapter inducing interferon- $\beta$  (TRIF), TRIF-related adapter molecule (TRAM), IL-1 receptor-associated kinases-1 and-4 (IRAK1 and IRAK4), and tumour-necrosis factor (TNF)-receptor associated factor 6 (TRAF 6), interferon regulatory factor-3 (IRF3), activated protein-1 (AP-1), extracellular signal-regulated kinases  $\frac{1}{2}$  (ERK 1/2), nuclear factor kappa-light-chain-enhancer of activated B cells (NF- $\kappa$ B), inhibitor of NF- $\kappa$ B (IKK), c-Jun NH<sub>2</sub>-terminal kinase (JNK).



The signaling cascade of TLR4 can be seen in Figure 1. In vitreous humor, LPS binds to LPS-binding protein (LBP) to form a complex which transfers LPS to cluster of differentiation-14 (CD14), a glycosylphosphatidylinositol-anchored membrane protein (Vaure and Liu, 2014). Subsequently LPS can interact with TLR4 to form a functional receptor complex.

Upon activation of TLR4, two signalling pathways are activated: (1) myeloid differentiation primary-response protein 88 (MyD88)-dependent pathway, (2) MyD88-independent signalling pathway also called the TIR-domain-containing adapter inducing interferon- $\beta$  (TRIF)/TRIF-related adapter molecule (TRAM), TRIF/TRAM pathway (Akira and Takeda, 2004). Kezic et al., (2011) showed using MyD88 genetic knockout mice that EIU involves

the MyD88 pathway (Kezic et al., 2011). Intracellular signalling of the MyD88 pathway includes activation of IL-1 receptor-associated kinases-1 and-4 (IRAK1 and IRAK4) and tumour-necrosis factor (TNF)-receptor associated factor 6 (TRAF6), which leads to activation of transcription factors such as NF- $\kappa$ B and AP-1 and subsequent upregulation of inflammatory cytokines (Kawasaki and Kawai, 2014). The TRIF-TRAM pathway activates the interferon regulatory factor-3 (IRF3) transcription factor which results in upregulation of type I interferons (IFNs) (Akira and Takeda, 2004). TNF- $\alpha$  is one of the cytokines produced by the TRIF/TRAM pathway which can contribute to late phase NF- $\kappa$ B activation upon interaction with TNF receptors (Vaure and Liu, 2014).

In the rat model of EIU generated by systemic LPS injection, inflammation peaks at 6-10 h post induction and then rapidly resolves after a couple days. Breakdown of the blood-aqueous barrier was reported to occur 2 h post LPS injection (Allensworth et al.,

2011; Smith et al., 1998). Histological studies reveal that there is an infiltration of leukocytes from 2-8 h with peak total cell numbers at 24 h in this model of EIU. Becker et al. (2000) using intravital microscopy (IVM) showed that there is peak leukocyte adhesion in the iridial microcirculation at 4-6 h post EIU in mice (Becker et al., 2000). The predominant infiltrating cells are neutrophils, which in addition to macrophages, contribute to the pathogenesis of EIU (Smith et al., 1998). Neutrophils are the primary effector cells in acute inflammation and phagocytose particles in the inflammatory site. Macrophages are a heterogeneous group of cells and participate in cell-mediated immunity, tissue repair and destruction of microbes, among other things (Smith et al., 1998). Rats are more susceptible to LPS than mice in generating EIU. In mice, EIU is normally generated by intravitreal injection of LPS, while in rats EIU can be induced by local or systemic LPS (Rosenbaum et al., 2011). Changes in the clinical signs during EIU are similar to those seen in humans with uveitis, including protein flare and cells that infiltrate in the anterior chamber, miosis, posterior synechiae (iris adheres to the lens), fibrin clots and hypopyon (leukocyte exudate in the anterior chamber) (Li et al., 1995; Rosenbaum et al., 1980; Smith et al., 1998).

## ***1.2 The immune response***

### ***1.2.1 Leukocyte recruitment and transmigration***

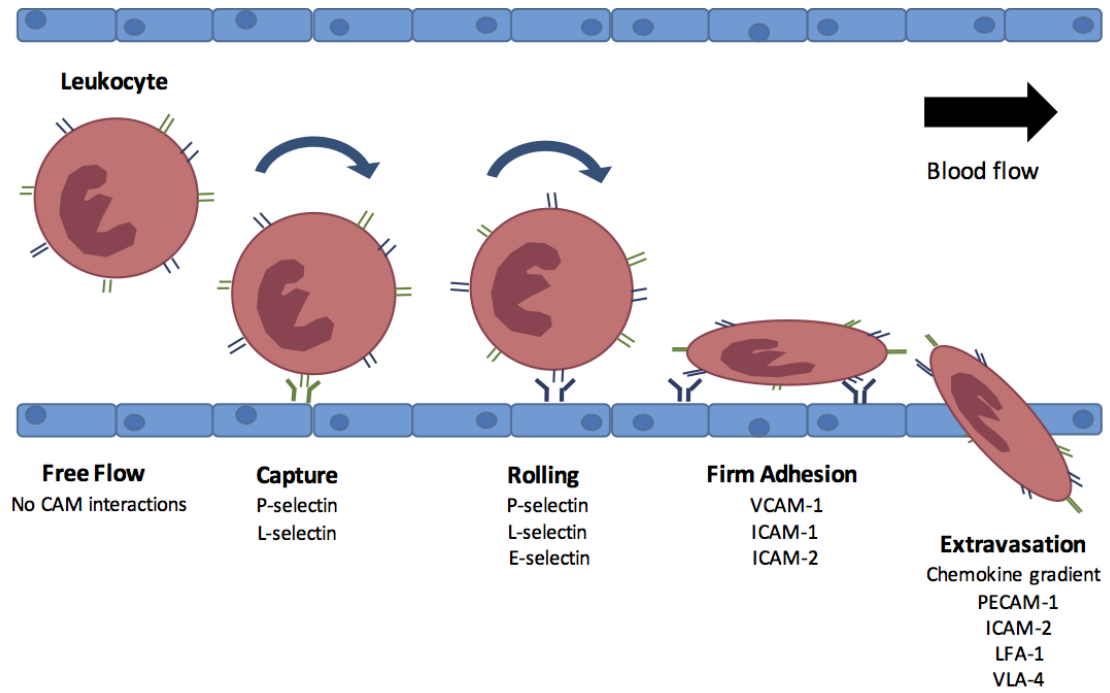
In normal healthy ocular tissues circulating leukocytes pass through the microvasculature at the same speed as the blood and do not attach since neither the leukocytes nor the endothelium are activated because there is no ongoing inflammation. During inflammation, a well-defined multi-step process involves cell adhesion molecules

(CAM) to recruit leukocytes (Figure 2). These infiltrating leukocytes contribute to local inflammation by releasing pro-inflammatory cytokines.

The first step of leukocyte recruitment is called leukocyte capture which is mediated by P-selectins on endothelial cells and P-selectin glycoprotein ligand-1 (PSG-1) on leukocytes. PSGL-1 is constitutively expressed on immune cells while P-selectin is only expressed on inflamed endothelium (Kolaczkowska and Kubes, 2013). P-selectin then interacts with PSG-1 on leukocytes to tether passing leukocytes and slow their velocities (de Oliveira et al., 2016). Selectins are membrane glycoproteins that have a distal lectin-like domain that can interact with specific carbohydrates. Glycosylation-dependent cell adhesion molecule-1 (GlyCAM-1), CD34, PSGL-1, and mucosal vascular addressin cell adhesion molecule 1 (MAdCAM-1) are sialylated carbohydrate moieties on mucin like CAMs (Nourshargh and Alon, 2014).

Once captured, leukocytes will begin a special type of binding to the endothelium called rolling which is mediated by P-selectin and E-selectin on endothelium with PSG-1. Circulating leukocytes also express L-selectin which can interact with CD34 and GlyCAM-1 expressed on the endothelium of lymph nodes (Golias et al., 2007). The shear force of the flowing blood can be strong enough to detach the leukocytes (Al-Banna et al., 2013). Once rolling, a chemokine, such as IL-8 or chemokine (C-X-C motif) ligand 2 (CXCL-2), binds to the G-protein coupled receptor (GPCR) IL-8 receptor (C-X-C chemokine receptor type 1, [CXCR1] and CXCR2) on neutrophils to activate them, which causes a conformational change in integrin molecules in the neutrophil membrane. Chemokine (C-C motif) ligand 4 (CCL4) is a chemokine that is recognized by C-C chemokine receptor type 5 (CCR5) on circulating monocytes and natural killer (NK) cells (Vestweber, 2015).

**Figure 2:** Leukocyte recruitment cascade and CAMs during inflammation. Cellular adhesion molecule (CAM), Vascular adhesion molecule-1 (VCAM-1), intercellular adhesion molecule-1 (ICAM-1), platelet endothelial cell adhesion molecule (PECAM-1), lymphocyte function-associated antigen-1(LFA-1), very late antigen-5 (VLA-4).



The conformational change on neutrophils to activated integrins increases their affinity for the binding to immunoglobulin (Ig)-super-family adhesion molecules on the endothelium. Integrin and Ig superfamily adhesion molecule interaction facilitates leukocyte arrest and adhesion. Lymphocyte function-associated antigen-1 (LFA-1) plays an important role in leukocyte adherence and interacts with intracellular adhesion molecule-1 (ICAM-1) on endothelium. In addition, vascular cell adhesion molecule-1 (VCAM-1) contributes to leukocyte adhesion by interacting with macrophage-1 antigen (MAC-1) on monocytes (Kolaczowska and Kubes, 2013).

Firmly adherent leukocytes can transmigrate into inflamed tissues, in a process known as extravasation. This is in response to local production of chemokines by endothelium and resident immune cells. Once the leukocyte transmigrates and reaches the site of inflammation it can enhance or attenuate the inflammation by phagocytosing pathogens and damaged tissue. These recruited leukocytes also contribute to the cytokines and chemokine gradient.

### *1.2.2 Resident immune cells and ocular immune response*

The eye, like the brain, pregnant uterus, and testis is a site of immune privilege in the body. It has been considered atypical immunologically since the first corneal transplant was performed in a human more than a hundred years ago, in which the graft was shown to survive longer than expected (Benhar et al., 2012; Niederkorn, 2013). The complexity of immune privilege is related to the special microenvironment and immunoregulatory mechanisms operating within the eye, which generally act to suppress the immune response. This is thought to be an evolutionary adaptation to preserve vulnerable ocular

tissues from potentially blinding damage resulting from an uncontrolled inflammatory immune response (Mérída et al., 2015). Both the innate and acquired immune responses function in ocular defense mechanisms. The eye is unique in that this organ has characteristics of both the central nervous system (CNS) and peripheral nervous system (PNS) immune system. The immune cells associated with PNS (cornea, ciliary body, iris, choroid) include macrophages and DCs. The retina is an extension of the CNS and has microglia as resident immune cells (Cairns et al., 2016).

There are several ways in which the eye protects itself from the deleterious consequences of ocular inflammation. These include physical barriers (formed by the blood-aqueous barrier and blood retinal barrier [BRB]), active immunomodulatory proteins in the aqueous humor, immunoregulation via cell-to-cell contact mechanisms with corneal and iris pigmented epithelium, and APC development of antigen tolerance (Cairns et al., 2016; London et al., 2013; Niederkorn, 2012; Streilein et al., 2002). Nevertheless, immune privilege is not insurmountable and intraocular inflammatory diseases, like uveitis, remains an important clinical problem.

The physical barriers in the eye include a BRB and a lack of efferent lymphatics in some ocular tissues, including cornea and retina, all of which protects these tissues against the potentially toxic free entry or exit of cells or large molecules (Chen, 2009; Zhou and Caspi, 2010). The outer third of the neural retina is protected by the tight junctions that close off the spaces between the retinal pigmented epithelium (RPE) cells. The inner two-thirds of the retina that is supplied by the central artery is protected by the tight junctions on its non-fenestrated capillaries (Freddo, 2001). The iris pigmented epithelium and ciliary pigmented epithelium are protected by the blood-aqueous barrier that forms tight junctions

between cells, preventing leakage into the anterior chamber (Nieder Korn, 2012). Additionally, the cornea is avascular and has reduced expression of major histocompatibility complex (MHC) class I molecules and no expression of class II molecules (Streilein, 2003).

There are several types of resident ocular cells that are potentially capable of communicating with the immune system, including: Langerhans, macrophages, astrocytes, DCs, microglia, Müller, and RPE cells. In particular, RPE cells have many characteristics of macrophages and have the capacity to migrate and engulf particles and exhibit properties that strongly suggest a capacity to participate in the local immune response. Furthermore, the RPE can be stimulated to release cytokines, most importantly IL-6 and RPE cells in culture have been reported to act as APCs for S-Antigen (S-Ag)-specific T cells (Percopo et al., 1990).

Kaplan, Stevens and Streilein discovered that alloantigenic cells placed in the anterior chamber of rat eye elicit a form of systemic immunity in which circulating antibodies are present, but the animal's ability to display T cell-mediated immunity is impaired (Nieder Korn, 2006). This was termed anterior chamber-associated immune deviation (ACAID). Antigen that is injected into a rat's eye is picked up by specialized macrophages that populate the anterior uvea and then these APCs migrate to the spleen and are associated with elevation of regulatory and NK T cells (Nieder Korn, 2012; Streilein, 1999). The innate tolerogenic ability of ACAID APCs can be explained by the presence of immunosuppressive cytokines such as tumor growth factor- $\beta$  (TGF- $\beta$ ) and alpha-melanocyte stimulating hormone ( $\alpha$ -MSH). TGF- $\beta$  *in-vitro* induces the ACAID APCs to become tolerogenic (Hara et al., 1992).

There are several extraocular physical and chemical barriers including blink reflexes, eye lids, and components in tears such as lysozyme, lactoferrin, complement and immunoglobulins. Lysozyme is effective against bacteria by destroying the cell wall (McClellan, 1997). Lactoferrin is also effective against bacteria since it strongly binds iron cations, an essential cofactor for bacterial growth. Tears transport secretory IgA (sIgA) to the ocular surface, which is produced in the lacrimal gland (Akpek and Gottsch, 2003). Additionally, the lacrimal gland produces immunosuppressive cytokines such as TGF- $\beta$ . Animal studies with TGF- $\beta$  and plasma cell deficient mice have demonstrated extensive ocular surface pathology (McClellan, 1997). Tears also contain neutrophils, which are significantly increased during sleep when the lids are closed for a long period (Akpek and Gottsch, 2003; Forrester et al., 2008).

Understanding the ocular immune response and identification of novel targets for ocular inflammatory disease is critical for decreasing vision loss and treating uveitis. It may prove beneficial to target the early acute inflammatory stage of ocular inflammatory disease with effective anti-inflammatory drugs before the disease can become chronic where adaptive immunity makes a large contribution. More research is needed to determine the best signalling pathway to decrease the acute phase of inflammation.

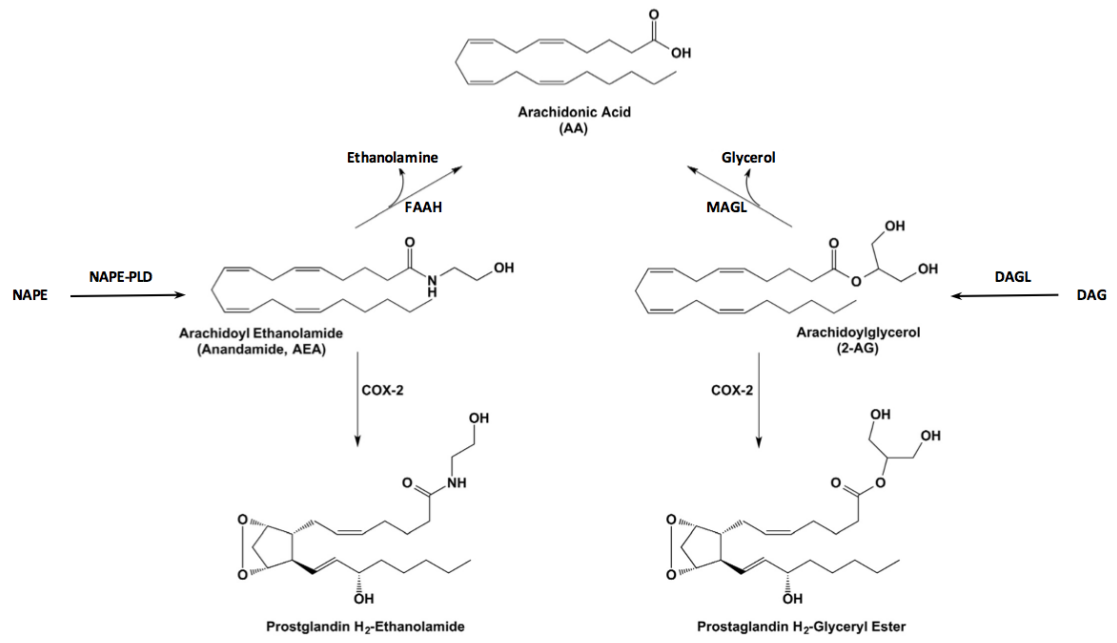
### ***1.3 The Endocannabinoid system***

The ECS has emerged as a potential anti-inflammatory target (Munoz-Luque et al., 2007; Pacher et al., 2006; Rajesh et al., 2010). The ECS is an endogenous lipid signaling system comprised of two GPCRs cannabinoid receptors (CB<sub>1</sub>R and CB<sub>2</sub>R), their endogenous endocannabinoids ligands, and enzymes responsible for endocannabinoid synthesis and degradation (Kreitzer and Stella, 2009; McPartland et al., 2015; Mechoulam

and Parker, 2013). The two most studied endocannabinoids are N-arachidonylethanolamine (AEA or anandamide) and 2-arachidonoyl glycerol (2-AG). Both AEA and 2-AG are non-selective agonists for CB<sub>1</sub>R and CB<sub>2</sub>R (Cairns et al., 2016). AEA is synthesised by an enzyme called N-acyl phosphatidylethanolamine phospholipase-D (NAPE-PLD) and degraded by fatty acid amide hydrolase (FAAH), while 2-AG is synthesised by diacylglycerol-lipase (DAGL) and degraded by monoacylglycerol lipase (MAGL) (Figure 3).

Both CB<sub>1</sub>R and CB<sub>2</sub>R on activation couple to G<sub>i/o</sub> proteins to inhibit adenylyl cyclase and stimulate mitogen-activated protein kinases (MAPK) signaling. CB<sub>1</sub>R is highly expressed in the CNS, and activation of this receptor regulates the presynaptic release of neurotransmitters, with resultant modulation of sensory, motor, and cognitive functions (Herkenham et al., 1991; Mackie, 2006). CB<sub>2</sub>R, in contrast, is localized primarily to immune cells (Galiegue et al., 1995; Munro et al., 1993), and drugs acting at this receptor lack psychotropic side-effects associated with cannabinoids that act at CB<sub>1</sub>R (Cairns et al., 2016). The crystal structure of the human CB<sub>1</sub>R in complex with the stabilizing CB<sub>1</sub>R agonists either tetrahydrocannabinol (AM11542) or hexahydrocannabinol (AM841) (Hua et al., 2017), antagonist AM6538 (Hua et al., 2016) or inverse agonist taranabant (Shao et al., 2016) has recently been published. These structures will aid in the development of new more selective cannabinoid drugs and provide novel insights into the structure-activity based relationship (SAR) of ligands, such as  $\Delta^9$ -tetrahydrocannabinol (THC), that bind to CB<sub>1</sub>R at the orthosteric site, or cannabinoids that interact with allosteric sites on CB<sub>1</sub>R such as cannabidiol (CBD) and other novel small molecules (Laprairie et al., 2015). An allosteric binding site is a topographically distinct site on the GPCR from the established

**Figure 3:** Major pathways for the synthesis and degradation of endocannabinoids (AEA and 2-AG). Adopted from (Blankman and Cravatt, 2013). 2-arachidonoylglycerol (2-AG), cyclooxygenase 2 (COX-2), diacylglycerol lipase (DAGL), fatty acid amide hydrolase (FAAH), monoacylglycerol lipase (MAGL), N-acylphosphatidylethanolamine (NAPE), NAPE-phospholipase D (NAPE-PLD).

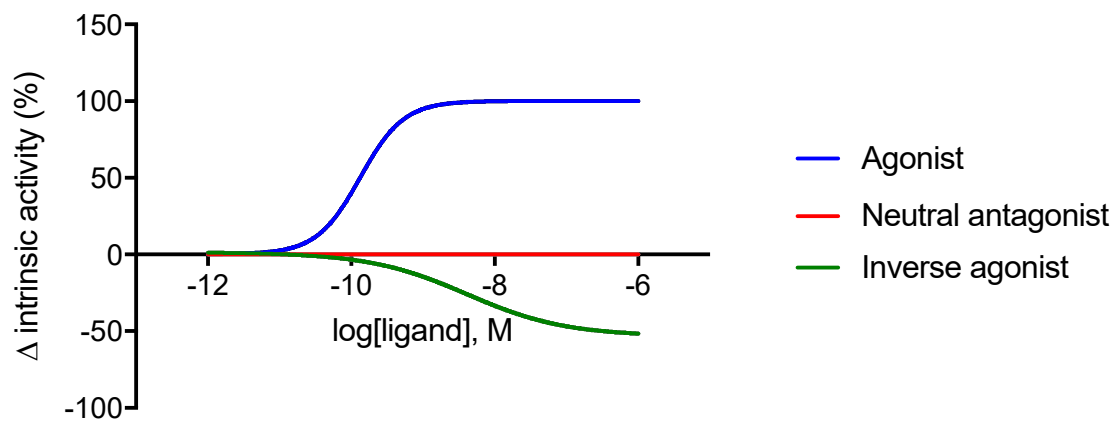


primary active orthosteric binding site (Wootten et al., 2013). Allosteric ligand binding is believed to induce a conformational change in the receptor that affects the receptor affinity and/or efficacy of the orthosteric ligand thereby modifying pre-existing actions of the orthosteric ligand (Laprairie et al., 2017; Ross, 2007). A pharmacological ligand can be described as an agonist if it binds to the receptor and activates it, a neutral antagonist if it binds to the receptor but has no activity and can block the activity of other agonists, or an inverse agonist, if it binds to the receptor but produces the opposite pharmacological response to that of the agonist. A prerequisite for an inverse agonist is that the receptor must have a constitutive activity level (basal receptor signalling that is present in the absence of an agonist). An inverse agonist binds to the receptor and decreases receptor activity (Figure 4).

### 1.3.1 ECS ligands

Cannabinoids are hydrophobic compounds that can bind to cannabinoid receptors. Phytocannabinoids are constituents of the cannabis plant, *Cannabis sativa*. There are over 400 active constituents in cannabis of which over 100 of these are cannabinoids, each possessing a multi-ring structure. The most abundant phytocannabinoid is THC, and ingestion of THC is associated with the psychotropic effects of cannabis. Another important phytocannabinoid is CBD, which has reported therapeutic effects and an apparent absence of the psychoactive properties associated with THC (Pertwee, 2006). Interest in CBD lies in its analgesic, anticonvulsant, antiemetic, antianxiety, and anti-inflammatory properties (Klein, 2005). Endocannabinoids are endogenous lipids derived from arachidonic acid in the cell membrane (Figure 3). AEA and 2-AG have a similar

**Figure 4:** Change in intrinsic (basal) receptor activity after different pharmacological treatments. Treatment: agonist, will increase receptor activity; neutral antagonist, block any change in activity and block the actions of an agonist; inverse agonist, requires that there be basal constitutive activity and it will reduce it.



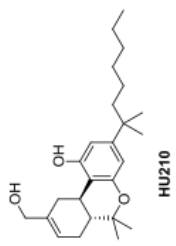
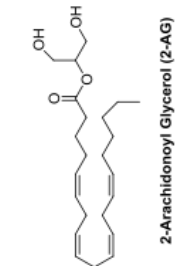
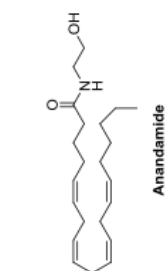
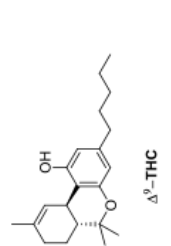
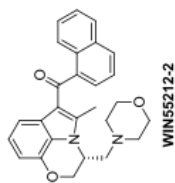
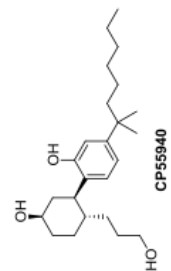
structure and function but different affinities for CB<sub>1</sub>R and CB<sub>2</sub>R and are produced and degraded by distinct enzymatic pathways (McHugh et al., 2008). AEA and 2-AG are more selective for the CB<sub>1</sub>R over the CB<sub>2</sub>R; however 2-AG is much more abundant and has higher affinity for the CB<sub>2</sub>R compared to AEA (Galiegue et al., 1995).

Isolation of phytocannabinoids such as THC, cannabidiol and cannabinol (Gaoni and Mechoulam, 1971, 1964) led to synthesis of synthetic cannabinoids and contributed to the cloning of cannabinoid receptors (Galiegue et al., 1995; Kaminski et al., 1992; Munro et al., 1993). The structural features of THC include a C3 side chain, phenolic hydroxyl, has three rings: the aromatic A-ring, pyran B-ring, and cyclohexenyl C-ring. Many of the synthetic cannabinoids (Figure 5) replace the pyran B-ring with an aliphatic chain, known as the southern aliphatic region which is the main structural feature of classical cannabinoids (Bow and Rimoldi, 2016). Many classical cannabinoids, including CP55940 have modifications to the C3 side chain, which alters potency and selectivity to the CB<sub>1</sub>R versus CB<sub>2</sub>R. Other non-classical cannabinoids have been developed such as, WIN 55,212-2, JWH-018, and SR141716 (Bow and Rimoldi, 2016).

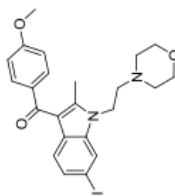
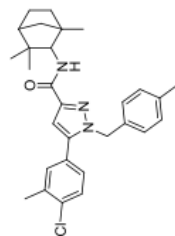
Knowledge of the CB<sub>1</sub>R crystal structure in complex with an agonist (Hua et al., 2017), antagonist (Hua et al., 2016) or inverse agonist (Shao et al., 2016) enabled the researchers to virtually dock various cannabinoids (THC, CP55940, WIN 55,212, JWH-018, AEA, and 2-AG) into the orthosteric binding site of the CB<sub>1</sub>R 3D model. These ligands mainly interact with extracellular loop 2 (ECL2), N-terminal loop, helices III, VI, and VII (Hua et al., 2016). The rings in THC and CP55940 lie between the N-terminal loop and ECL2. AEA and 2-AG were also modeled and formed a C-shape conformation and interact

**Figure 5:** Structures of different classical and non-classical cannabinoid ligands.

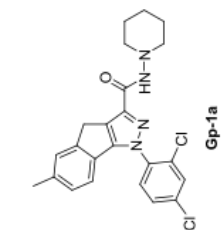
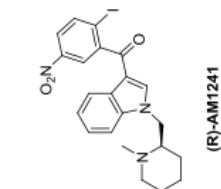
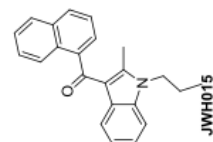
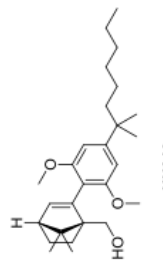
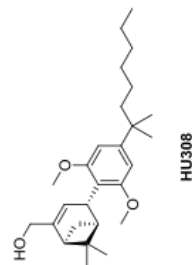
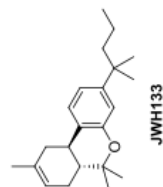
**Non-selective agonists**



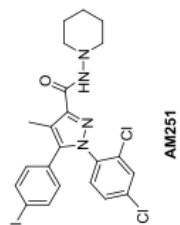
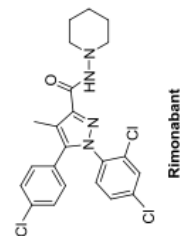
**Selective CB<sub>2</sub>R antagonist**



**Selective CB<sub>2</sub>R agonists**



**Selective CB<sub>1</sub>R antagonist**



similar to THC in the orthosteric binding site. JWH-018 and WIN55,212 were modeled to bind deeper in the orthosteric binding pocket of CB<sub>1</sub>R (Hua et al., 2016).

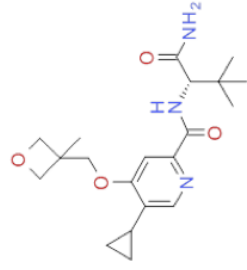
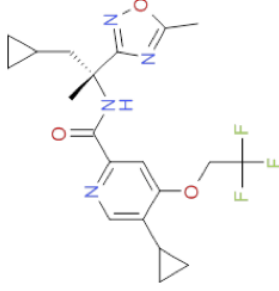
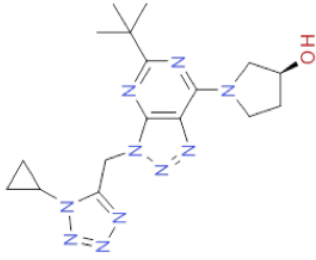
The pharmacology of endocannabinoids and phytocannabinoids is increasingly complex since many of these ligands are non-selective and may be mediating their actions through CB<sub>1</sub>R and CB<sub>2</sub>R, and possibly other non-CB<sub>1</sub>R and non-CB<sub>2</sub>R receptors, such as transient receptor potential cation channel subfamily V member 1 (TRPV1), G protein-coupled receptor 55 (GPR55), GPR18, GPR19, peroxisome proliferator-activated receptor gamma (PPAR $\gamma$ ) and serotonin 1A receptor (5-HT<sub>1A</sub>) (McHugh et al., 2008). In addition, most synthetic cannabinoids that have been developed, such as WIN55,212-2, CP55940, GP1a, JWH018, SR141716a (rimonabant), show non-CB<sub>2</sub>R and CB<sub>1</sub>R mediated activity (Atwood and Mackie, 2010; Klein, 2005; Soethoudt et al., 2017). Table 1 shows well established cannabinoid ligands with their selectivity for CB<sub>2</sub>R over CB<sub>1</sub>R. For the purposes of target validation and drug development it is necessary to have synthetic agonists that are highly selective and induce well-defined receptor signalling pathways. Therefore, the objective of the present study was to examine the anti-inflammatory actions of the new highly potent and selective CB<sub>2</sub>R agonists, RO6871304 and RO6871085, that originate from two chemically diverse series, and a structurally related novel CB<sub>2</sub>R inverse agonist, RO6851228, in a well-established mouse model of EIU (Table 2) (Kezic et al., 2011; Rosenbaum et al., 2011; Szczesniak et al., 2017; Toguri et al., 2015). All these novel cannabinoids have affinities that are significantly higher for CB<sub>2</sub>R than the endocannabinoids, AEA and 2-AG, and phytocannabinoids such as THC. These novel selective CB<sub>2</sub>R agonists may be of value as lead compounds for a selective CB<sub>2</sub>R drug given, that their effects are mediated through binding CB<sub>2</sub>R and not CB<sub>1</sub>R.

**Table 1:** Binding selectivity and bias signalling for cannabinoids for human cannabinoid receptors. CB<sub>2</sub>R selectivity for all cannabinoid receptor reference ligands are presented as  $10^{(pKi\ CB_2R - pKi\ CB_1R)}$ . CP55940 was used as the reference compound since it performed as a full agonist at both CB<sub>1</sub>R and CB<sub>2</sub>R with similar potencies in all assays. This data was reported in (Soethoudt et al., 2017).

	Selectivity for human CB <sub>2</sub> R over CB <sub>1</sub> R	Bias signalling on human CB <sub>2</sub> R
WIN55212-2	1	Bias towards GIRKs over cAMP
HU910	166	Equally balanced at all transduction pathways
HU308	278	Equally balanced at all transduction pathways
JWH015	28	Bias toward GIRK over cAMP
AEA	1	Bias toward pERK and GIRK over cAMP
2-AG	1	Bias toward GIRK over G proteins
THC	0.5	Bias toward G protein (pERK) signalling over $\beta$ -arrestin and GTP $\gamma$ s

**Table 2:** Chemical structures, physicochemical properties, binding affinity and selectivity for human and mouse cannabinoid receptors for a novel series of CB<sub>2</sub>R ligands. CB<sub>2</sub>R selectivity for all cannabinoid receptor reference ligands are presented as ratio of mean pK<sub>i</sub> values between CB<sub>2</sub>R and pK<sub>i</sub> values between CB<sub>1</sub>R from human orthologues. <sup>a</sup>distribution coefficient values. <sup>b</sup>Parallel artificial membrane permeability assay (PAMPA) was used to determine membrane permeation coefficient values (P<sub>eff</sub>). <sup>c</sup>aqueous solubility in phosphate buffer pH 6.5. <sup>d</sup>Human and mouse microsomal stability assessed by clearance.

Comp:	RO6871304	RO6871085	RO6851228
MW (g/mol)	384	424	390
h/m CB <sub>2</sub> R cAMP EC <sub>50</sub> [nM](%eff)	0.7(103%)/0.4(101)	0.5(91%)/0.7(89%)	26(-159%)/5(-174%)
EC <sub>50</sub> ratio hCB <sub>1</sub> /hCB <sub>2</sub> R	>14286	>2062	>61855
h CB <sub>2</sub> R Ki [nM]	8	25	27
Ki Ratio hCB <sub>1</sub> R/hCB <sub>2</sub> R	>1250	122	250
logD <sup>a</sup>	2.8	3.9	3.2
Pampa Peff [cm/s*10 <sup>-6</sup> ] <sup>b</sup>	3	2	5
Lysa [mg/mL] <sup>c</sup>	162	4	174
Mic. CL (h/m) [μL/min/kg] <sup>d</sup>	<10/71	10/26	34/53



### 1.3.2 *CB<sub>2</sub>R signaling pathways*

CB<sub>2</sub>R are class A Rhodopsin-like family of G protein-coupled receptors. As such they are single polypeptides that have a seven transmembrane  $\alpha$ -helix domain and a short extracellular domain that binds cannabinoids in the orthosteric binding site (Atwood et al., 2012). CB<sub>2</sub>R predominantly couple to G $\alpha_{i/o}$  subunits of G proteins (Howlett, 2002). Activation of CB<sub>2</sub>R (Figure 6) results in activation of multiple signal transduction pathways, including inhibition of adenylyl cyclase and stimulation of several MAPKs including ERK-1/2, c-June NH<sub>2</sub>-terminal kinase (JNK), p38 (Kishimoto et al., 2003). Depending on both the cell type and state of immune activation, CB<sub>2</sub>R can also activate additional signaling pathways including: small G proteins (such as RhoA, Rac, and cdc42), G-protein-coupled inward rectifying K<sup>+</sup>-channels (GIRKs), recruitment of  $\beta$ -arrestin, and activation of phospholipase C (PLC) leading to the release of intracellular Ca<sup>2+</sup>, and stimulation of signaling via the phosphatidyl inositol 3 kinase (PI3K)/Akt pathway, with downstream JNK activation, ceramide production and gene transcription (Ryberg et al., 2007; Henstridge et al., 2000; Atwood & Mackie, 2010).

Different agonists may stabilize distinct conformations of the receptor leading to biased receptor signalling or functional selectivity wherein a particular agonist may bias the receptor to favour one signalling pathway over another signalling pathway (Figure 7) (Kenakin, 2012). Understanding receptor bias is important in drug discovery and translational studies, given that receptor activation may activate multiple signaling pathways and can be different between rodent and human receptor orthologues (Soethoudt et al., 2017). Table 1 shows results from Soethoudt et al (2017) who reported the different biased signalling of different CB<sub>2</sub>R agonists. HU910, HU308 and JWH133 have biased

**Figure 6:** CB<sub>2</sub>R activation signalling pathway. Adenylate cyclase (AC), activated protein-1 (AP-1); adenosine triphosphate (ATP), 2-arachidonoyl glycerol (2-AG), cannabinoid 2 receptor (CB<sub>2</sub>R), extracellular signal-regulated kinases 1/2 (ERK 1/2), nuclear factor kappa-light-chain-enhancer of activated B cells (NF-κB), protein kinase A (PKA), protein kinase C (PKC).

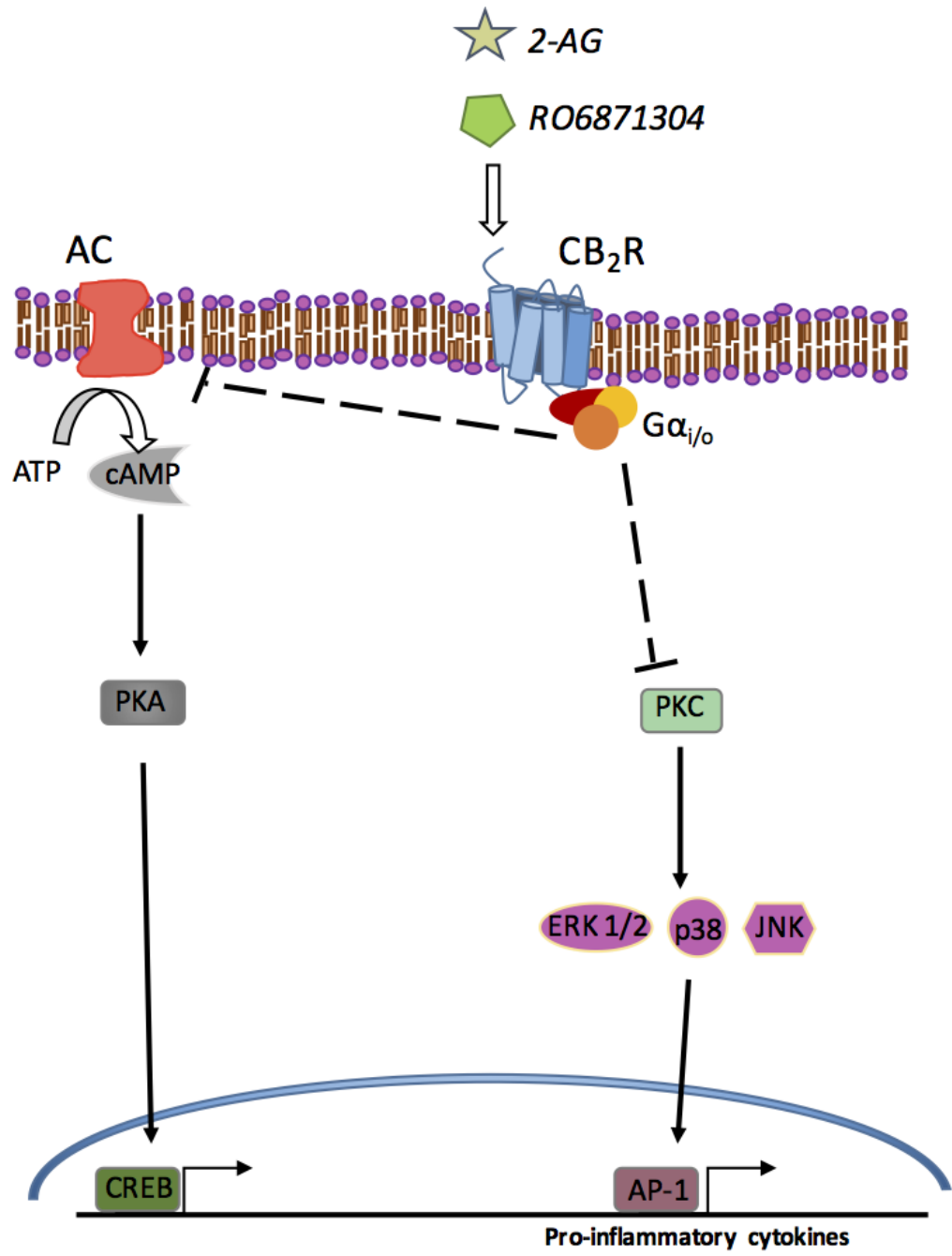
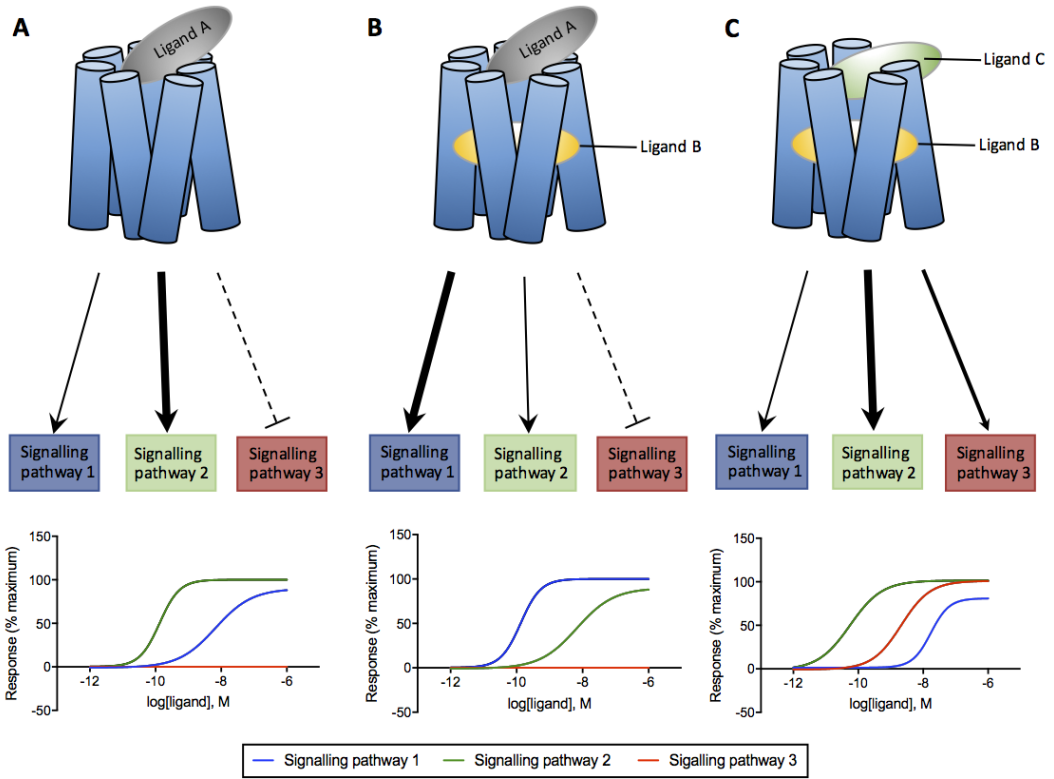


**Figure 7:** Signalling bias of ligands for different receptor activation signalling pathways. There is co-binding of an allosteric modulator in B and C. (A) Ligand A binds to the orthosteric binding site and causes potent activation of signalling pathway 2, modest activation of signalling pathway 1, and does not activate signalling pathway 3. (B) binding of Ligand B to the allosteric site changes the signalling of Ligand A causing potentiation of signalling pathway 1 and decreased potency to activate signalling pathway 2, and does not activate signalling pathway 3. (C) Ligand C binding to the orthosteric binding site and Ligand B binding to the allosteric site causes potent activation of signalling pathway 2, activation of signalling pathway 3 and decreased potency to activate signalling pathway 1.



signalling toward G protein signalling over  $\beta$ -arrestin and cAMP signalling in mouse CB<sub>2</sub>R. The advantages of understanding the signalling bias are that drugs can be developed that have a selectivity for a certain therapeutic pathway and less for an unwanted pathway that produces potential side-effects, for example  $\beta$ -arrestin recruitment and receptor downregulation.

### *1.3.3 CB<sub>2</sub>R distribution and expression*

CB<sub>2</sub>R, often called the ‘peripheral’ cannabinoid receptor, is highly expressed on cells of the immune system and is found in abundance in lymphoid tissues (Croxford and Yamamura, 2005). The human CB<sub>2</sub>R was cloned in 1993 from the promyelocytic leukaemia cell line HL-60 (Munro et al., 1993). Of specific immune cells, the highest levels of CB<sub>2</sub>R mRNA in order are found in: B cells > NK cells >> monocytes > neutrophils > CD8<sup>+</sup> T cells > CD4<sup>+</sup> T cells (Galiegue et al., 1995). CB<sub>2</sub>R are expressed on many monocyte-derived cells. These include microglia, circulating macrophages, osteocytes, osteoclasts, DCs, and hepatic Kupffer cells (Atwood & Mackie, 2010). The high CB<sub>2</sub>R expression associated with immune cells suggests the involvement of the ECS and CB<sub>2</sub>R in modulating the immune system. Unfortunately, primary antibodies for CB<sub>2</sub>R, as with many other GPCRs, lack specificity and this makes it difficult to study protein expression.

Macrophage and microglial CB<sub>2</sub>R mRNA levels are dependent upon the activation state of the cells. Under normal physiological conditions, CB<sub>2</sub>R mRNA is barely detectable in the CNS (Carlisle et al., 2002; Griffin et al., 1999; Schatz et al., 1997). Conversely, in inflammatory and neurodegenerative conditions, CB<sub>2</sub>R expression is considerably increased (Benito et al., 2003; Maresz et al., 2005; Carrier et al., 2004; Eljaschewitsch et

al., 2006; Ramirez et al., 2005). For example, in an experimental model of encephalomyelitis, CB<sub>2</sub>R mRNA expression was 10-fold greater in activated microglia cells, as compared to resting cells (Maresz et al., 2005).

Taken together, these studies indicate that CB<sub>2</sub>R expression is increased during pathological states; however, the factors that are involved in the increased or decreased expression are far from understood. The presence of CB<sub>2</sub>R on immune cells in the periphery and the anti-inflammatory properties associated with receptor activation, make CB<sub>2</sub>R an attractive therapeutic target for immunomodulation in ocular inflammation, as well as for other systemic and CNS inflammatory diseases.

#### *1.3.4 CB<sub>2</sub>R and the immune system*

The ECS plays a prominent role in immune homeostasis and all immune cells examined to-date express cannabinoids receptors, in particular CB<sub>2</sub>R, as well as enzymes for the production and degradation of endocannabinoids. *In vitro* studies have shown that stimulation with LPS increases production of AEA and 2-AG by immune cells including macrophages, peripheral-blood mononuclear cells (PBMCs) and DCs (Croxford and Yamamura, 2005). Interestingly, in animal studies with herpes simplex virus, *Listeria monocytogenes*, *Staphylococcus epidermidis*, *Treponema pallidum* and *Legionella pneumophila*, exogenous cannabinoid treatment is protective and suppresses host resistance to infection (Klein, 2005). Further suggesting a role for CB<sub>2</sub>R in immunomodulation, Buckley *et al*, (2000) showed that THC treatment inhibited the activation of T helper cells through activity on macrophages, and was blocked in CB<sub>2</sub>R<sup>-/-</sup> mice (Buckley et al., 2000).

Cumulative evidence indicates that activation of CB<sub>2</sub>R is immunosuppressive and that CB<sub>2</sub>R may function as an endogenous auto-protective receptor to prevent inflammation; CB<sub>2</sub>R are strongly up-regulated in inflamed tissue, and selective activation of these receptors reduces inflammation (Rom et al., 2013). In support of this, previous studies in various animal models have shown that administration of synthetic CB<sub>2</sub>R agonists, suppressed disease severity of experimental autoimmune encephalomyelitis (EAE), sepsis (Lehmann et al., 2012, 2011), uveitis (Toguri et al., 2014), rheumatoid arthritis, multiple sclerosis (MS), Alzheimer's disease (AD), Huntington's disease (HD), Parkinson's disease, head injury, and ischemia-reperfusion (Downer, 2011).

#### *1.3.5 CB<sub>2</sub>R and macrophages*

There has been a significant number of cannabinoid studies focussed on ECS signaling in macrophages (reviewed in Miller and Stella, 2008), since these cells are important mediators in both innate and adaptive immunity. Macrophages migrate toward diseased tissue, engulf damaged cells and infectious agents, and present antigens to T cells of the adaptive immune system. They mediate their effects through production of acute phase cytokines (TNF- $\alpha$ , IL-1, IL-6 and IL-10), phagocytosis of infectious agents, and release inflammatory mediators such as nitric oxide (NO) and arachidonic acid metabolites. Studies on *in vitro* murine peritoneal macrophages and in *in vivo* mouse models, showed that CB<sub>2</sub>R agonists consistently suppressed various functions including cell migration, spreading, phagocytosis, cytokine production, and antigen presentation (reviewed in Atwood and Mackie, 2010b). Furthermore, Steffens et al (2005) show that THC treatment decreases macrophage migration and that this is mediated through CB<sub>2</sub>R since these effects

were lost in macrophages treated with the pharmacological CB<sub>2</sub>R antagonist, SR144528, or in CB<sub>2</sub>R<sup>-/-</sup> macrophages (Steffens et al., 2005).

Molecular changes in macrophages have been reported following cannabinoid treatment. For example, THC and AEA treatment of macrophages inhibit LPS-induced NO, an important inflammatory mediator, and also inhibit IL-6 release (Chang et al., 2001). In addition, the LPS-induced expression of pro-inflammatory cytokines can be inhibited by cannabinoids in murine macrophages and microglia (Croxford and Yamamura, 2005). LPS-induced NO production in macrophages was also shown to be inhibited by WIN 55,212-2 treatment *in vivo*, an effect blocked by the CB<sub>2</sub>R antagonist SR144528 (Ross et al., 2000). Similar findings have also been found in other cells types including microglia, astrocytes and neurons (Martínez-Orgado et al., 2007; Shmist et al., 2006). The decrease in pro-inflammatory cytokines by cannabinoids acting at CB<sub>2</sub>R may occur by the inhibition of transcription factors that induce cytokine gene expression. For example, TNF, a major cytokine released by microglia cells in a number of pathological conditions, is inhibited by the activation of CB<sub>2</sub>R via the inhibition of NF-κB (Rajesh et al., 2007). Given that cannabinoids have been shown to negatively regulate proinflammatory cytokines, NF-κB activation, NO production and granulocyte macrophage colony-stimulation factor (GM-CSF), this would suggest that activation of CB<sub>2</sub>R signalling pathways may be an essential mechanism responsible for the inhibition of the inflammatory response (Gertsch and Anavi-Goffer, 2012; Pacher and Mackie, 2012).

### 1.3.6 CB<sub>2</sub>R involvement in the ocular immune response

The eye contains all the components of the ECS including expression of both CB<sub>1</sub>R and CB<sub>2</sub>R. CB<sub>1</sub>R is expressed throughout the retina and in the trabecular meshwork, while CB<sub>2</sub>R expression is more limited and localized to resident immune cells and retinal glial cells (Toguri et al., 2016). Until very recently, the involvement of the ECS, and more specifically, CB<sub>2</sub>R, in the ocular immune response has not been examined. Xu *et al.* (2007), using a model of experimental autoimmune uveitis, reported that modulation of the ECS, in particular activation of CB<sub>2</sub>R, with the synthetic cannabinoid, JWH133, was anti-inflammatory. JWH133 decreased leukocyte infiltration into the inflamed retina and prevented retinal structural changes. The authors of this study proposed a mechanism that involved JWH133-mediated inhibition of the activation and function (response to antigen presentation) of autoreactive T cells and prevented their proliferation. JWH133 treatment was also associated with decreased TNF- $\alpha$ , interferon- $\gamma$  (INF- $\gamma$ ), IL-6, and IL-10 (Xu et al., 2007).

More recent work by our group (Toguri et al., 2014), using a rat model of EIU, has demonstrated that activation of CB<sub>2</sub>R reduces leukocyte-endothelial interactions, and decreases the levels of pro-inflammatory cytokines (IL-1 $\beta$ , IL-6, TNF- $\alpha$ , INF- $\gamma$ , chemokine [C-C motif] ligand 5 [CCL5], CXCL2) and transcription factors responsible for production of pro-inflammatory mediators (NF- $\kappa$ B and AP-1). This study also demonstrated that in EIU, CB<sub>2</sub>R agonists were more efficacious than clinically used topical agents, including corticosteroids and NSAIDs in a single dose regimen. In a later study, Toguri et al. (2015) showed that there is upregulation of CB<sub>2</sub>R mRNA during EIU in mice, suggesting that there is increased constitutive activity of this receptor during ocular

inflammation (Toguri, 2015). This was supported by use of a pharmacological antagonist to block CB<sub>2</sub>R, which resulted in exacerbated leukocyte adhesion in the iridial microcirculation.

Work from our lab, has also showed in a model of chronic ocular inflammation, proliferative vitreoretinopathy (PVR), that CB<sub>2</sub>R activation with the potent and selective CB<sub>2</sub>R agonist, HU308, decreased histopathological scores, the number of activated microglia, and leukocyte adhesion compared to vehicle-treated eyes. Conversely, an increase in histopathological scores, and activated microglia, and elevated levels of cytokines was observed in CB<sub>2</sub>R<sup>-/-</sup> mice compared to WT mice (Szczesniak et al., 2017). Taken together, these studies demonstrate the immunomodulatory properties of CB<sub>2</sub>R activity and indicate the potential of developing novel ligands that activate CB<sub>2</sub>R with favourable drug properties for the treatment of ocular inflammatory disease.

## **1.4 Novel selective CB<sub>2</sub>R ligands**

### *1.4.1 Currently used CB<sub>2</sub>R agonists and their pharmacokinetics (PK) and pharmacodynamics (PD)*

There are currently several different chemical classes that have been described as CB<sub>2</sub>R agonists. These include endocannabinoids, phytocannabinoids, and synthetic cannabinoids such as GP1a, JWH133, JWH015, AM1241 and HU308. CB<sub>2</sub>R antagonists include AM630 and SR144528 (Figure 5). Many of these commonly used ligands show both CB<sub>2</sub>R and CB<sub>1</sub>R-mediated activity since these two receptors share high homogeneity in their respective orthosteric ligand binding sites (Atwood and Mackie, 2010; Klein,

2005). CB<sub>2</sub>R ligands have a range of affinities and selectivities for CB<sub>2</sub>R over CB<sub>1</sub>R. All these ligands are highly lipophilic molecules (high distribution-coefficient [logD]), which negatively affects their solubility and absorption, distribution, metabolism and excretion (ADME)-properties (Soethoudt et al., 2017). Most of the commonly used ligands have membrane permeation coefficients (PAMPA)  $P_{\text{eff}}$  that allow the molecules to cross cell membranes. Several of the “gold standard” CB<sub>2</sub>R agonists, HU308 and HU910, have been shown to have good bioavailability after administration of 1 mg/kg i.v. in mice and reach maximal plasma concentration approximately 1 h post injection (Soethoudt et al., 2017).

#### *1.4.2 High-throughput screen and lead optimization for CB<sub>2</sub>R ligands*

In collaboration with Roche Pharmaceuticals, who performed a high-throughput screen to identify potent and selective CB<sub>2</sub>R agonists, a series of candidate ligands were selected to identify useful lead compounds. This analysis was conducted by assessment of potency at CB<sub>2</sub>R (cAMP assay) and selectivity for CB<sub>2</sub>R versus CB<sub>1</sub>R (cAMP assay) (Nettekoven et al., 2016). Lead hits included heterocyclic triazolopyrimidines rings which were used to rationalize a SAR. Nettekoven et al (2016) outline this high through-put screen approach and lead optimized for enhanced potency and physico-chemical properties. The novel ligands used in this study (RO6871304, RO6871085, and RO6851228) dock well into the orthosteric ligand binding site of the 3D homology model of CB<sub>2</sub>R, which is based on the X-ray crystal structure of activated bovine rhodopsin (Nettekoven et al., 2016). The basic SAR for RO6871304 is that each substituent on the triazolopyrimidine ring, at positions 3 and 5 (Table 2), are in contact with the external loop

region of CB<sub>2</sub>R, while position 7 points downwards within the binding pocket towards the transmembrane.

#### 1.4.3 Physico-chemical properties of CB<sub>2</sub>R ligands: PK and ADME

The compounds selected for further pharmacodynamics studies were the result of lead ADME optimization to improve drug-likeness and pharmacokinetics (PK). The physico-chemical properties of the three compounds tested are listed in Table 2. Molecular weights range from 387 g/mol for RO6871304 up to 424 g/mol for RO6871085. Importantly, all novel selective CB<sub>2</sub>R agonists are lipophilic molecules. To decrease lipophilicity, aromaticity of the parent ligand was decreased by substitution. The lowest lipophilicity value (logD), calculated to be 2.8 for RO6871304 while RO6871085 is the most lipophilic with a logD value of 3.2. The PAMPA P<sub>eff</sub> is high for each of the ligands meaning that they can cross biological barriers. Furthermore, these compounds have enhanced metabolic stability as evidenced by low *in vitro* clearance of human and mouse microsomes.

These compounds have low plasma protein binding, with a fraction unbound (fu) of 0.9 in mouse to 13.1% in humans, and also have high efflux ratios (ER), indicating they are suitable for peripheral diseases. These ligands also do not inhibit the human ether-a-go-go-related gene (hERG) potassium channel and, therefore, are unlikely to have any reactive metabolites. Furthermore, these compounds do not inhibit cytochrome P450 (CYP) (3A4/2CP/2D6) (Nettekoven et al., 2016). After i.v. 1 mg/kg administration in mice, the cannabinoid ligands tested reach peak concentration approximately 1 h after injection, have low clearance rate, good volume of distribution (V<sub>ss</sub>; 1 - 4 [L/kg]), and good half-

lives (0.3 h to 4.2 h). Since the route of administration used for ocular delivery in this study was topical the PK data values are assumed to be lower but still have good bioavailability. Furthermore, we assume these ligands reach high concentration within the ocular tissues.

#### *1.4.4 Affinity and selectivity in the CBR binding studies*

[<sup>3</sup>H]-CP55940 displacement assays were performed by Roche Pharmaceuticals using membrane fractions of CHO cells expressing recombinant human (or mouse) CB<sub>2</sub>R or CB<sub>1</sub>R (Table 2). The novel ligands exhibited strong K<sub>i</sub> values for CB<sub>2</sub>R and have high selectivity for human and mouse CB<sub>2</sub>R versus CB<sub>1</sub>R, suggesting that they lack CB<sub>1</sub>R off-target activity. RO6871304, RO6871085, RO6851228 possess 1250-, 122-, 250-fold higher respective affinities for human CB<sub>2</sub>R than for CB<sub>1</sub>R.

#### *1.4.5 Activity of CBR signaling pathways and selectivity in the CBR binding studies*

To determine the functional activity and selectivity (towards CB<sub>2</sub>R over CB<sub>1</sub>R) of the ligands, Roche Pharmaceuticals carried out cAMP assays using both human CB<sub>2</sub>R and human CB<sub>1</sub>R (Table 2). All ligands were also tested using mouse CB<sub>2</sub>R to determine interspecies behavior. Efficacy of the ligands is normalized to the effect produced by CP55940 (10 μM). RO6871304 and RO6871085 behave as potent full agonists with high selectivity at human and mouse CB<sub>2</sub>R with EC<sub>50</sub> for human and mouse for each being 0.7/0.4 nM and 0.5/0.7 nM, respectively. RO6851228 behaved as a potent inverse agonist with high selectivity at human and mouse CB<sub>2</sub>R with an EC<sub>50</sub> 26 nM and 5 nM for each, respectively.

#### *1.4.6 Clinical advantage of improved drug-likeness*

Improved potent and selective CB<sub>2</sub>R agonists with good ADME profiles, bioavailability and half-life for ocular delivery have many clinical implications including: (1) improved patient compliance due to less frequent dosing, (2) better correspondence between dose and plasma concentration, (3) improved extrapolation from animal studies to human studies (4) low patient variability due to differences in drug metabolism and (5) less active metabolites (Pattern, 2009).

### **1.5 Hypothesis and Objectives**

The overall purpose of this thesis was to examine the pharmacology of a new series of selective CB<sub>2</sub>R ligands in an experimental model of uveitis, EIU.

My work tested the hypothesis that activation of CB<sub>2</sub>R is anti-inflammatory during ocular inflammation by inhibiting activation of resident ocular immune cells and decreasing neutrophil migration and adhesion.

The specific objectives tested were:

- 1) To evaluate the effects of the novel selective CB<sub>2</sub>R agonists, RO6871304, RO6871085, and HU910, and an inverse agonist, RO6851228, on leukocyte interactions in an experimental model of EIU in WT and CB<sub>2</sub>R genetic knockout (CB<sub>2</sub>R<sup>-/-</sup>) mice
- 2) Compare the anti-inflammatory effects of the selective CB<sub>2</sub>R agonist RO6871304 to a clinical steroid drug, dexamethasone, used to treat ocular inflammation.

- 3) Determine the therapeutic time window for CB<sub>2</sub>R agonist treatment in EIU.
- 4) Examine the ability of a selective CB<sub>2</sub>R agonist or inverse agonist to modify neutrophil migration *in vitro*.
- 5) Further identify which immune cell type(s) is/are responsible for the CB<sub>2</sub>R mediated reduction in leukocyte adhesion.

## Chapter II: Methods and Materials

### 2.1 Animals

Male BALB/c wild-type (WT; 25-30 g; Charles River, QC, Canada) and age matched (6-8 weeks) CB<sub>2</sub>R knockout mice (CB<sub>2</sub>R<sup>-/-</sup>) were used for experiments. CB<sub>2</sub>R<sup>-/-</sup> mice were obtained by crossing male C57BL/6J CB<sub>2</sub>R<sup>-/-</sup> mice (strain B6.129P2-Cnr2tm1Dgen/J; Jackson Laboratory, Bar Harbour, ME, USA) with inbred BALB/c female mice (Charles River) for ten generations. Heterozygote mice from separate parents were then bred for a homozygote knock-out of the CB<sub>2</sub>R<sup>-/-</sup>. CB<sub>2</sub>R<sup>-/-</sup> was confirmed via genotyping. BALB/c mice were used for IVM experiments as the absence of pigment allowed for visualization of leukocyte-endothelial interactions in the iridial microvasculature. Animals were maintained on a 12 h light/dark cycle with unrestricted access to food and water. All experiments were conducted in accordance with the standards and procedures of the Canadian Council on Animal Care and were approved by the Dalhousie University Committee on Laboratory Animals. All studies involving animals are reported in accordance with the ARRIVE guidelines for reporting experiments involving animals (<http://www.nc3rs.org.uk/>; Kilkenny et al., 2010; McGrath et al., 2010).

### 2.2 Genotyping CB<sub>2</sub>R<sup>-/-</sup> animals

PCR genotyping was carried out using DNA extracted from ear punches with an Accustart II Mouse Genotyping Kit (Quanta Biosciences, MD, USA) according to manufacturer's instructions. The following PCR primers were used: moIMR0086 (5'-GGGGATCGATCCGTCCTGTAAGTCT-3'; mutant forward), oIMR7552 (5'-GACTAGAGCTTTGTAGGTAGGCGGG-3'; common reverse), and oIMR7565 (5'-

GGAGTTCAACCCCATGAAGGAGTAC-3'; WT forward). The expected results were a single product at ~550 bp for CB<sub>2</sub>R<sup>-/-</sup>, a single product at ~385 bp for wild-type and two products at ~550 and 385 bp for heterozygous animals.

### **2.3 Induction of endotoxin-induced uveitis (EIU)**

EIU was induced in BALB/c mice, as previously described (Becker et al., 2000; Toguri et al., 2014), using an intravitreal injection of LPS (2 µl; 125 ng/µl; *E. coli* 0111:B4 L084M4118V; Sigma-Aldrich, ON, Canada) in saline. Animals were anesthetized with 4.0% isoflurane for induction, and 2.0% isoflurane for maintenance (in O<sub>2</sub>) and anesthesia was monitored by toe pinch. Under anesthesia, animals were injected intravitreally through the *pars plana* with sterile saline (control) or LPS solution using a 30G needle and Hamilton syringe (Hamilton Company, Reno, NV, USA) with the assistance of a WILD M37 dissecting microscope (Leitz Canada, Kitchener, ON, Canada). Once the injection was completed, the puncture wound was glued shut with 3M Vetbond Tissue Adhesive (3M Animal Products, St. Paul, MN, USA), and animals recovered.

### **2.4 Intravital microscopy**

IVM was conducted as previously described (Toguri et al., 2014). The iridial microcirculation was imaged 6 h after induction of EIU. Animals were anesthetized with pentobarbital (i.p., 54 mg/kg). 15 min before initiating IVM, Rhodamine 6G (1.5 mL/kg; Sigma-Aldrich) was injected intravenously (i.v.) to visualize leukocytes within the vasculature, while fluorescein isothiocyanate (FITC) conjugated albumin (i.v., 1 mL/kg; Sigma-Aldrich) allowed for visualization of blood flow. The iridial microcirculation was

observed using an Olympus OV100 Small Animal Imaging System (Olympus, Tokyo, Japan), which contains an MT-20 light source, fluorescence excitation from a xenon lamp (150W) and an excitation filter for rhodamine-6G (excitation 515-560 nm, emission 590 nm). Images were captured in real-time by a black and white DP70 CCD C-mount camera and digitally recorded with HImage software (Hamamatsu, Herrsching, Germany).

For adoptive transfer experiments leukocytes were visualized by fluorescent light (495 nm excitation for calcein-AM) in the iridial microcirculation using a Leica DMLM epifluorescence microscope (Leica, Wetzlar, Germany) equipped with a mercury-arc light source (LEG EBQ 100, Carl Zeiss, Jena, German) and captured by a CCD video camera (SIT 68, DAGE MTI, Michigan, IN, USA). Videos were recorded on a computer using WinDV Capture software (Mourek, Prague, Czech Republic) and stored on an external hard drive.

During IVM animals were placed on a heating pad in a stereotactic frame, and Tear-Gel® (Novartis Pharmaceuticals Canada Inc., Dorval, QC, Canada) was applied to their cornea. The iris was divided into four equal quadrants by drawing two superficial lines, lengthwise and widthwise. IVM was carried out in each of these quadrants. Two to four videos of each quadrant were recorded for 30 s each. Videos were analyzed off-line without knowledge of the treatment groups. Adherent leukocytes were defined as the number of leukocytes that did not detach from the endothelial surface during the 30 s observation period in venules (capillaries with blood flowing away from the pupil). Using imaging software (ImageJ, National Institute of Health, Bethesda, MD, USA) the number of adherent leukocytes within each vessel segment was calculated by measuring the diameter and length of vessel segment studied, assuming a cylindrical geometry of blood vessels.

Adherent leukocytes were expressed as number of cells per mm<sup>2</sup> of endothelial surface. Rolling leukocytes were classified as cells that moved along the endothelium and crossed a predetermined cross-sectional line of the venule. The number of rolling leukocytes was counted for 30 s and used to estimate the number of rolling leukocytes per min. IVM was conducted 6 h after induction of EIU.

## **2.5 Isolation of murine bone marrow cell neutrophils**

As described previously (Kezic et al., 2011), mouse neutrophils were isolated from the bone marrow of mice. Mice were euthanized, femur and tibia were dissected and flushed with ice-cold 1x Hanks balanced salt solution (HBSS; supplemented with 10 nM HEPES, pH7.5 and 0.5 mM EDTA; Invitrogen) through a sterile filter (70 µm). The suspension was centrifuged at 300 g for 12 min at 4°C. STEMCELL™ negative selection neutrophil isolation kit (Vancouver, BC, Canada) was used to isolate neutrophils according to the manufacturer's instructions. The isolated neutrophils were then washed once and the pelleted cells were suspended in RPMI (Invitrogen) containing 1% heat-inactivated fetal bovine serum (FBS, Invitrogen) and used immediately for neutrophil migration experiments. The murine neutrophil isolation protocol routinely yields cell suspensions that are >95% pure and viable as determined by cresyl violet and trypan blue exclusion, respectively.

## **2.6 Neutrophil migration assay**

Neutrophil migration assays were performed using a Boyden chamber, as previously described (Sun et al., 2013; Tole et al., 2009). Isolated neutrophils ( $1 \times 10^5$

cells/ 100  $\mu$ L) from WT or CB2R<sup>-/-</sup> mice were incubated with vehicle alone (0.01% DMSO), or various concentrations of RO8671304 or RO6851228 at 37 °C, 5% CO<sub>2</sub> for 30 min. Cells were then loaded into the upper chamber of a 3  $\mu$ m Transwell insert (Corning Life Sciences, Corning, NY, USA) coated with protein (5% FBS in RPMI) in a 24-well plate. This Transwell system is separated from the bottom chamber containing RPMI (1% FBS) alone or 10<sup>-8</sup> M chemokine (C-X-C motif) ligand 2 (CXCL2)/ monocyte inflammatory protein-2 (MIP-2) (Peprotech, Rocky Hill, NJ, USA). Migration took place over 1 h at 37 °C, 5% CO<sub>2</sub>. To determine the number of neutrophils which had migrated from the top to the bottom chamber, the filter was removed and neutrophils in the lower chamber gently pipetted up and down to evenly distribute and sink to the bottom of the plate. An Olympus inverted bright-field microscope with an Infinity 3 camera (Lumenera, Ottawa, ON, Canada) was used to photograph 12 random fields (10X magnification) of each well. The number of migrated neutrophils was then determined using ImageJ. The data represents the mean value of cells per field  $\pm$  standard deviation (SD) from at least three independent experiments for each treatment condition performed in triplicate.

## **2.7 Neutrophil-depletion and adoptive transfer**

Neutrophils were depleted *in vivo* using mAb Gr-1 (RB6-8C5, BioXcell, West Lebanon, NH, USA) administered 24 h prior to induction of EIU, as previously described (Sieve et al., 2009). Mice were injected with a single dose of 50  $\mu$ g in 100  $\mu$ L Gr-1 (i.p.) or isotype control antibody (IgG2b; BioXcell). Treatment with this dose of antibody induced severe neutropenia for up to 48 h (>99% depletion of neutrophils by flow cytometry of Ly6G<sup>+</sup> expression of peripheral blood). EIU was induced 24 h after Gr-1

treatment. Directly after induction of EIU mice were treated with topical vehicle (Tocrisolve) or RO6871304 (1.5% w/v). Leukocytes were isolated from mouse bone marrow, as described above, using 1X RBC lysis buffer (Sigma-Aldrich) according to the manufacturer's instructions. Leukocytes were stained with 1  $\mu$ M Calcein-AM (Life Technologies, Gaithersburg, MD, USA) at 37 °C, 5% CO<sub>2</sub> for 30 min, washed and resuspended in PBS for injection. One hour before IVM (5 h after induction of EIU), animals were anesthetized and adoptively transferred i.v. with  $1.5 \times 10^7$  calcein-AM pre-loaded leukocytes in 100  $\mu$ L. FITC (i.v., 1 mL/kg) was injected 10 min before IVM.

## **2.8 Peripheral blood leukocyte isolation**

To characterize the efficiency of neutrophil depletion using Gr-1 depletion antibody, blood was obtained 24 h following injection of anti-Gr-1 depletion antibody. Submandibular venipuncture was performed to collect 70  $\mu$ L of blood in 10  $\mu$ L of heparin (10,000 U/mL; Sigma-Aldrich). RBC lysis was performed by adding 2 mL of lysis buffer for 1 min and neutralized by adding an equal volume of PBS. Samples were centrifuged for 5 min at 300g, supernatant was discarded and the blood leukocytes were resuspended in 200  $\mu$ L of PBS. The frequency of Gr1<sup>+</sup> CD11b<sup>+</sup> cells was determined using flow cytometry.

## **2.9 Antibodies and flow cytometry**

The following antibodies were obtained from eBioscience (San Diego, CA): FITC-conjugated rat IgG2b (clone A95-1), FITC-anti-CD11b (clone M1/70); phycoerythrin (PE)-conjugated rat IgG2b (clone A95-1), PE-anti-Gr1 (clone RB6-8C5). Prior to staining,

all cell samples were pre-incubated with anti-CD16/32 to block non-specific binding. Flow cytometry was performed using a two laser FACSCalibur with BD CellQuest Pro software (BD Biosciences, Mississauga, ON, Canada) and data analysis was performed using FlowJo (V10.2; FlowJo, LLC; Ashland, OR).

## 2.10 Pharmacological treatments

CB<sub>2</sub>R agonists, RO6871304, RO6871085 and the CB<sub>2</sub>R inverse agonist, RO6851228, were provided by Hoffman-la Roche Ltd. (Basel, Switzerland), and were dissolved in Tocrisolve™ 100 (Tocris Bioscience, Ellisville, MO, USA), which is a 1:4 ratio of soya oil/water, that is emulsified with the block co-polymer Pluronic F68. In mice with EIU, RO6871304, RO6871085 or RO6851228 was applied topically on the eye either directly after, hourly after, or 3 h after injection of LPS at the dose of 1.5% (w/v) (5 µL/animal). See Figures 8-11 for an experimental timeline. Control animals received (5 µL) vehicle (Tocrisolve) or positive controls received 0.1% (w/v) dexamethasone (Sigma-Aldrich) in Tocrisolve (5 µL/animal). The CB<sub>2</sub>R agonist, HU308 (4-[4-(1,1-dimethylheptyl)-2,6-dimethoxyphenyl]-6,6-dimethylbicyclo[3.1.1]hept-2-ene-2-methanol) (Hanus et al., 1999) was purchased from Tocris Bioscience (Bristol, UK), and were dissolved in dimethyl sulfoxide (DMSO) (Sigma-Aldrich) and sterile saline (3:7) for i.v. administration. HU308 was administered i.v. at a dose of 0.1-10 mg/kg (100 µL/animal) 15 min after intravitreal injection of LPS. Control animals received i.v. 100 µL DMSO and saline (3:7).

## 2.11 Statistical analysis

Individual animals in each treatment group were coded and experiments were analyzed blinded. All data are expressed as mean  $\pm$  SD, and results were analyzed using Prism 5 software (GraphPad Software, La Jolla, CA, USA). The Kolmogorov-Smirnov test was used to confirm normal distribution of the data. A two-tailed unpaired t-test was used to compare two groups of data. Significance was set at  $p < 0.05$ . One-way analysis of variance (ANOVA) with a Dunnett's *post hoc* test was used to compare all experimental groups to the WT + LPS + vehicle-treated group or WT + CXCL2 + vehicle. Significance was set at  $p < 0.05$ .

**Figure 8:** Experimental timeline for EIU studies in mice. Animals were treated topically directly after LPS with either CB<sub>2</sub>R agonist, inverse agonist, DEX, or vehicle.

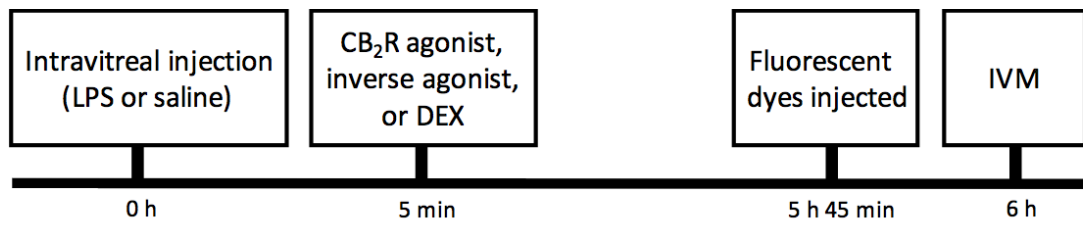


**Figure 9:** Experimental timeline for animals treated 3 h post-LPS with CB<sub>2</sub>R agonist to examine the therapeutic time window.

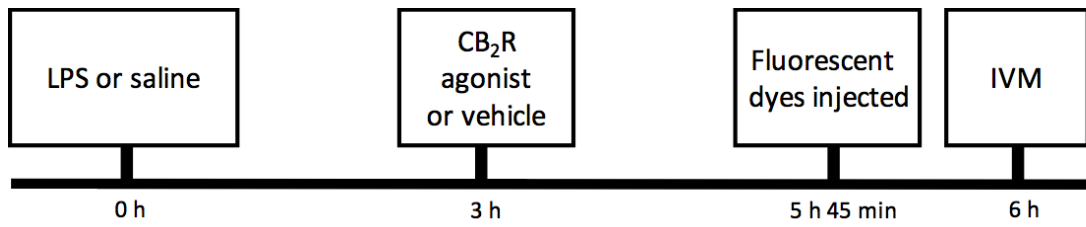
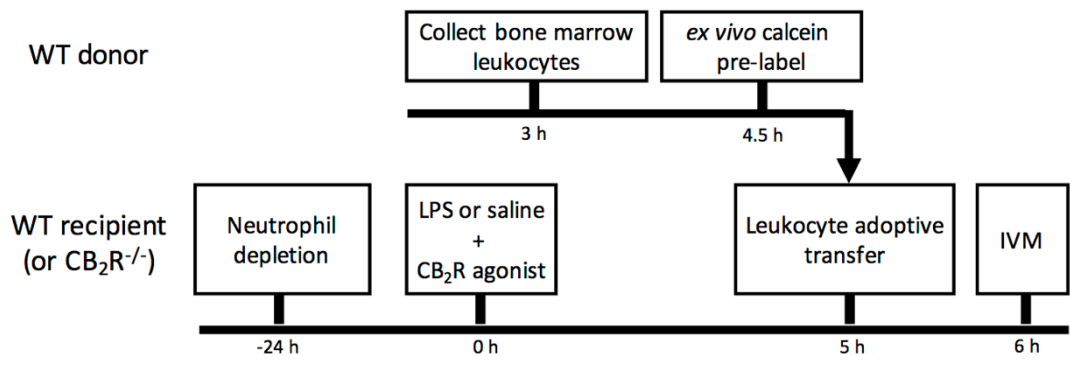


**Figure 10:** Experimental timeline for EIU adoptive transfer studies in mice. Animals were depleted of neutrophils by Gr-1 treatment and subsequently induced with EIU + treatment with topical CB<sub>2</sub>R agonist. Pre-labeled leukocytes were adoptively transferred 5 h later and IVM conducted at 6 h.



## Chapter III: Results

### 3.1 Intravital microscopy

#### 3.1.1 *CB<sub>2</sub>R* activation decreases leukocyte-endothelial interactions in the iridial microcirculation

IVM was carried out to screen the anti-inflammatory properties of a new series of selective CB<sub>2</sub>R agonists (RO6871304 and RO6871085) in mice with EIU. HU910 and HU308 are well established selective CB<sub>2</sub>R agonists, which are based on the phytocannabinoid chemical structure backbone, and were tested for comparison. The bar graph in Figure 11 shows that intravitreal injection of LPS in WT animals + topical vehicle (Tocrisolve) produced a significant increase (29 fold increase) in the number of adherent leukocytes to the endothelium ( $540 \pm 164$  cells/mm<sup>2</sup>) in the iridial microcirculation at 6 h compared to animals receiving intravitreal saline injection + vehicle (control;  $17 \pm 2$  cells/mm<sup>2</sup>;  $p < 0.05$ ). There was no significant difference in the number of rolling leukocytes for all treatment groups (Table 3,  $p > 0.05$ ). Topical treatment with 1.5% w/v HU910 ( $133 \pm 29$  cells/mm<sup>2</sup>), RO6871304 ( $126 \pm 60$  cells/mm<sup>2</sup>), or RO6871085 ( $230 \pm 94$  cells/mm<sup>2</sup>) significantly attenuated LPS-induced leukocyte-endothelial interactions at 6 h compared to vehicle treated eyes ( $p < 0.05$ ). The dose used was selected based on a previous study using a synthetic selective CB<sub>2</sub>R agonist, HU308, in a rat model of EIU, that was shown to be anti-inflammatory (Toguri et al., 2014).

Figure 12 shows a log dose response with HU910 (0.03, 0.3, and 3.0 mg/kg) administered i.v. directly after intravitreal LPS injection. Treatment with 3.0 mg/kg HU910 ( $244 \pm 176$  cells/mm<sup>2</sup>) significantly reduced leukocyte adhesion in the iridial microcirculation at 6 h after LPS compared to LPS + vehicle (micelles;  $690 \pm 424$

**Figure 11:** A screen of novel selective CB<sub>2</sub>R agonists to determine the most efficacious ligand in reducing leukocyte-adhesion in the iridial microcirculation during EIU in BALB/c mice. Bar graph represents the mean number of adherent leukocytes 6 h after intravitreal injection of: saline (control) + topical vehicle (n=4), LPS (250 ng) + topical vehicle (n=10), LPS + topical HU910 (1.5% w/v; n=6), LPS + topical RO6871304 (1.5% w/v; n=6), or LPS + topical RO6871085 (1.5% w/v; n=6). Data presented as mean ± SD. One-way ANOVA with Dunnett; \* p < 0.05 compared to LPS + vehicle.

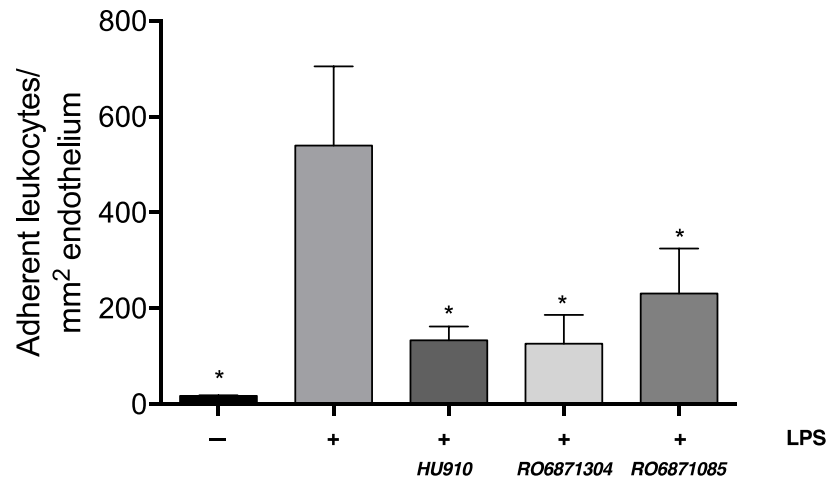
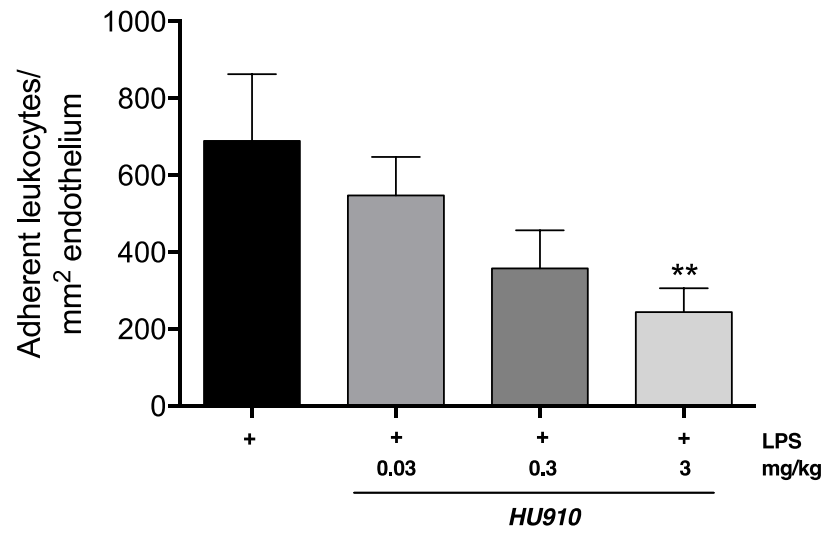


**Table 3:** Leukocyte-endothelial rolling in the iridial microcirculation 6 h after intravitreal injection of LPS and treatment with a CB<sub>2</sub>R agonist (RO6871304) or inverse agonist (RO6851228). Table shows the mean number of rolling leukocytes per min after intravitreal injection of: saline + vehicle (topical; Tocrisolve; n=6), LPS + vehicle (n=6), LPS + RO6871304 (1.5% w/v; n=6), or LPS + RO6851228 (1.5% w/v; n=6). Data presented as mean ± SD. No significant difference between groups were found (One-way ANOVA with Dunnet; p > 0.05).

	Saline	LPS	LPS + RO6871304	LPS + RO6851228
Rolling leukocytes per min	$0.15 \pm 0.27$	$0.38 \pm 0.59$	$0.05 \pm 0.07$	$0.45 \pm 0.47$

**Figure 12:** Dose response for the CB<sub>2</sub>R agonist, HU910. Bar graph represents the mean number of adherent leukocytes 6 h after intravitreal injection of: LPS (250 ng) + vehicle (i.v.; micelles; n=6) or LPS + HU910 (i.v.; 0.03 – 3.0 mg/kg; n=6). Data presented as mean ± SD. One-way ANOVA with Dunnett; \*\* p < 0.01 compared to LPS + vehicle.



cells/mm<sup>2</sup>;  $p < 0.01$ ). Similarly, Figure 13 shows a log dose response with HU308 (0.1, 1.0, and 10.0 mg/kg) administered i.v. directly after induction of EIU. Intravenous treatment with 1.0 and 10.0 mg/kg HU308 ( $309 \pm 90$  cells/mm<sup>2</sup> and  $225 \pm 75$  cells/mm<sup>2</sup>, respectively) significantly reduced (0.5 and 0.6 fold reduction, respectively) leukocyte adhesion 6 h after induction of EIU compared to LPS + vehicle (3:7, DMSO:saline;  $574 \pm 176$  cells/mm<sup>2</sup>;  $p < 0.01$ ).

Of the CB<sub>2</sub>R agonists tested, RO6871304 (topical; 1.5% w/v) was the most efficacious CB<sub>2</sub>R agonist at reducing leukocyte-endothelial adhesion in the iridial microcirculation at 6 h following induction of EIU. RO6871304 also had the highest selectivity for the CB<sub>2</sub>R over the CB<sub>1</sub>R (Table 2). Therefore, this compound was used for the remainder of the studies examining the CB<sub>2</sub>R therapeutic time window, CB<sub>2</sub>R effects on neutrophil migration and whether selective CB<sub>2</sub>R agonists act on resident ocular immune cells.

### *3.1.2 Comparison of CB<sub>2</sub>R agonist to a clinically used anti-inflammatory drug to treat uveitis*

Leukocyte-endothelial interactions in the iridial microcirculation were also examined after treatment with dexamethasone, a commonly used ocular anti-inflammatory drug which served as a positive control. Mice with EIU treated once immediately after LPS with dexamethasone (0.1% w/v, topically;  $481 \pm 97$  cells/mm<sup>2</sup>) did not have a significant difference in the number of adherent leukocytes in the iridial microcirculation at 6 h (Figure 14;  $p > 0.05$ ) compared with vehicle ( $540 \pm 164$  cells/mm<sup>2</sup>). This is in contrast to treatment

**Figure 13:** Dose response for the CB<sub>2</sub>R agonist, HU308. The bar graph represents the mean number of adherent leukocytes 6 h after intravitreal injection of: LPS (250 ng) + vehicle (i.v.; 3:7, DMSO:saline; n=6) or LPS + HU308 (i.v.; 0.1 – 10.0 mg/kg; n=5-8). Data presented as mean ± SD. One-way ANOVA with Dunnett; \*\* p < 0.01 compared to LPS + vehicle.

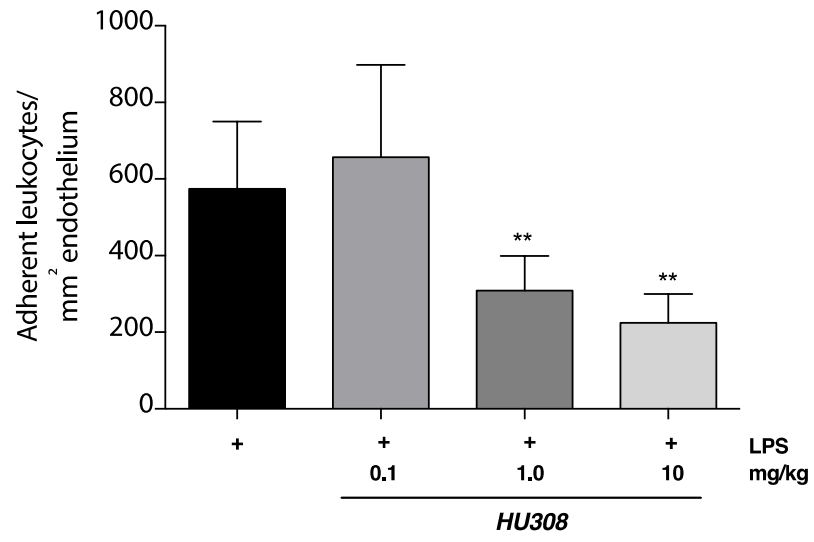
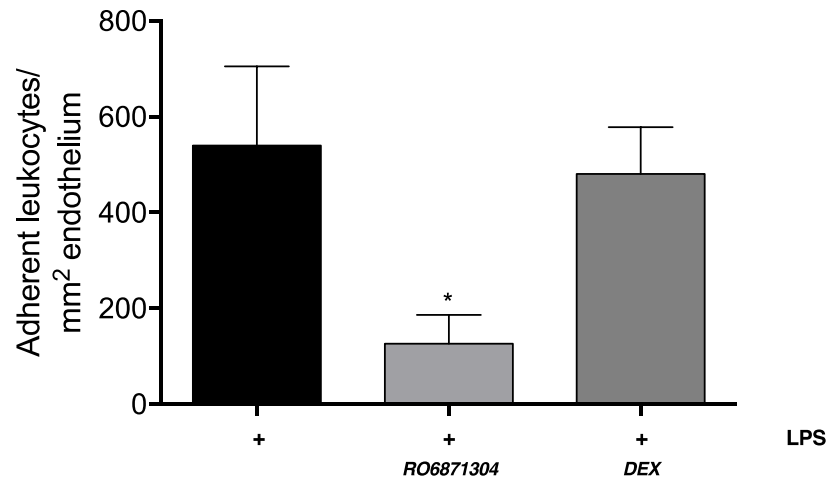


**Figure 14:** A comparison of the effects of the CB<sub>2</sub>R agonist, RO6871304, compared to the clinically-used steroid, dexamethasone, on leukocyte adherence in the iridial microcirculation in mice with EIU. Bar graph represents the mean number of adherent leukocytes 6 h after intravitreal injection of: LPS (250 ng) + topical vehicle (n=10), LPS + topical RO6871304 (1.5% w/v; n=5), or LPS + topical dexamethasone (0.1% w/v; n=8). Data presented as mean ± SD. One-way ANOVA with Dunnett; \* p < 0.05 compared to LPS + vehicle.



with RO6871304 which produced a significant reduction in iridial leukocyte adherence (1.5% w/v;  $126 \pm 29$  cells/mm<sup>2</sup>;  $p < 0.05$ ).

### *3.1.3 Determining the therapeutic time window for treatment with the CB<sub>2</sub>R agonist to modulate leukocyte adhesion during EIU*

The bar graph in Figure 15 shows that there was no decrease in LPS-induced leukocyte-endothelial interactions (adhesion) at 6 h when RO6871304 was applied topically at 3 h post-EIU ( $634 \pm 185$  cells/mm<sup>2</sup>) compared to vehicle ( $560 \pm 125$  cells/mm<sup>2</sup>;  $p > 0.05$ ) suggesting that CB<sub>2</sub>R activation is required early during EIU or that a multiple dosing regimen may be required for efficacy when topical drug therapy is delayed.

### *3.1.4 The effects of CB<sub>2</sub>R genetic deletion (CB<sub>2</sub>R<sup>-/-</sup>) or decrease in constitutive CB<sub>2</sub>R activity on leukocyte-endothelial interactions in the iridial microcirculation during EIU*

To further examine the involvement of CB<sub>2</sub>R in the EIU pathologies and to validate CB<sub>2</sub>R as the target for these new selective CB<sub>2</sub>R agonists *in vivo*, CB<sub>2</sub>R<sup>-/-</sup> mice were used for experiments. The bar graph in Figure 16 shows that LPS-induced inflammation in CB<sub>2</sub>R<sup>-/-</sup> mice + vehicle ( $762 \pm 173$  cells/mm<sup>2</sup>) was significantly increased relative to WT + LPS-injected + vehicle animals ( $540 \pm 164$  cells/mm<sup>2</sup>;  $p < 0.05$ ). There was no significant difference in leukocyte adherence in CB<sub>2</sub>R<sup>-/-</sup> mice treated with RO6871304 (1.5% w/v;  $694 \pm 216$  cells/mm<sup>2</sup>) compared to vehicle ( $762 \pm 173$  cells/mm<sup>2</sup>;  $p > 0.05$ ). Consistent with this, the bar graph in Figure 17 shows that treatment of WT mice with the novel selective CB<sub>2</sub>R inverse agonist RO6851228 (1.5% w/v;  $819 \pm 79$  cells/mm<sup>2</sup>)

**Figure 15:** Determining the therapeutic time window for CB<sub>2</sub>R agonist treatment to reduce leukocyte-adhesion in the iridial microcirculation during EIU in mice. A single dose of RO6871304 was applied topically at 3 h post EIU. Bar graph represents the mean number of adherent leukocytes 6 h after intravitreal injection of: LPS (250 ng) + topical vehicle (n=6) or LPS + topical RO6871304 (1.5% w/v; n=8). Two tailed unpaired t-test;  $p > 0.05$  compared to LPS + vehicle.

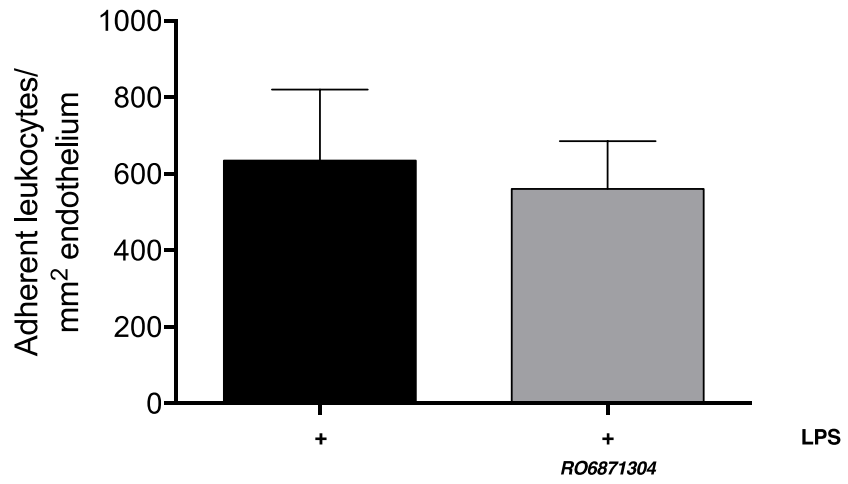


**Figure 16:** RO6871304 exerts its anti-inflammatory effects through CB<sub>2</sub>R. CB<sub>2</sub>R<sup>-/-</sup> mice with EIU exhibit increased iridial leukocyte-adhesion compared to WT. Bar graph represents the mean number of adherent leukocytes in WT or CB<sub>2</sub>R<sup>-/-</sup> mice 6 h following intravitreal injection of LPS and topical treatment with either vehicle (n=7) or RO6871304 (1.5%; w/v; n=6). One-way ANOVA with Dunnett; \* p < 0.05 compared to LPS + vehicle in WT mice.

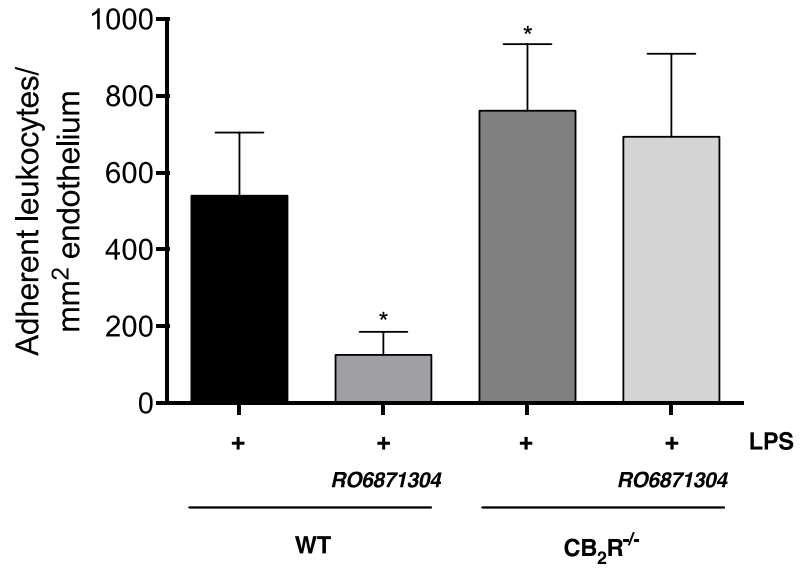
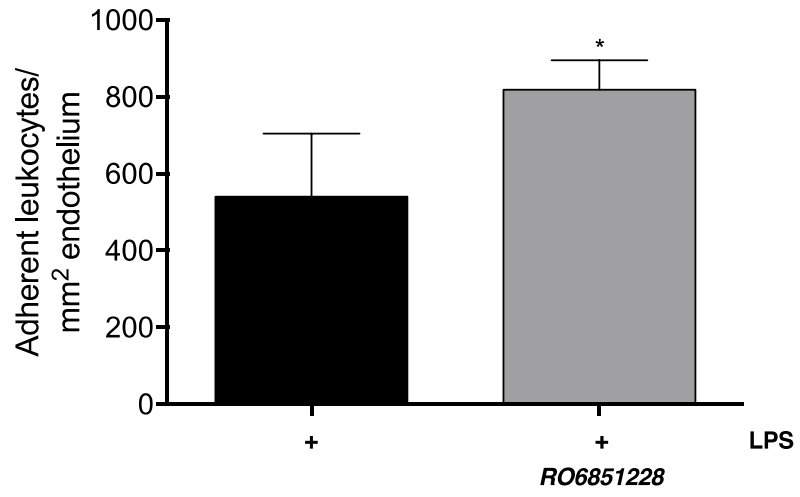


**Figure 17:** The CB<sub>2</sub>R inverse agonist, RO6851228 increases leukocyte adhesion in the iridial microcirculation during EIU. Bar graph represents the mean number of adherent leukocytes at 6 h post-intravitreal injection of LPS and following topical treatment with either vehicle (n=10) or RO6871228 (1.5%; n=6). Two tailed unpaired t-test; \* p < 0.05 compared to LPS + vehicle.



increased leukocyte-adhesion at 6 h post-intravitreal injection of LPS compared to treatment with vehicle ( $540 \pm 164$  cells/mm<sup>2</sup>;  $p < 0.05$ ).

## 3.2 Neutrophil migration

### 3.2.1 *CB<sub>2</sub>R* activation decreases neutrophil migration in-vitro

To determine whether the *CB<sub>2</sub>R* agonist, RO6871304, modulates neutrophil migration towards a chemoattractant signal, a Boyden chamber Transwell Migration (Corning) assay was performed with CXCL2 placed in the lower chamber. CXCL2 is a potent neutrophil chemoattractant. As expected, basal migration of mouse neutrophils was minimal ( $4 \pm 3$  cells/field; Figure 18A and D), but increased in the presence of CXCL2 ( $10^{-8}$   $\mu$ M) chemotactic gradient ( $95 \pm 15$  cells/field; Figure 18B and D;  $p < 0.001$ ). RO6871304 inhibited neutrophil migration towards CXCL2 in a dose-dependent fashion (compare Figure 18B and C; Figure 8D) compared to vehicle ( $p < 0.01$ ). RO6871304 (0.01 – 1.0  $\mu$ M) produced a 0.3 to 0.5 fold decrease in the number of neutrophils migrating towards CXCL2 (Figure 8D; CXCL2 + vehicle;  $95 \pm 15$  cells/field; CXCL2 + 0.01  $\mu$ M RO6871304;  $69 \pm 17$  cells/field; CXCL2 + 0.1  $\mu$ M RO6871304;  $50 \pm 5$  cells/field; CXCL2 + 1.0  $\mu$ M RO6871304;  $58 \pm 3$  cells/field). The  $IC_{50}$  for RO6871304 inhibition of neutrophil migration was 6.6 nM (Figure 19). There was no difference in the number of *CB<sub>2</sub>R*<sup>-/-</sup> neutrophils that migrated toward CXCL2 compared to WT cells (Figure 18;  $p > 0.05$ ). However, the effect of RO6871304 on migration was lost in *CB<sub>2</sub>R*<sup>-/-</sup> neutrophils (Figure 18D; no chemoattractant + vehicle;  $3 \pm 0$  cells/field; CXCL2 + vehicle;  $91 \pm 25$  cells/field; CXCL2 + 0.01  $\mu$ M RO6871304;  $101 \pm 31$  cells/field; CXCL2 + 0.1  $\mu$ M RO6871304;  $90 \pm 25$  cells/field; CXCL2 + 1.0  $\mu$ M RO6871304;  $110 \pm 26$  cells/field;  $p > 0.05$ ). Together, this

data demonstrates that RO6871304 inhibits CXCL2-induced chemotaxis of primary mouse neutrophils in a dose-dependent fashion and is dependent on the presence of CB<sub>2</sub>R.

### *3.2.2 Loss of constitutively activity of CB<sub>2</sub>R activation does not affect neutrophil migration in-vitro*

Next, neutrophils were treated with the CB<sub>2</sub>R inverse agonist, RO6851228, to determine the effect of the CB<sub>2</sub>R inverse agonist on migration. Treatment of neutrophils with RO6851228 (0.01 – 1.0 μM) did not affect CXCL2-induced neutrophil migration compared to vehicle (Figure 18E; no chemoattractant + vehicle; 4 ± 3 cells/field; CXCL2 + vehicle; 98 ± 15 cells/field; CXCL2 + 0.01 μM RO6871304; 102 ± 6 cells/field; CXCL2 + 0.1 μM RO6871304; 109 ± 5 cells/field; CXCL2 + 1.0 μM RO6871304; 108 ± 14 cells/field; p > 0.05) suggesting that neutrophil migration is already at its maximal in this system or that there is no increased constitutive CB<sub>2</sub>R activity in this system.

### *3.2.3 RO6871304 and RO6851228 do not affect cell viability*

Using the trypan blue exclusion method, the estimated percentage viability of neutrophils incubated for 30 min in vehicle or 1.0 μM RO6871304 and RO6851228 was 97 ± 0.38% and 96 ± 0.6%, respectively. These values were not significantly different from one another (data not shown; p > 0.05; n=3) and indicate that these CB<sub>2</sub>R ligands have no effect on neutrophil viability.

**Figure 18:** CB<sub>2</sub>R activation reduces neutrophil migration towards chemoattractant. (A-C), representative images (20X magnification) of neutrophils from WT mice that migrated in a Boyden chamber setup: (A) RPMI + vehicle, (B) CXCL2 + vehicle, (C) CXCL2 + RO6871304 (1 μM). (D) Bar graph represents the mean number of neutrophils from WT or CB<sub>2</sub>R<sup>-/-</sup> mice pre-treated with various concentrations of the CB<sub>2</sub>R agonist, RO6871304, that migrated to the lower chamber of a Boyden Chamber setup when using CXCL2 (10<sup>-8</sup>M) as a chemoattractant. Neutrophils were counted from 12 random microscopic fields of view per well. (E) Bar graph represents the mean number of neutrophils from WT mice pre-treated with various concentrations of the CB<sub>2</sub>R inverse agonist, RO6851228, that migrated in the Boyden chamber setup. Data is presented as the mean neutrophil migration per microscopic field of view ± SD from at least 3 independent experiments conducted in triplicate each. One-way ANOVA with Dunnett; \*\* p < 0.01 compared to WT neutrophils + CXCL2 + vehicle.

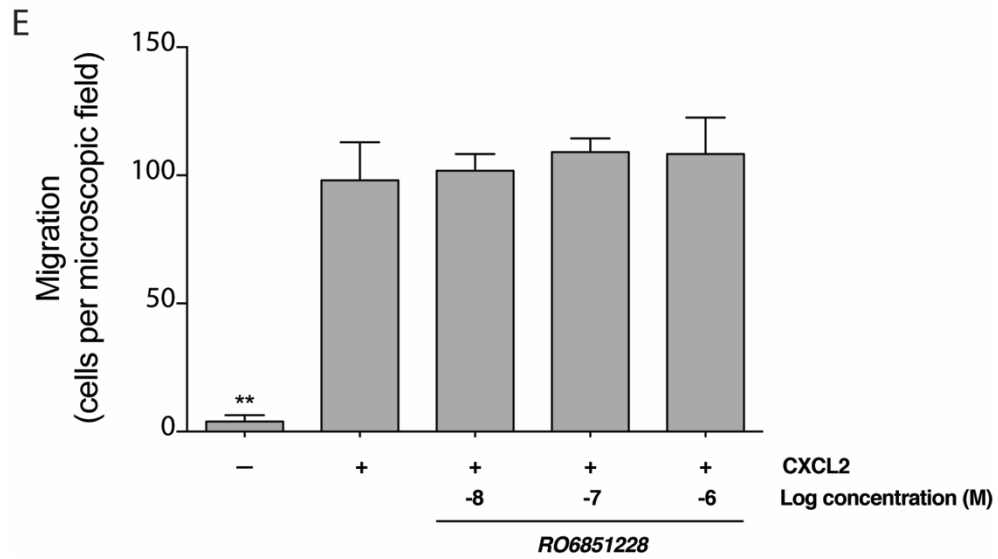
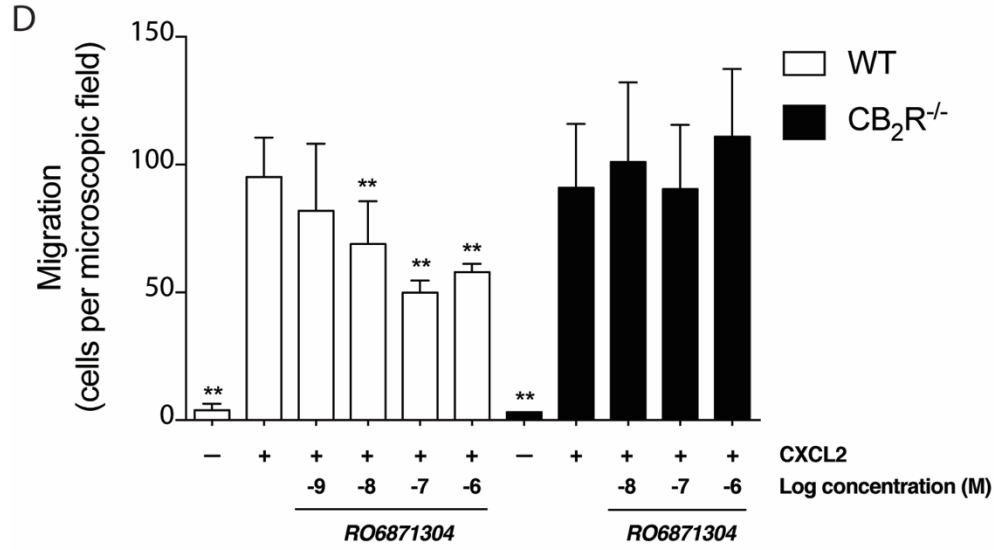
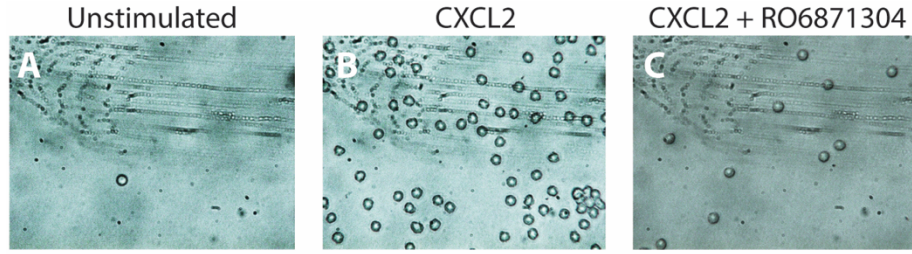
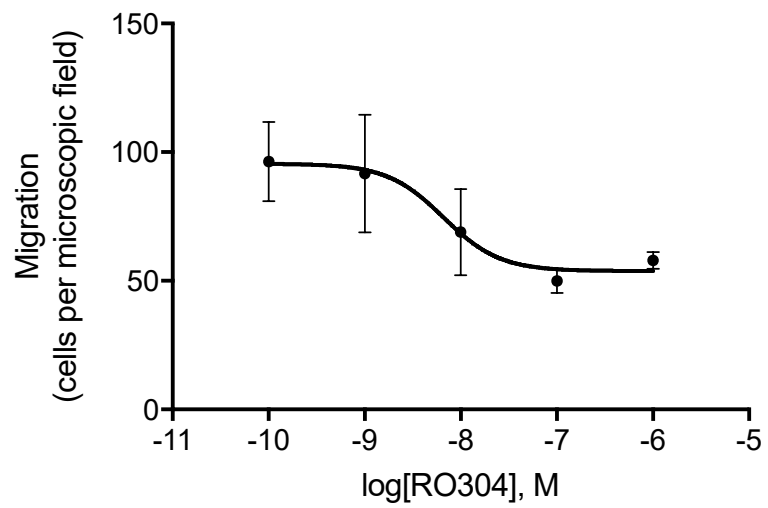


**Figure 19:** Pre-treatment with RO6871304 versus level of neutrophil migration towards CXCL2 chemoattractant to determine the IC<sub>50</sub>. Data was fitted using GraphPad nonlinear regression equation, log(inhibitor) versus response - variable slope (four parameters). Data is presented as the mean neutrophil migration per microscopic field of view  $\pm$  SD from at least 3 independent experiments conducted in triplicate each.



### 3.3 Adoptive transfer

#### 3.2.1 *CB<sub>2</sub>R* activation on resident ocular immune cells mediates *CB<sub>2</sub>R* leukocyte-adherence effects

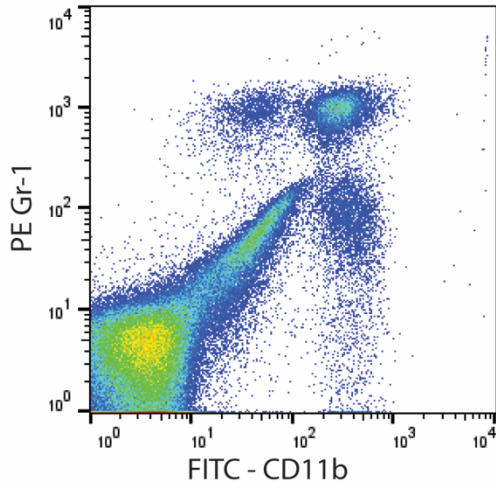
To determine the contribution of resident ocular immune cells to the *CB<sub>2</sub>R*-mediated decrease in leukocyte adhesion in the iridial microcirculation seen after *CB<sub>2</sub>R* agonist treatment (RO6871304 and RO6871085), donor bone-marrow leukocytes from naïve mice were adoptively transferred at 5 h post-EIU. Treatment with Gr-1 antibody (50 µg in PBS; i.p.) ablated circulating neutrophils in the peripheral blood of host mice after 24 h compared to isotype control (Figure 20), as determined by FACS analysis of peripheral blood for Ly6G<sup>+</sup>. As expected, neutrophil depletion in EIU mice without adoptive transfer showed absence of LPS-induced leukocyte (autologous) adherence response in the iridial microcirculation compared to isotype controls (Figure 21;  $p < 0.01$ ), suggesting that neutrophils are the primary cells adhering to the iridial endothelium. The bar graph in Figure 22 shows that i.p. administration of 50 µg Gr-1 in WT + LPS animals significantly decreased leukocyte-endothelial adhesion ( $22 \pm 21$  cells/mm<sup>2</sup>) compared to isotype controls ( $985 \pm 347$  cells/mm<sup>2</sup>;  $p < 0.01$ ).

Figure 22 A and B show representative images of the iris microcirculation after adoptive transfer of naïve bone-marrow derived leukocytes at 5 h post-EIU or saline control neutrophil-depleted mice. IVM was performed at 6 h. The bar graph in Figure 22C shows that at 6 h post-EIU in neutrophil depleted mice there was a significant increase (28 fold) in the number of adoptively transferred leukocytes adherent to the iridial microcirculation ( $174 \pm 23$  cells/mm<sup>2</sup>) compared to animals receiving intravitreal saline control ( $6 \pm 7$  cells/mm<sup>2</sup>;  $p < 0.0001$ ). Topical treatment with the *CB<sub>2</sub>R* agonist, RO6871304 (Figure

22C; 1.5% w/v) in neutrophil-depleted mice with EIU significantly decreased (64 fold) the LPS-induced leukocyte adhesion of adoptively-transferred leukocytes ( $63 \pm 22$  cells/mm<sup>2</sup>) compared to vehicle ( $174 \pm 23$  cells/mm<sup>2</sup>;  $p < 0.0001$ ). There was no difference in the number of WT adoptively transferred leukocytes adherent to the iridial endothelium in neutrophil-depleted WT mice with EIU compared to neutrophil-depleted CB<sub>2</sub>R<sup>-/-</sup> mice with EIU ( $p > 0.05$ ). Figure 22D shows that the effect of RO6871304 (1.5% w/v;  $161 \pm 58$  cells/mm<sup>2</sup>) was lost in CB<sub>2</sub>R<sup>-/-</sup> mice compared to vehicle ( $158 \pm 65$  cells/mm<sup>2</sup>;  $p > 0.05$ ), consistent with a selective CB<sub>2</sub>R action of this ligand.

**Figure 20:** Gr-1 antibody depletes neutrophils in the peripheral blood after 24 h. Flow cytometry analysis of peripheral blood for Gr-1<sup>+</sup> cells from mice following *in vivo* administration of neutrophil depleting Gr-1 antibody. WT mice injected with isotype control or 50 µl Gr-1 i.p. 24 h before FACS analysis and generation of EIU. Representative example. n=2. This data was generated by Simon Gebremeskel from Dr. Brent Johnston's Lab (Dalhousie University).

**Isotype control**



**Gr-1 depletion**

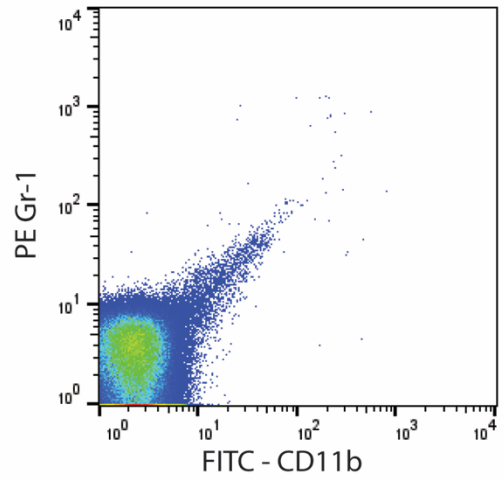


**Figure 21:** Neutrophil depletion abolishes leukocyte adhesion to iridial microvasculature at 6 h post-EIU induction. Bar graph represents mean number of adherent leukocytes in the iris microcirculation of isotype control and Gr-1 antibody treated mice at 6 h post-LPS injection. Rhodamine 6G was used to fluorescently label autologous leukocytes 15 min prior to IVM analysis. n=6-8, Two tailed unpaired t-test; \*\* p < 0.01 compared to LPS + isotype control.

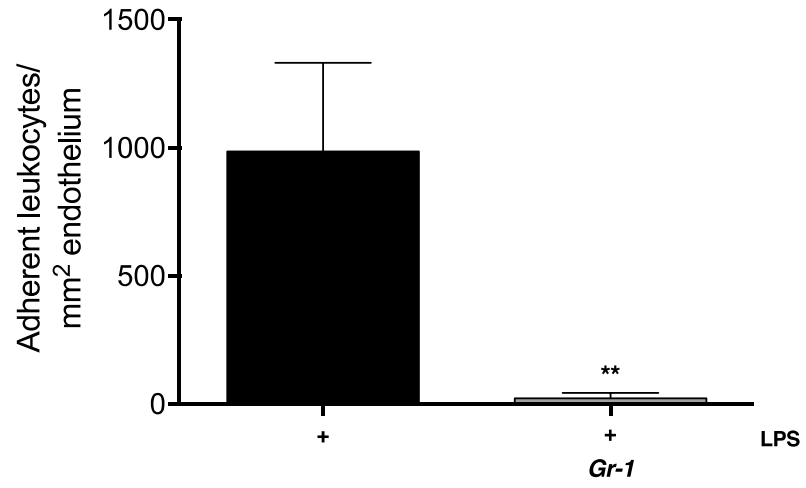
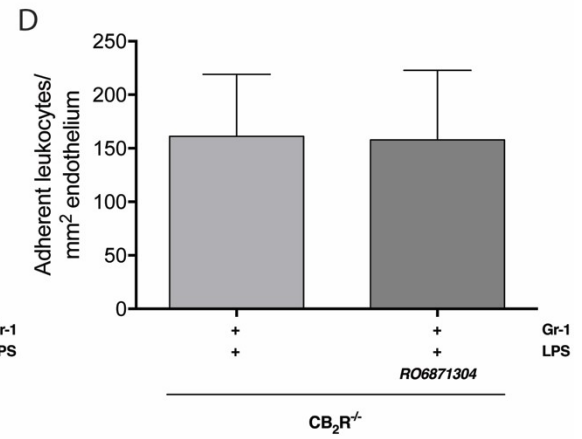
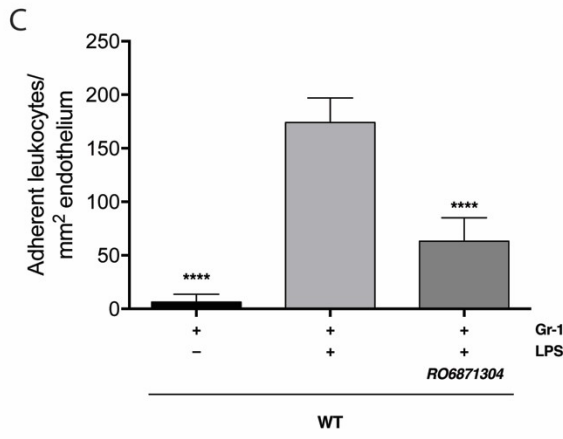
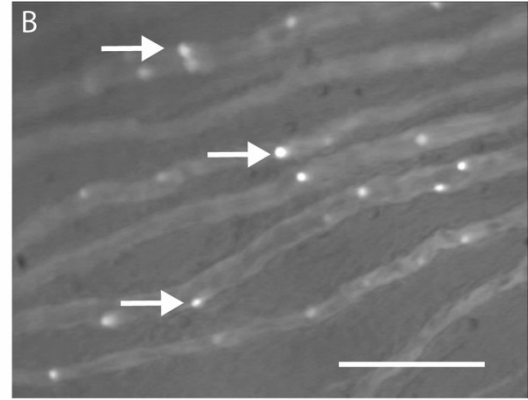
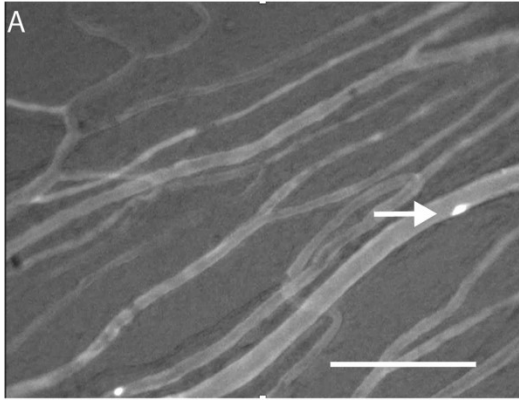


**Figure 22:** CB<sub>2</sub>R activation in neutrophil-depleted EIU mice with accompanying leukocyte adoptive transfer reduces leukocyte-adhesion in the iridial microcirculation. Representative IVM images of the iridial microcirculation of neutrophil-depleted mice showing the number of adoptively transferred adherent leukocytes (calcein-AM pre-labeled) 6 h after intravitreal saline (A) or LPS (B). Arrows indicate adherent leukocytes. Scale bar = 100 μm. (C) bar graph represents the mean number of adoptively transferred WT leukocytes adherent to the iris microcirculation 6 h after EIU induction with LPS injection or saline control in neutrophil-depleted WT mice treated topically with vehicle (Tocrisolve) or RO6871304 (1.5% w/v). n=6-8; one-way ANOVA with Dunnett; \*\*\*\* p < 0.0001 compared to LPS + vehicle. (D) bar graph represents the mean number of adoptively transferred WT leukocytes adherent to the iris microcirculation 6 h after EIU in neutrophil-depleted CB<sub>2</sub>R<sup>-/-</sup> mice treated topically with vehicle or RO6871304. n=6-8; two tailed unpaired t-test; \*\*\*\* p > 0.05 compared to LPS + vehicle.



## Chapter IV: Discussion

My study used novel cannabinoids that are highly selective for the CB<sub>2</sub>R over CB<sub>1</sub>R. These ligands were chosen for further investigation because prior studies indicated decreased lipophilicity compared to other published cannabinoids, good solubility, passive membrane permeability, and enhanced lower microsomal clearance, as well as good oral bioavailability and half-life (Porter et al., in preparation; and unpublished observations from Roche Pharmaceuticals). My results demonstrate that selective CB<sub>2</sub>R ligands attenuate leukocyte adhesion to the iridial microvasculature in EIU, decrease neutrophil migration *in vitro* and also mediate part of their actions via resident ocular immune cells. In my thesis, I used an experimental model of a pan-uveitis-like pathology generated via injection of LPS into the posterior chamber of the eye to investigate CB<sub>2</sub>R selective ligands. In this model, I observed increased leukocyte-endothelial interactions at 6 h correlated with inflammation. These findings are consistent with a previously published study which used a similar EIU model (intravitreal injection of LPS at 250 ng / $\mu$ L) and showed gradual development of EIU like pathology, including acute innate immune system response, breakdown of the BRB, neutrophil and macrophage recruitment, microglia activation, vision loss, pain and production of proinflammatory cytokines and chemokines, in both the anterior and posterior chambers of the eye (Becker et al., 2000; Planck et al., 2008; Toguri et al., 2014).

### *4.1.1 Effect of CB<sub>2</sub>R activation on leukocyte-endothelial interactions*

Pan-uveitis affects tissues in the anterior chamber of the eye, including the iris (Becker et al., 2000). Therefore, we took advantage of IVM which allowed us to non-

invasively observe and quantify the behavior of leukocytes in the iridial microvasculature in live animals with EIU in order to screen CB<sub>2</sub>R agonists. Our goal was to identify ligands that were potent and selective for CB<sub>2</sub>R and devoid of potential off-target effects. Off-target activity could arise due to actions at other receptors, including CB<sub>1</sub>R as well as other non-cannabinoid receptors, or activity at enzymes involved in endocannabinoid regulation or direct effects on ion channels (Soethoudt et al., 2017).

In-line with the competitive ligand binding assays carried out by colleagues at Roche that demonstrated that the ligands, RO6871304, RO6871085, HU910, are highly selective for CB<sub>2</sub>R over CB<sub>1</sub>R (Table 2), results from my thesis study indicated that the novel cannabinoids, RO6871304, RO6871085, HU910, are selective agonists at CB<sub>2</sub>R; all ligands displayed anti-inflammatory efficacy comparable or better than the well-characterized CB<sub>2</sub>R-selective agonist, HU308. My work further demonstrated that CB<sub>2</sub>R are important in the modulation of leukocyte adhesion during the inflammatory response. I showed that intravitreal injection of LPS increased leukocyte-endothelial interactions in the iridial microcirculation, a step which precedes the transendothelial migration of leukocyte into the affected tissue (Rom et al., 2013). Topical treatment of animals with the selective CB<sub>2</sub>R agonists, RO6871304, RO6871085, or HU910, decreased adhesion of leukocytes to the endothelium (Figure 11). Similarly, HU910 or HU308 administered i.v., dose-dependently reduced leukocyte adhesion in mice with EIU (Figure 12 and 13). As RO6871304 was the most efficacious of the ligands tested in reducing leukocyte adhesion (independent of route of delivery) and also had the highest selectivity *in vitro* for the human CB<sub>2</sub>R over CB<sub>1</sub>R compared to the other tested ligands, this cannabinoid was used for the majority of the pharmacological studies including validation of target. I showed that the

anti-inflammatory effect of RO6871304 is selective for the CB<sub>2</sub>R and its effect is absent in CB<sub>2</sub>R<sup>-/-</sup> animals with EIU (Figure 16). A topical drug delivery system was the preferred route of administration for these studies; topical delivery avoids systemic effects and is the most commonly used method for applying ophthalmic medications.

#### *4.1.2 Effect of pharmacological block of CB<sub>2</sub>R activity and genetic loss of CB<sub>2</sub>R, on leukocyte-endothelial interactions*

CB<sub>2</sub>R has been reported to be upregulated in inflammation (Benito et al., 2003; Carrier et al., 2004; Eljaschewitsch et al., 2006; Maresz et al., 2005; Ramirez, 2005). In keeping with these findings, work from our laboratory in a mouse model of EIU indicates that CB<sub>2</sub>R mRNA is increased in ocular inflammation (Toguri, 2015) and that constitutive activity and/or endogenous activation of CB<sub>2</sub>R may be important in modulating the ensuing inflammatory response to endotoxin (Toguri et al., 2014). My work, using the selective CB<sub>2</sub>R inverse agonist, RO6851228, further supports these findings of Toguri et al. (2014) and indicates that CB<sub>2</sub>R upregulation leads to increased activity of this receptor in EIU; exposure to the inverse agonist, RO6851228, produced an increase in leukocyte adhesion (enhanced inflammation) in mice with EIU (Figure 17). To my knowledge, this is the first time it has been shown that topical treatment with a CB<sub>2</sub>R inverse agonist increases inflammation when administered after induction of inflammation in an experimental model. Systemic administration of a CB<sub>2</sub>R inverse agonist administered prior to endotoxin induction of sepsis in mice was reported to enhance inflammatory damage (Sardinha et al., 2014). In models of PVR and EIU (Szczesniak et al., 2017; Toguri et al., 2014), systemic pre-administration of CB<sub>2</sub>R antagonist/inverse agonist also increased inflammation.

Consistent with these studies, my results from the use of the inverse agonist, RO6851228, also found that  $CB_2R^{-/-}$  mice showed increased leukocyte adhesion during EIU compared to WT mice. Taken together, this suggests that there is increased constitutive activity of  $CB_2R$  during ocular inflammation which may contribute to an auto-protective role of this receptor.

#### *4.1.3 Comparison of a $CB_2R$ agonist to steroid treatment on leukocyte-endothelial interactions*

In my study using a model of acute ocular inflammation, topical treatment with a steroid, dexamethasone, did not significantly decrease leukocyte-endothelial adhesion in the iris microcirculation at the 6 h time point. This lack of anti-inflammatory efficacy may reflect the dosing regimen I used; animals received a single dose of steroid rather than dosing with dexamethasone at multiple time points (hourly) following EIU induction. Hourly dosing (topical) was shown to be effective in reducing inflammation, specifically proinflammatory cytokines, in other studies using the same model of EIU in rats (Kanai et al., 2012). Future studies should consider this dosing regimen when comparing  $CB_2R$  agonists and other drugs (see also 4.1.4).

#### *4.1.4 Therapeutic time window for $CB_2R$ treatment*

To establish a therapeutic time window for dosing with a topical  $CB_2R$  agonist during acute ocular inflammation, I tested cannabinoid treatment at 3 h rather than 0 h after EIU induction. I found that the beneficial effects of selective  $CB_2R$  agonist treatment on

leukocyte adhesion are diminished with a single dosing regimen when there is a delay in topical administration of CB<sub>2</sub>R agonist in EIU. This supports the idea that drugs targeting the early acute stage of inflammation involving the innate immune response, are more effective if administered within a few hours after injury. While these results suggest that in this murine model of EIU early topical treatment provides the greatest immunosuppressive effect, it remains to be determined whether a multiple dosing regimen initiated at later time points in mice with EIU can decrease pathology. There are limited studies optimizing dosing schedule and therapeutic window for cannabinoid therapies in different disease models and more work is necessary to determine the exact therapeutic window for CB<sub>2</sub>R treatment (Ashton and Glass, 2007). However, in a model of cerebral ischemia, the therapeutic time window for treatment with the phytocannabinoid, CBD, has been shown to be 3 h after onset of ischemia, with benefits maintained up to 3 days post-treatment. Furthermore, decreased numbers of ionizing calcium-binding adapter molecule 1 (Iba-1, marker expressed by microglia) and glial fibrillary acidic protein (GFAP; marker expressed by astrocytes)-positive cells, and improved neurological score and motor coordination were still present at 3 days post CBD treatment (administered i.p. 3 h post-ischemia) (Hayakawa et al., 2010, 2008).

#### *4.1.5 Effect of CB<sub>2</sub>R modulation on neutrophil migration in vitro*

In my thesis, I examined immune cell targets and mechanisms that may contribute to the immunosuppressive actions of CB<sub>2</sub>R activation. My work demonstrated the effects of a selective CB<sub>2</sub>R agonist, RO6871304, on mouse neutrophil migration. RO6871304 dose-dependently inhibited neutrophil migration toward the chemoattractant, CXCL2

(Figure 18A-D). This finding suggests that selective CB<sub>2</sub>R activation can act to inhibit migration of circulating neutrophils towards the site of ocular inflammation. Decreasing constitutive activity of CB<sub>2</sub>R with pre-treatment with the inverse agonist, RO6851228, had no effect on neutrophil migration compared to vehicle (Figure 18E). The lack of observed pro-migratory activity following RO6851228 treatment could be due to several factors; the maximal number of neutrophils able to migrate was already at the assay's threshold or lack of CB<sub>2</sub>R upregulation and absence of constitutive CB<sub>2</sub>R activity in neutrophils in this *in vitro* system.

#### *4.1.6 Cell type(s) responsible for the CB<sub>2</sub>R mediated anti-inflammatory effects*

CB<sub>2</sub>R activation has been shown to reduce leukocyte adhesion using IVM in several studies (Lehmann et al., 2012; Rom et al., 2013; Sardinha et al., 2014; Xu et al., 2007); however, these studies did not investigate the cellular targets (resident immune cells, circulating neutrophils, or endothelium) responsible for the reduction in leukocyte adhesion seen after agonist treatment. This is because the IVM approach used for the majority of my experiments does not easily allow discrimination between fluorescent labelled individual immune cell subtypes. Therefore, to obtain further information on specific immune cells involved in the inflammatory response in EIU, I adopted an alternative method to help distinguish specific cell types mediating the anti-inflammatory effects of CB<sub>2</sub>R activation. The approach I used was to selectively deplete WT mice of their circulating neutrophils prior to the induction of EIU and subsequently treat EIU eyes topically with the CB<sub>2</sub>R agonist (Figure 22). This approach ensures that the effects of RO6871304, are largely exerted via binding to CB<sub>2</sub>R on the ocular resident immune cells

(macrophages and/or microglia) and/or endothelium rather than neutrophils. Adoptive transfer of naïve leukocytes was then performed at a later time point and IVM used to test whether in EIU animals treated with the CB<sub>2</sub>R agonist there is an effect on neutrophil adhesion to the iridial vascular walls. This approach allowed me to discern immune cell targets contributing to CB<sub>2</sub>R mediated inhibition of leukocyte adhesion. The results showed that CB<sub>2</sub>R activation in resident ocular immune cells and/or endothelium significantly inhibited adhesion of adoptively transferred leukocytes compared to vehicle treated eyes (Figure 22C). Neutrophil-depleted CB<sub>2</sub>R<sup>-/-</sup> mice with EIU showed similar adhesion levels of adoptively transferred WT leukocytes compared to WT control mice and were not affected by RO6871304 treatment (Figure 22D), further validating ligand selectivity for CB<sub>2</sub>R.

## **4.2 Comparisons of our findings to other studies in the field**

### *4.2.1 ECS and the eye*

Toguri et al. (2014 and 2015) reported similar findings using rodent models of EIU to my study in mice and showed that CB<sub>2</sub>R activation with the CB<sub>2</sub>R agonist, HU308, was able to decrease leukocyte adhesion in the iridial microvasculature with observed decreases in the levels of pro-inflammatory cytokines (Toguri, 2015; Toguri et al., 2014). The effects of HU308 in this previous study, however, could not be fully attributed to CB<sub>2</sub>R since HU308 still produced a reduction in leukocyte adhesion in CB<sub>2</sub>R<sup>-/-</sup> mice. This finding may be attributed to off-target activity of HU308, possibly via CB<sub>1</sub>R (Atwood et al., 2012; Soethoudt et al., 2017), and underscores the need for improved selectivity of CB<sub>2</sub>R agonist

ligands being developed. Our study has identified several such highly selective cannabinoid ligands for both human and mouse CB<sub>2</sub>R. These CB<sub>2</sub>R ligands did not produce any discernible actions at CB<sub>1</sub>R when tested *in vivo* and *in vitro*, as confirmed using both pharmacological block and genetic knock-out of CB<sub>2</sub>R in my thesis.

In keeping with other studies investigating the regulation of CB<sub>2</sub>R expression during inflammation (Beltramo et al., 2006; Maresz et al., 2005), Toguri et al (2015) reported that the receptor mRNA gene expression is upregulated in ocular tissues during ocular inflammation, suggesting that CB<sub>2</sub>R could be a selective pharmacological target for ocular inflammatory disease; CB<sub>2</sub>R is only upregulated in inflamed tissues (Toguri, 2015). Increases in ocular CB<sub>2</sub>R mRNA also support the increased constitutive activity of CB<sub>2</sub>R that I observed in my mouse model of EIU. In further support of increased CB<sub>2</sub>R activity in EIU, Toguri et al (2014) also found that pharmacological blockade of CB<sub>2</sub>R with the CB<sub>2</sub>R antagonist, AM630, or genetic deletion (CB<sub>2</sub>R<sup>-/-</sup>) exacerbated leukocyte-endothelial interactions in the iridial microvasculature compared to vehicle or WT controls (Toguri, 2015).

Increased release of endocannabinoids, such as AEA, has also been reported in numerous pathologies, including the eye, and this increased “endocannabinoid tone” may contribute to increased CB<sub>2</sub>R activation in inflammation. For example, Matias et al. (2006) reported elevated AEA levels in the retina of post-mortem eyes from patients with diabetic retinopathy (DR), a retinal disease associated with chronic inflammation and neovascularization. The same study found elevated AEA levels in retinas of post-mortem eyes of patients with age related macular degeneration (AMD), a degenerative retinal disease leading to RPE atrophy with oxidative stress as a contributing factor (Matias et al.,

2006). A later study by Wei et al. (2009) found that exposing human RPE cells and an RPE cell line to hydrogen peroxide-induced oxidative stress upregulated expression of CB<sub>1</sub>R and CB<sub>2</sub>R, and downregulated FAAH (Wei et al., 2009). Downregulation of FAAH may contribute to the increased levels of AEA found in post-mortem AMD eyes.

My findings that the CB<sub>2</sub>R agonists inhibit leukocyte adhesion via activation of CB<sub>2</sub>R on resident ocular immune cells are also in-line with Toguri et al. (2015). This study used immunohistochemical staining for Ly6G following the induction of EIU and demonstrated increased recruitment of neutrophils into the iris, an effect that was inhibited by CB<sub>2</sub>R agonist treatment (Toguri, 2015). The authors proposed that CB<sub>2</sub>R agonist modifies activation of resident microglia and macrophages since depletion of these cells negated the effects of CB<sub>2</sub>R activation on leukocyte adhesion. Taken together, these findings and my reported results indicate that CB<sub>2</sub>R activation may be decreasing the LPS-induced activation of resident ocular microglia and macrophages and/or endothelium with a resultant decrease in the production of pro-inflammatory mediators, such as CXCL2 or CXCL5, and inhibition of neutrophil recruitment and adhesion.

#### *4.2.2 ECS and immune cell migration*

Cannabinoids have been shown to inhibit chemokine-induced migration of a variety of immune cells, including neutrophils, lymphocytes, macrophages, monocytes, and microglia (Cabral G. A., 2009; Miller and Stella, 2008). Consistent with my results, Murikinati et al. (2010) showed that *in vitro* CB<sub>2</sub>R activation of human neutrophils with pre-treatment with the cannabinoid, JWH133, inhibited chemotaxis of neutrophils toward

CXCL2 (Murikinati et al., 2010). This action of JWH133 was dependent on activation of MAPK p38. The same study also reported that CB<sub>2</sub>R activation decreases infarct volume during cerebral ischemia by decreasing neutrophil migration. McHugh et al (2008) also showed that several endocannabinoids and phytocannabinoids are inhibitors of human neutrophil migration *in vitro* toward the bacterial component *N*-formyl-L-methionyl-L-leucyl-L-phenylalanine (fMLP) (McHugh et al., 2008).

#### 4.2.3 ECS and other inflammatory diseases

My hypothesis that CB<sub>2</sub>R activation is mediating its effects through resident ocular immune cells is contrary to findings reported by Rom et al. (2013), who showed in an LPS-induced encephalitis model that *ex vivo* treatment of the adoptively transferred leukocytes with CB<sub>2</sub>R agonists, JWH133 or GP1a, decreased leukocyte adhesion to the endothelium of cortical vessels (Rom et al., 2013). Similarly, their study found that there was an increase in adhesion of adoptively transferred leukocytes derived from CB<sub>2</sub>R<sup>-/-</sup> mice injected into either WT or CB<sub>2</sub>R<sup>-/-</sup> recipient mice compared to adoptive transfer of WT leukocytes. These results are in contrast to my findings that CB<sub>2</sub>R activation in resident ocular immune cells is necessary to decrease leukocyte adhesion. Rom et al (2013) also showed that CB<sub>2</sub>R agonist treatment of monocytes attenuated their adhesion in an *in vitro* blood-brain barrier (BBB) system and also inhibited their migration across primary brain microvascular endothelial cells, thereby improving barrier function. To examine a mechanism responsible for the decreased monocyte-BBB interactions effects, these researchers found that CB<sub>2</sub>R activation on monocytes decreased active conformations of the integrins, LFA-1, and very late antigen 4 (VLA-4) (Rom et al., 2013).

Recently another group has shown that CB<sub>2</sub>R activation in experimental models of sepsis can decrease inflammation (Lehmann et al., 2012, 2011; Sardinha et al., 2014). Sepsis is a disease characterised by dysfunctional microcirculation due to systemic inflammation. Lehmann et al. (2012) reported that in two experimental models of sepsis in mice, either colon ascendens stent peritonitis (CASP) or systemic LPS-induced endotoxemia, CB<sub>2</sub>R activation with HU308 reduced intestinal leukocyte adhesion (Lehmann et al., 2012). Furthermore HU308 reduced the levels of inflammatory mediators in the CASP model, including proinflammatory cytokines (TNF- $\alpha$ , IL-1 $\beta$ ), adhesion molecules (ICAM, VCAM) and chemokines (CCL5, CXCL2). The same group in a later study showed in a mouse model of endotoxemia that inhibition of enzymes FAAH (URB597 treatment) and MAGL (JZL184 treatment), which are responsible for the degradation of endocannabinoids, produced similar results and decreased intestinal leukocyte adhesion (Sardinha et al., 2014). An anti-inflammatory and immunomodulatory role for CB<sub>2</sub>R in sepsis is also consistent with the reported reduced survival in mice lacking CB<sub>2</sub>R (Tschöp et al., 2009).

## **4.3 Limitations**

### *4.3.1 Other models of ocular inflammation*

Results presented in this study were conducted using an experimental model of acute ocular inflammation, specifically EIU in mice. It would be beneficial to test these selective CB<sub>2</sub>R ligands in other models of chronic ocular inflammation including autoimmune uveitis, proliferative vitreoretinopathy, age-related macular degeneration, endophthalmitis and diabetic retinopathy, which are associated with higher incidence of

vision loss, and complications like cataracts and glaucoma due to increased steroid use (McCluskey et al., 2000). Chronic ocular inflammatory pathologies also involve the adaptive immune response. There have only been two studies published to date that I am aware of investigating the role of CB<sub>2</sub>R in models of chronic ocular inflammation (Szczesniak et al., 2017; Xu et al., 2007). Further research is required to better understand the effects of CB<sub>2</sub>R modulation of the adaptive immune response, including effects on T cells and B cells, both of which contribute to the pathogenesis of certain ocular inflammatory diseases, including autoimmunity. It would also be useful to test these compounds in species other than mice. This would allow us to determine whether the anti-inflammatory effect of this series of compounds is effective across different species. Another limitation to our study is that I only used male mice. Performing similar tests in female mice is important to understand sex difference in the effects of CB<sub>2</sub>R modulation and ECS changes associated with inflammation. There are limited studies investigating the sex differences in ECS tone. One study reported that the amygdala (important for social, cognitive and emotional behaviors) of females showed higher levels of endocannabinoids, while the amygdala of males contained greater concentrations of their primary metabolic enzymes, MAGL and FAAH (Krebs-Kraft et al., 2010). These differences may contribute to sexual dimorphism in the amygdala.

#### *4.3.2 Markers of inflammation and ocular function*

This study only assessed leukocyte adhesion and rolling as a measurable outcome of inflammation. There are several other means to assess inflammation and function within the eye during ocular inflammatory diseases. These include histopathological scores

(inflammatory cell infiltration, granulomas, and retinal damage), clinical scores (fundus assessment, vasculitis, papilledema, retinal detachment, and lesions), immunohistochemical staining for neutrophil or retinal glial cell activation (Iba-1 for microglia and GFAP for astrocytes), and visual function (electroretinography [ERG]) (Agarwal et al., 2012; Szczesniak et al., 2017). For further assessment of markers of inflammation, myeloid cell recruitment can be quantified and the M1 (pro-inflammatory) versus M2 (anti-inflammatory) polarization status of the resident ocular microglia and macrophages within EIU eyes following treatment with vehicle or CB<sub>2</sub>R agonist can be evaluated using FACS analysis. There has recently been two studies published reporting FACS analysis to assess neutrophil, monocyte, macrophage, and T-cell infiltration during the late acute inflammatory phase of EIU (18 - 48 h) (Chu et al., 2016; Liyanage et al., 2016). Future studies, outside the scope of this present work, should incorporate flow cytometry approaches in further assessment of the role of CB<sub>2</sub>R in ocular inflammation and involvement of neutrophil adhesion and migration, such as expression of PSGL-1 and LFA-1.

#### *4.3.3 CB<sub>2</sub>R expression*

A previous study from our lab (Toguri et al., 2015) demonstrated that there is increased CB<sub>2</sub>R mRNA expression during EIU; however, to-date, commercially available CB<sub>2</sub>R antibodies have not proved to be specific enough to confirm protein levels (Cécycy et al., 2013). One way to circumvent this is to use transgenic CB<sub>2</sub>R-GFP reporter mice, which have recently become available (Schmole et al., 2015). This allows the use of fluorescence imaging to trace CB<sub>2</sub>R protein expression and confirm upregulation of this

receptor in the specific tissues during EIU. This approach would provide information as to how receptor expression in specific cells and tissues is affected by inflammation and by treatment with cannabinoids and small molecules that bind CB<sub>2</sub>R. It is also possible to use immunohistochemical staining for Ly6G, Iba-1, GFAP, cluster of differentiation 31 (CD31; endothelium) in tissue from transgenic CB<sub>2</sub>R-GFP reporter mice to determine cell-specific CB<sub>2</sub>R expression. While upregulated CB<sub>2</sub>R expression in resident immune cells and glia during inflammation may account for the increased ocular expression of CB<sub>2</sub>R in EIU, it may also be possible that the increased CB<sub>2</sub>R mRNA expression may be due to the increased recruitment of neutrophils expressing CB<sub>2</sub>R. Probing this may be possible using novel fluorescent tagged CB<sub>2</sub>R ligands, several of which have recently been developed by our collaborators at Roche Pharmaceuticals. These ligands can be used as probes for confocal imaging or flow cytometry to visualize CB<sub>2</sub>R-ligand binding on immune cells and better understand CB<sub>2</sub>R protein expression in disease (Petrov et al., 2011; Sexton et al., 2011).

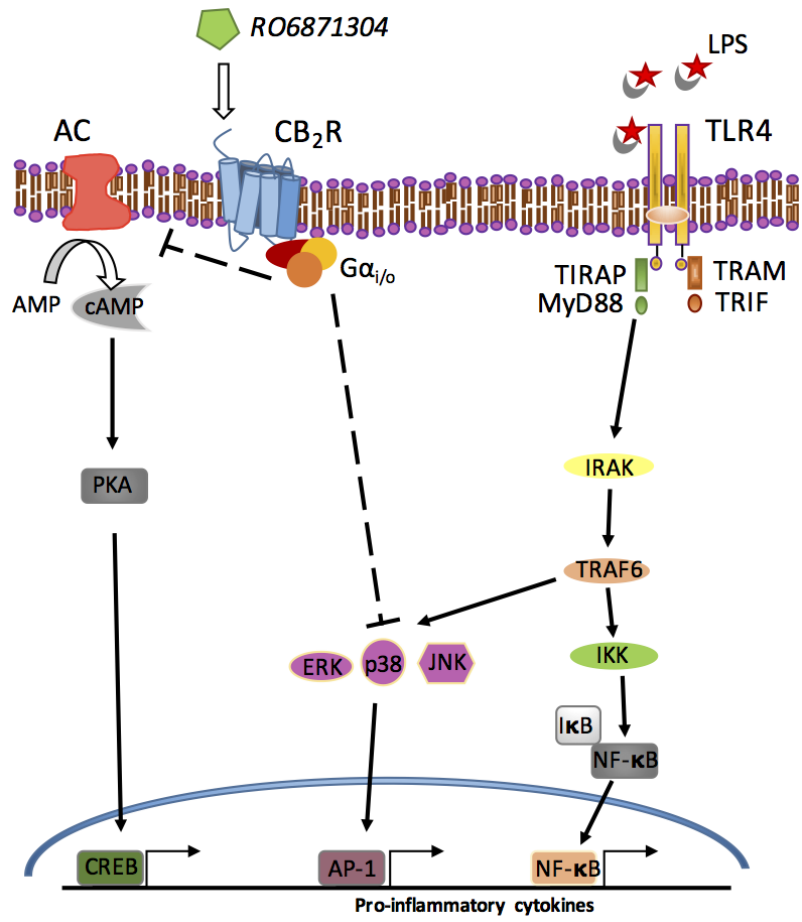
#### *4.3.4 Optimizing neutrophil depletion*

Although the Gr-1 mAb has been used extensively to deplete Ly6G expressing neutrophils, it also binds to Ly6C on eosinophils, DCs, monocytes and macrophages (Stirling et al., 2009). Future studies should explore a more specific protocol and use the specific Ly6G mAb, which has been demonstrated as an improved method to deplete neutrophils (Daley et al., 2007).

#### **4.4 Proposed CB<sub>2</sub>R anti-inflammatory signalling mechanism**

Based on previous studies and together with my research results, I hypothesize that CB<sub>2</sub>R agonist treatment is decreasing ocular inflammation through activation of CB<sub>2</sub>R on resident ocular macrophages, microglia and/or endothelium, through Gβγ, which inhibits MAPK and CREB to inhibit ERK, JNK, and p38 phosphorylation (Figure 23). ERK, JNK, and p38 phosphorylation are also downstream of the TLR4 pathway which activates AP-1 and NF-κB transcription factors to cause transcription of pro-inflammatory cytokines and chemokines including IL-1β, TNF-α, IL-6, CXCL2, CCL5. Therefore, I propose that CB<sub>2</sub>R activation is reducing TLR4-mediated phosphorylation of MAPK signaling and inhibiting the production of pro-inflammatory cytokines and chemokines, thereby preventing recruitment of neutrophils and reducing inflammation within the eye. Although, I did not explore in detail these or other signalling pathways in my thesis, future work could address this in the EIU model by: 1) immunohistochemical staining of EIU + CB<sub>2</sub>R agonist-treated eyes for NF-κB (phosphorylated-p65), 2) use of LPS-stimulated RAW 264.7 macrophage-like cells treated with specific CB<sub>2</sub>R ligands with agonist and quantification of protein in nuclear extracts using Western blot with specific antibodies against phosphorylated-p65 (Kalariya et al., 2012).

**Figure 23:** Schematic representation of the proposed CB<sub>2</sub>R activation signaling pathway which modulates EIU-induced ocular inflammation. CB<sub>2</sub>R activation blocks the TLR4-mediated phosphorylation of MAPK signalling and inhibits the production of pro-inflammatory cytokines, thereby preventing recruitment of neutrophils and consequential tissue damage and inflammation.



## **4.5 Conclusion**

My results demonstrate that novel cannabinoid ligands, which have high selectivity to bind and activate CB<sub>2</sub>R over CB<sub>1</sub>R, attenuate leukocyte adhesion to the iridial microvasculature in EIU, an effect which is consistent with the proposed anti-inflammatory role for this receptor. From the research I carried out for my thesis, I propose that these ligands exert their effects at multiple immune cell targets to decrease inflammation. These include neutrophils, since pre-treatment of neutrophils with these ligands decreases their migration *in vitro* toward CXCL2, and resident ocular microglia, monocytes and/or endothelium, given that these CB<sub>2</sub>R selective ligands still reduce leukocyte adhesion in neutrophil-depleted EIU mice. My results strongly suggest that drugs targeting CB<sub>2</sub>R may have efficacy in the treatment of uveitis by decreasing neutrophil recruitment and activation of resident ocular immune cells and preventing consequent tissue damage.

## **4.6 Future directions**

There are several future experiments that would be useful to expand the scope of work presented in this thesis and would provide additional information for selection of lead compounds to develop as therapeutic drugs for treating uveitis. In order to provide further valuable information on pharmacodynamics and pharmacokinetics of CB<sub>2</sub>R ligands in our model, I propose the following experiments:

#### 4.6.1 Markers of inflammation

I plan to investigate the effects of selective CB<sub>2</sub>R agonist treatment on mRNA (by qPCR) and protein (using cytokine ELISA multiplex assay kits) levels of pro-inflammatory cytokines and cellular adhesion molecules, including Iba-1, GFAP, CD68 (monocytes/macrophages), Ly6G, IL-1 $\beta$ , TNF- $\alpha$ , IL-6, IL-10, TGF- $\beta$ , CXCL2, CCL5 AP-1, I $\kappa$ B $\alpha$ , ICAM-1, ICAM-2, VCAM-1, PSGL-1, LFA-1, VLA-4, MAC-1, L-selectin, E-selectin, and P-selectin. I also plan to investigate the effects of CB<sub>2</sub>R modulation on neutrophil function such as phagocytosis, reactive oxygen species, degranulation, and neutrophil extracellular traps. It would also be beneficial to examine the effects of CB<sub>2</sub>R activation on endothelium, such as NF- $\kappa$ B and RhoA activation, ICAM-1 and VCAM-1 upregulation, CCL2 expression, and blood-ocular barrier integrity (tight junction protein expression).

#### 4.6.2 Retinal pathology

Optical coherence tomography (OCT) offers the ability to non-invasively image *in vivo* in real time cells infiltrating into the retina, vitreous, or optic nerve, and retinal edema. This imaging tool used in ophthalmology provides cross-sectional images of the retina and can be used for serial observation of different retinal diseases in patients with AMD, glaucoma, or posterior uveitis. OCT has been applied to experimental models of EAU (Chen et al., 2013) and most recently EIU (Chu et al., 2016). This method can be correlated with retinal histology and immunohistochemical analysis of neutrophil and monocyte/macrophage recruitment, funduscopy, and visual function by ERG. OCT will

allow us to quantitatively assess retinal pathology and monitor CB<sub>2</sub>R drug treatment effects over time in our EIU pan-uveitis model.

#### *4.6.3 PK and Systemic effects*

Future work should continue PK analysis and refining the topical delivery vehicle. Studies are required to determine how much of the drug gets absorbed across the cornea and how much is transported out of the ocular tissues and into systemic circulation. At this time, we do not know whether topical delivery of cannabinoids has systemic effects. One way to test if the drug is absorbed systemically would be to apply the drug topically to the naïve contralateral eye (right) and examine whether there is still a reduction of leukocyte adhesion in the EIU eye (left). This data is important to be used for PK modelling and scaled up for humans. We also need to determine if we can treat EIU topically at 3 h after inflammation by adjusting the dosing regimen to hourly dosing and/or using a loading dose followed by an hourly dose.

These future experiments will extend our findings and are required for move preclinical studies to the clinic, as well as to better understand the pharmacology of the CB<sub>2</sub>R and the ECS in the eye.

## References

- Agarwal, R.K., Silver, P.B., Caspi, R.R., 2012. Rodent models of experimental autoimmune uveitis. *Methods Mol. Biol.* 900, 443–469. doi:10.1007/978-1-60761-720-4\_22
- Akira, S., Takeda, K., 2004. Toll-like receptor signaling. *Nat. Rev. Immunol.* 4, 499–511. doi:10.1038/nri1391
- Akpek, E.K., Gottsch, J.D., 2003. Immune defense at the ocular surface. *Eye* 17, 949–956. doi:10.1038/sj.eye.6700617
- Al-Banna, N.A., Toguri, J.T., Kelly, M.E.M., Lehmann, C.H., 2013. Leukocyte-endothelial interactions within the ocular microcirculation in inflammation and infection. *Clin. Hemorheol. Microcirc.* 55, 423–443. doi:10.3233/PPR-2012-0009
- Allensworth, J.J., Planck, S.R., Rosenbaum, J.T., Rosenzweig, H.L., 2011. Investigation of the differential potentials of TLR agonists to elicit uveitis in mice. *J. Leukoc. Biol.* 90, 1159–1166. doi:10.1189/jlb.0511249
- Ashton, J.C., Glass, M., 2007. The cannabinoid CB2 receptor as a target for inflammation-dependent neurodegeneration. *Curr. Neuropharmacol.* 5, 73–80.
- Atwood, B.K., Mackie, K., 2010. CB2: a cannabinoid receptor with an identity crisis. *Br. J. Pharmacol.* 160, 467–479. doi:10.1111/j.1476-5381.2010.00729.x
- Atwood, B.K., Straiker, A., Mackie, K., 2012. CB<sub>2</sub>: therapeutic target-in-waiting. *Prog. Neuropsychopharmacol. Biol. Psychiatry* 38, 16–20. doi:10.1016/j.pnpbp.2011.12.001
- Babu, K., Mahendradas, P., 2013. Medical management of uveitis - current trends. *Indian J. Ophthalmol.* 61, 277–283. doi:10.4103/0301-4738.114099
- Becker, M.D., Nobiling, R., Planck, S.R., Rosenbaum, J.T., 2000. Digital video-imaging of leukocyte migration in the iris: intravital microscopy in a physiological model during the onset of endotoxin-induced uveitis. *J. Immunol. Methods* 240, 23–37.
- Beltramo, M., Bernardini, N., Bertorelli, R., Campanella, M., Nicolussi, E., Fredduzzi, S., Reggiani, A., 2006. CB2 receptor-mediated antihyperalgesia: Possible direct involvement of neural mechanisms. *Eur. J. Neurosci.* 23, 1530–1538. doi:10.1111/j.1460-9568.2006.04684.x
- Benhar, I., London, A., Schwartz, M., 2012. The privileged immunity of immune privileged organs: The case of the eye. *Front. Immunol.* 3, 1–6. doi:10.3389/fimmu.2012.00296
- Benito, C., Núñez, E., Tolón, R.M., Carrier, E.J., Rábano, A., Hillard, C.J., Romero, J., 2003. Cannabinoid CB2 receptors and fatty acid amide hydrolase are selectively overexpressed in neuritic plaque-associated glia in Alzheimer's disease brains. *J. Neurosci.* 23, 11136–11141.

- Blankman, J.L., Cravatt, B.F., 2013. Chemical probes of endocannabinoid metabolism. *Pharmacol. Rev.* 65, 849–871. doi:10.1124/pr.112.006387
- Bow, E.W., Rimoldi, J.M., 2016. The structure-function relationships of classical cannabinoids: CB1/CB2 modulation. *Perspectives Med. Chem.* 28, 17–39.
- Buckley, N.E., McCoy, K.L., Mezey, É., Bonner, T., Zimmer, A., Felder, C.C., Glass, M., Zimmer, A., 2000. Immunomodulation by cannabinoids is absent in mice deficient for the cannabinoid CB2 receptor. *Eur. J. Pharmacol.* 396, 141–149. doi:10.1016/S0014-2999(00)00211-9
- Cabral G. A., G.-T.L., 2009. Emerging role of the CB2 cannabinoid receptor in immune regulation and therapeutic prospects. *Expert Rev. Mol. Med.* 11, 1–31. doi:10.1017/S1462399409000957.Emerging
- Cairns, E.A., Toguri, T.J., Porter, R.F., Szczesniak, A.M., Kelly, M.E.M., 2016. Seeing over the horizon: targeting the endocannabinoid system for the treatment of ocular disease. *J. Basic Clin. Physiol. Pharmacol.* 27, 253–265. doi:10.1515/jbcpp-2015-0065
- Carlisle, S.J., Marciano-Cabral, F., Staab, A., Ludwick, C., Cabral, G.A., 2002. Differential expression of the CB2 cannabinoid receptor by rodent macrophages and macrophage-like cells in relation to cell activation. *Int. Immunopharmacol.* 2, 69–82. doi:10.1016/S1567-5769(01)00147-3
- Carrier, E.J., Kearns, C.S., Barkmeier, A.J., Breese, N.M., Yang, W., Nithipatikom, K., Pfister, S.L., Campbell, W.B., Hillard, C.J., 2004. Cultured rat microglial cells synthesize the endocannabinoid 2-arachidonylglycerol, which increases proliferation via a CB2 receptor-dependent mechanism. *Mol. Pharmacol.* 65, 999–1007. doi:10.1124/mol.65.4.999
- Cécylre, B., Zabouri, N., Huppé-Gourgues, F., Bouchard, J.-F., Casanova, C., 2013. Roles of cannabinoid receptors type 1 and 2 on the retinal function of adult mice. *Investig. Ophthalmology Vis. Sci.* 54, 8079. doi:10.1167/iovs.13-12514
- Chang, Y.H., Lee, S.T., Lin, W.W., 2001. Effects of cannabinoids on LPS-stimulated inflammatory mediator release from macrophages: Involvement of eicosanoids. *J. Cell. Biochem.* 81, 715–723. doi:10.1002/jcb.1103
- Chen, J., Qian, H., Horai, R., Chan, C.C., Caspi, R.R., 2013. Use of optical coherence tomography and electroretinography to evaluate retinal pathology in a mouse model of autoimmune uveitis. *PLoS One* 8, 1–8. doi:10.1371/journal.pone.0063904
- Chen, L., 2009. Ocular lymphatics: state-of-the-art review. *Lymphatics* 42, 66–76. doi:10.1016/j.bbamem.2015.02.010
- Chu, C.J., Gardner, P.J., Copland, D.A., Liyanage, S.E., Gonzalez-Cordero, A., kleine Holthaus, S.-M., Luhmann, U.F.O., Smith, A.J., Ali, R.R., Dick, A.D., 2016. Multimodal analysis of ocular inflammation using the endotoxin-induced uveitis mouse model. *Dis. Model. Mech.* 9, 473–481. doi:10.1242/dmm.022475

- Croxford, J.L., Yamamura, T., 2005. Cannabinoids and the immune system: potential for the treatment of inflammatory diseases? *J. Neuroimmunol.* 166, 3–18. doi:10.1016/j.jneuroim.2005.04.023
- Daley, J.M., Thomay, A.A., Connolly, M.D., Reichner, J.S., Albina, J.E., 2007. Use of Ly6G-specific monoclonal antibody to deplete neutrophils in mice. *J. Leukoc. Biol.* 83, 64–70. doi:10.1189/jlb.0407247
- de Oliveira, S., Rosowski, E.E., Huttenlocher, A., 2016. Neutrophil migration in infection and wound repair: going forward in reverse. *Nat. Rev. Immunol.* 16, 378–391. doi:10.1038/nri.2016.49
- Downer, E.J., 2011. Cannabinoids and innate immunity: taking a toll on neuroinflammation. *ScientificWorldJournal.* 11, 855–865. doi:10.1100/tsw.2011.84
- Eljaschewitsch, E., Witting, A., Mawrin, C., Lee, T., Schmidt, P.M., Wolf, S., Hoertnagl, H., Raine, C.S., Schneider-Stock, R., Nitsch, R., Ullrich, O., 2006. The endocannabinoid anandamide protects neurons during CNS inflammation by induction of MKP-1 in microglial cells. *Neuron* 49, 67–79. doi:10.1016/j.neuron.2005.11.027
- Forrester, J. V, Klaska, I.P., Yu, T., Kuffova, L., 2013. Uveitis in mouse and man. *Int. Rev. Immunol.* 32, 76–96. doi:10.3109/08830185.2012.747524
- Forrester, J. V, Xu, H., Lambe, T., Cornall, R., 2008. Immune privilege or privileged immunity? *Mucosal Immunol.* 1, 372–381. doi:10.1038/mi.2008.27
- Fraunfelder, F.W., Rosenbaum, J.T., 1997. Drug-induced uveitis. Incidence, prevention and treatment. *Drug Saf.* 17, 197–207. doi:10.2165/00002018-199717030-00005
- Freddo, T.F., 2001. Shifting the paradigm of the blood-aqueous barrier. *Exp. Eye Res.* 73, 581–592. doi:10.1006/exer.2001.1056
- Galiegue, S., Mary, S., Marchand, J., Dussossoy, D., Carriere, D., Carayon, P., Bouaboula, M., Shire, D., Le Fur, G., Casellas, P., 1995. Expression of central and peripheral cannabinoid receptors in human immune tissues and leukocyte subpopulations. *Eur. J. Biochem.* 232, 54–61. doi:10.1111/j.1432-1033.1995.tb20780.x
- Gaoni, Y., Mechoulam, R., 1971. The isolation and structure of delta-1-tetrahydrocannabinol and other neutral cannabinoids from hashish. *J. Am. Chem. Soc.* 93, 217–224. doi:10.1021/ja00730a036
- Gaoni, Y., Mechoulam, R., 1964. Isolation, structure, and partial synthesis of an active constituent of hashish. *J. Am. Chem. Soc.* 86, 1646–1647. doi:10.1021/ja01062a046
- Gertsch, J., Anavi-Goffer, S., 2012. Methylhonokiol attenuates neuroinflammation: a role for cannabinoid receptors? *J. Neuroinflammation* 9, 1–5. doi:10.1186/1742-2094-9-135

- Golias, C., Tsoutsi, E., Matziridis, A., Makridis, P., Batistatou, A., Charalabopoulos, K., 2007. Leukocyte and endothelial cell adhesion molecules in inflammation focusing on inflammatory heart disease. *In Vivo* 21, 757–69. doi:0258-851X/2007
- Griffin, G., Wray, E.J., Tao, Q., McAllister, S.D., Rorrer, W.K., Aung, M., Martin, B.R., Abood, M.E., 1999. Evaluation of the cannabinoid CB2 receptor-selective antagonist, SR144528: further evidence for cannabinoid CB2 receptor absence in the rat central nervous system. *Eur. J. Pharmacol.* 377, 117–125. doi:10.1016/S0014-2999(99)00402-1
- Hanus, L., Breuer, A., Tchilibon, S., Shiloah, S., Goldenberg, D., Horowitz, M., Pertwee, R.G., Ross, R. a, Mechoulam, R., Frider, E., 1999. HU-308: a specific agonist for CB(2), a peripheral cannabinoid receptor. *Proc. Natl. Acad. Sci. U. S. A.* 96, 14228–14233.
- Hara, Y., Caspi, R.R., Wiggert, B., Dorf, M., Streilein, J.W., 1992. Analysis of an in vitro-generated signal that induces systemic immune deviation similar to that elicited by antigen injected into the anterior chamber of the eye. *J. Immunol.* 149, 1531–1538.
- Hayakawa, K., Mishima, K., Fujiwara, M., 2010. Therapeutic potential of non-psychoactive cannabidiol in ischemic stroke. *Pharmaceuticals* 3, 2197–2212. doi:10.3390/ph3072197
- Hayakawa, K., Mishima, K., Irie, K., Hazekawa, M., Mishima, S., Fujioka, M., Orito, K., Egashira, N., Katsurabayashi, S., Takasaki, K., Iwasaki, K., Fujiwara, M., 2008. Cannabidiol prevents a post-ischemic injury progressively induced by cerebral ischemia via a high-mobility group box 1-inhibiting mechanism. *Neuropharmacology* 55, 1280–1286. doi:10.1016/j.neuropharm.2008.06.040
- Herkenham, M., Lynn, a B., Johnson, M.R., Melvin, L.S., de Costa, B.R., Rice, K.C., 1991. Characterization and localization of cannabinoid receptors in rat brain: a quantitative in vitro autoradiographic study. *J. Neurosci.* 11, 563–583. doi:10.1073/pnas.87.5.1932
- Howlett, A.C., 2002. International Union of Pharmacology. XXVII. classification of cannabinoid receptors. *Pharmacol. Rev.* 54, 161–202. doi:10.1124/pr.54.2.161
- Hua, T., Vemuri, K., Nikas, S.P., Laprairie, R.B., Wu, Y., Qu, L., Pu, M., Korde, A., Jiang, S., Ho, J.-H., Han, G.W., Ding, K., Li, X., Liu, H., Hanson, M.A., Zhao, S., Bohn, L.M., Makriyannis, A., Stevens, R.C., Liu, Z.-J., 2017. Crystal structures of agonist-bound human cannabinoid receptor CB1. *Nature* 547, 468–471. doi:10.1038/nature23272
- Hua, T., Vemuri, K., Pu, M., Qu, L., Han, G.W., Wu, Y., Zhao, S., Shui, W., Li, S., Korde, A., Laprairie, R.B., Stahl, E.L., Ho, J.H., Zvonok, N., Zhou, H., Kufareva, I., Wu, B., Zhao, Q., Hanson, M.A., Bohn, L.M., Makriyannis, A., Stevens, R.C., Liu, Z.J., 2016. Crystal structure of the human cannabinoid receptor CB1. *Cell* 167, 750–762.e14. doi:10.1016/j.cell.2016.10.004

- Kalariya, N.M., Shoeb, M., Ansari, N.H., Srivastava, S.K., Ramana, K. V., 2012. Antidiabetic drug metformin suppresses endotoxin-induced uveitis in rats. *Investig. Ophthalmol. Vis. Sci.* 53, 3431–3440. doi:10.1167/iovs.12-9432
- Kaminski, N.E., Abood, M.E., Kessler, F.K., Martin, B.R., Schatz, A.R., 1992. Identification of a functionally relevant cannabinoid receptor on mouse spleen cells that is involved in cannabinoid-mediated immune modulation. *Mol. Pharmacol.* 42, 736–742.
- Kanai, K., Ito, Y., Nagai, N., Itoh, N., Hori, Y., Chikazawa, S., Hoshi, F., Higuchi, S., 2012. Effects of instillation of eyedrops containing disulfiram and hydroxypropyl- $\beta$ -cyclodextrin inclusion complex on endotoxin-induced uveitis in rats. *Curr. Eye Res.* 37, 124–131. doi:10.3109/02713683.2011.622853
- Kawasaki, T., Kawai, T., 2014. Toll-like receptor signaling pathways. *Front. Immunol.* 5, 1–8. doi:10.3389/fimmu.2014.00461
- Kenakin, T., 2012. The potential for selective pharmacological therapies through biased receptor signalling. *BMC Pharmacol. Toxicol.* 13, 1–8.
- Kersey, J.P., Broadway, D.C., 2006. Corticosteroid-induced glaucoma: a review of the literature. *Eye* 20, 407–416. doi:10.1038/sj.eye.6701895
- Kezic, J., Taylor, S., Gupta, S., Planck, S.R., Rosenzweig, H.L., Rosenbaum, J.T., 2011. Endotoxin-induced uveitis is primarily dependent on radiation-resistant cells and on MyD88 but not TRIF. *J. Leukoc. Biol.* 90, 305–311. doi:10.1189/jlb.0111036
- Kilkenny, C., Browne, W., Cuthill, I.C., Emerson, M., Altman, D.G., 2010. Animal research: Reporting in vivo experiments: The ARRIVE guidelines. *Br. J. Pharmacol.* 160, 1577–1579. doi:10.1111/j.1476-5381.2010.00872.x
- Kishimoto, S., Gokoh, M., Oka, S., Muramatsu, M., Kajiwara, T., Waku, K., Sugiura, T., 2003. 2-arachidonoylglycerol induces the migration of HL-60 cells differentiated into macrophage-like cells and human peripheral blood monocytes through the cannabinoid CB2 receptor-dependent mechanism. *J. Biol. Chem.* 278, 24469–24475. doi:10.1074/jbc.M301359200
- Klein, T.W., 2005. Cannabinoid-based drugs as anti-inflammatory therapeutics. *Nat. Rev. Immunol.* 5, 400–11. doi:10.1038/nri1602
- Kolaczowska, E., Kubes, P., 2013. Neutrophil recruitment and function in health and inflammation. *Nat. Rev. Immunol.* 13, 159–175. doi:10.1038/nri3399
- Krebs-Kraft, D.L., Hill, M.N., Hillard, C.J., McCarthy, M.M., 2010. Sex difference in cell proliferation in developing rat amygdala mediated by endocannabinoids has implications for social behavior. *Proc. Natl. Acad. Sci. U. S. A.* 107, 20535–20540. doi:10.1073/pnas.1005003107
- Kreitzer, F.R., Stella, N., 2009. The therapeutic potential of novel cannabinoid receptors. *Pharmacol. Ther.* 122, 83–96. doi:10.1016/j.pharmthera.2009.01.005

- Laprairie, R.B., Bagher, A.M., Kelly, M.E.M., Denovan-Wright, E.M., 2015. Cannabidiol is a negative allosteric modulator of the type 1 cannabinoid receptor. *Br. J. Pharmacol.* 172, 4790–4805. doi:10.1002/bph.13250
- Laprairie, R.B., Kulkarni, P.M., Deschamps, J.R., Kelly, M.E.M., Janero, D.R., Cascio, M.G., Stevenson, L.A., Pertwee, R.G., Kenakin, T.P., Denovan-Wright, E.M., Thakur, G.A., 2017. Enantiospecific allosteric modulation of cannabinoid 1 receptor. *ACS Chem. Neurosci.* 8, 1188–1203. doi:10.1021/acschemneuro.6b00310
- Lehmann, C., Kianian, M., Zhou, J., Cerny, V., Kelly, M., 2011. The endocannabinoid system in sepsis—a potential target to improve microcirculation? *Signa Vitae* 6, 7–13.
- Lehmann, C., Kianian, M., Zhou, J., Küster, I., Kuschnerit, R., Whynot, S., Hung, O., Shukla, R., Johnston, B., Cerny, V., Pavlovic, D., Spassov, A., Kelly, M.E.M., Kuster, I., Kuschnerit, R., Whynot, S., Hung, O., Shukla, R., Johnston, B., Cerny, V., Pavlovic, D., Spassov, A., Kelly, M.E.M., 2012. Cannabinoid receptor 2 activation reduces intestinal leukocyte recruitment and systemic inflammatory mediator release in acute experimental sepsis. *Crit. Care* 16, 1–22. doi:10.1186/cc11248
- Li, Q., Peng, B., Whitcup, S.M., Jang, S.U., Chan, C.C., 1995. Endotoxin induced uveitis in the mouse: susceptibility and genetic control. *Exp. Eye Res.* 61, 629–632. doi:10.1016/S0014-4835(05)80056-9
- Liyanage, S.E., Gardner, P.J., Ribeiro, J., Cristante, E., Sampson, R.D., Luhmann, U.F.O., Ali, R.R., Bainbridge, J.W., 2016. Flow cytometric analysis of inflammatory and resident myeloid populations in mouse ocular inflammatory models. *Exp. Eye Res.* 151, 160–170. doi:10.1016/j.exer.2016.08.007
- London, A., Benhar, I., Schwartz, M., 2013. The retina as a window to the brain—from eye research to CNS disorders. *Nat. Rev. Neurol.* 9, 44–53. doi:10.1038/nrneurol.2012.227
- Mackie, K., 2006. Mechanisms of CB1 receptor signaling: endocannabinoid modulation of synaptic strength. *Int. J. Obes.* 30, 19–23. doi:10.1038/sj.ijo.0803273
- Maresz, K., Carrier, E.J., Ponomarev, E.D., Hillard, C.J., Dittel, B.N., 2005. Modulation of the cannabinoid CB2 receptor in microglial cells in response to inflammatory stimuli. *J. Neurochem.* 95, 437–445. doi:10.1111/j.1471-4159.2005.03380.x
- Martin, T.M., Smith, J.R., Rosenbaum, J.T., 2002. Anterior uveitis: current concepts of pathogenesis and interactions with the spondyloarthropathies. *Curr. Opin. Rheumatol.* 14, 337–341. doi:10.1097/00002281-200207000-00001
- Martínez-Orgado, J., Fernández-López, D., Lizasoain, I., Romero, J., 2007. The seek of neuroprotection: introducing cannabinoids. *Recent Pat. CNS Drug Discov.* 2, 131–139. doi:10.2174/157488907780832724

- Matias, I., Wang, J.W., Moriello, A.S., Nieves, A., Woodward, D.F., Di Marzo, V., 2006. Changes in endocannabinoid and palmitoylethanolamide levels in eye tissues of patients with diabetic retinopathy and age-related macular degeneration. *Prostaglandins Leukot. Essent. Fat. Acids* 75, 413–418. doi:10.1016/j.plefa.2006.08.002
- Matsuda, S., Koyasu, S., 2000. Review: Mechanisms of action of cyclosporine. *Immunopharmacology* 47, 119–125.
- McClellan, K., 1997. Mucosal defense of the outer eye. *Surv. Ophthalmol.* 42, 233–246.
- McCluskey, P., Towler, H., Lightman, S., 2000. Regular review: Management of chronic uveitis. *BMJ* 320, 555–558. doi:10.1136/bmj.320.7234.555
- McGrath, J.C., Drummond, G.B., McLachlan, E.M., Kilkenny, C., Wainwright, C.L., 2010. Editorial: Guidelines for reporting experiments involving animals: The ARRIVE guidelines. *Br. J. Pharmacol.* 160, 1573–1576. doi:10.1111/j.1476-5381.2010.00873.x
- McHugh, D., Tanner, C., Mechoulam, R., Pertwee, R.G., Ross, R.A., 2008. Inhibition of human neutrophil chemotaxis by endogenous cannabinoids and phytocannabinoids: evidence for a site distinct from CB1 and CB2. *Mol. Pharmacol.* 73, 441–450. doi:10.1124/mol.107.041863
- McPartland, J.M., Duncan, M., Di Marzo, V., Pertwee, R., 2015. Are cannabidiol and  $\Delta(9)$ -tetrahydrocannabinol negative modulators of the endocannabinoid system? A systematic review. *Br. J. Pharmacol.* 172, 737–753. doi:10.1111/bph.12944
- Mechoulam, R., Parker, L.A., 2013. The endocannabinoid system and the brain. *Annu. Rev. Psychol.* 64, 21–47. doi:10.1146/annurev-psych-113011-143739
- Mérida, S., Palacios, E., Navea, A., Bosch-Morell, F., 2015. New immunosuppressive therapies in uveitis treatment. *Int. J. Mol. Sci.* 16, 18778–18795. doi:10.3390/ijms160818778
- Mérida, S., Palacios, E., Navea, A., Bosch-Morell, F., 2015. Macrophages and uveitis in experimental animal models. *Mediators Inflamm.* 2015, 1–10. doi:10.1155/2015/671417
- Miller, A., Stella, N., 2008. CB2 receptor-mediated migration of immune cells: it can go either way. *Br. J. Pharmacol.* 153, 299–308. doi:10.1038/sj.bjp.0707523
- Munoz-Luque, J., Ros, J., Fernandez-Varo, G., Tugues, S., Morales-Ruiz, M., Alvarez, C.E., Friedman, S.L., Arroyo, V., Jimenez, W., 2007. Regression of fibrosis after chronic stimulation of cannabinoid CB2 receptor in cirrhotic rats. *J. Pharmacol. Exp. Ther.* 324, 475–483. doi:10.1124/jpet.107.131896
- Munro, S., Thomas, K.L., Abu-Shaar, M., 1993. Molecular characterization of peripheral receptor for cannabinoids. *Nature* 365, 61–65.

- Murikinati, S., Jüttler, E., Keinert, T., Ridder, D.A., Muhammad, S., Waibler, Z., Ledent, C., Zimmer, A., Kalinke, U., Schwaninger, M., 2010. Activation of cannabinoid 2 receptors protects against cerebral ischemia by inhibiting neutrophil recruitment. *Fed. Am. Soc. Exp. Biol.* 24, 788–798. doi:10.1096/fj.09-141275
- Nettekoven, M., Adam, J.M., Bendels, S., Bissantz, C., Fingerle, J., Grether, U., Grüner, S., Guba, W., Kimbara, A., Ottaviani, G., Püllmann, B., Rogers-Evans, M., Röver, S., Rothenhäusler, B., Schmitt, S., Schuler, F., Schulz-Gasch, T., Ullmer, C., 2016. Novel triazolopyrimidine-derived cannabinoid receptor 2 agonists as potential treatment for inflammatory kidney diseases. *ChemMedChem* 11, 179–189. doi:10.1002/cmdc.201500218
- Nieder Korn, J.Y., 2013. Corneal transplantation and immune privilege. *Int. Rev. Immunol.* 32, 57–67. doi:10.3109/08830185.2012.737877.Corneal
- Nieder Korn, J.Y., 2012. Ocular immune privilege and ocular melanoma: parallel universes or immunological plagiarism? *Front. Immunol.* 3, 1–10. doi:10.3389/fimmu.2012.00148
- Nieder Korn, J.Y., 2006. See no evil, hear no evil, do no evil: the lessons of immune privilege. *Nat. Immunol.* 7, 354–359. doi:10.1038/ni1328
- Nourshargh, S., Alon, R., 2014. Leukocyte migration into inflamed tissues. *Immunity* 41, 694–707. doi:10.1016/j.immuni.2014.10.008
- Pacher, P., Batkai, S., Kunos, G., 2006. The endocannabinoid system as an emerging target of pharmacotherapy. *Pharmacol. Rev.* 58, 389–462. doi:10.1124/pr.58.3.2
- Pacher, P., Mackie, K., 2012. Interplay of cannabinoid 2 (CB2) receptors with nitric oxide synthases, oxidative and nitrative stress, and cell death during remote neurodegeneration. *J. Mol. Med.* 90, 347–351. doi:10.1007/s00109-012-0884-1
- Pasadhika, S., Rosenbaum, J.T., 2014. Update on the use of systemic biologic agents in the treatment of noninfectious uveitis. *Biol. Targets Ther.* 8, 67–81. doi:10.2147/BTT.S41477
- Pattern, C., 2009. Strategies for in vitro metabolic stability testing. *Biochem. Pharmacol.* 3, 1–43.
- Percopo, C.M., Hooks, J., Shinohara, T., Caspi, R., Detrick, B., 1990. Cytokine-mediated activation of neuronal retinal resident cell provokes antigen presentation. *J. Immunol.* 145, 4101–4107.
- Pertwee, R.G., 2006. Cannabinoid pharmacology: the first 66 years. *Br. J. Pharmacol.* 147, 163–171. doi:0706406 [pii] 10.1038/sj.bjp.0706406
- Petrov, R.R., Ferrini, M.E., Jaffar, Z., Thompson, C.M., Roberts, K., Diaz, P., 2011. Design and evaluation of a novel fluorescent CB2 ligand as probe for receptor visualization in immune cells. *Bioorganic Med. Chem. Lett.* 21, 5859–5862. doi:10.1016/j.bmcl.2011.07.099

- Planck, S.R., Becker, M.D., Crespo, S., Choi, D., Galster, K., Garman, K.L., Nobile, R., Rosenbaum, J.T., 2008. Characterizing extravascular neutrophil migration in vivo in the iris. *Inflammation* 31, 105–111. doi:10.1007/s10753-007-9055-x
- Porter, R., Szczesniak, A., Toguri, J., Gebremeskel, S., Johnston, B., Lehmann, C., Grether, U., Ullmer, C., Kelly, M., n.d. Selective cannabinoid 2 receptor agonists as potential therapeutic drugs for the treatment of endotoxin-induced uveitis. *Mol. Pharmacol.*
- Rajesh, M., Mukhopadhyay, P., Bátkai, S., Haskó, G., Liaudet, L., Huffman, J.W., Csiszar, A., Ungvari, Z., Mackie, K., Chatterjee, S., Pacher, P., 2007. CB2-receptor stimulation attenuates TNF-alpha-induced human endothelial cell activation, transendothelial migration of monocytes, and monocyte-endothelial adhesion. *Am. J. Physiol. Heart Circ. Physiol.* 293, 2210–2218. doi:10.1152/ajpheart.00688.2007
- Rajesh, M., Mukhopadhyay, P., Bátkai, S., Patel, V., Saito, K., Matsumoto, S., Kashiwaya, Y., Horváth, B., Mukhopadhyay, B., Becker, L., Haskó, G., Liaudet, L., Wink, D.A., Veves, A., Mechoulam, R., Pacher, P., 2010. Cannabidiol attenuates cardiac dysfunction, oxidative stress, fibrosis, and inflammatory and cell death signaling pathways in diabetic cardiomyopathy. *J. Am. Coll. Cardiol.* 56, 2115–2125.
- Ramirez, B.G., 2005. Prevention of Alzheimer's disease pathology by cannabinoids: neuroprotection mediated by blockade of microglial activation. *J. Neurosci.* 25, 1904–1913. doi:10.1523/JNEUROSCI.4540-04.2005
- Rom, S., Zuluaga-Ramirez, V., Dykstra, H., Reichenbach, N.L., Pacher, P., Persidsky, Y., 2013. Selective activation of cannabinoid receptor 2 in leukocytes suppresses their engagement of the brain endothelium and protects the blood-brain barrier. *Am. J. Pathol.* 183, 1548–1558. doi:10.1016/j.ajpath.2013.07.033
- Rosenbaum, J.T., McDevitt, H.O., Guss, R.B., Egbert, P.R., 1980. Endotoxin-induced uveitis in rats as a model for human disease. *Nature* 286, 611–613. doi:10.1038/286611a0
- Rosenbaum, J.T., Woods, A., Kezic, J., Planck, S.R., Rosenzweig, H.L., 2011. Contrasting ocular effects of local versus systemic endotoxin. *Investig. Ophthalmol. Vis. Sci.* 52, 6472–6477. doi:10.1167/iovs.11-7742
- Ross, R.A., 2007. Allosterism and cannabinoid CB1 receptors: the shape of things to come. *Trends Pharmacol. Sci.* 28, 567–572. doi:10.1016/j.tips.2007.10.006
- Ross, R.A., Brockie, H.C., Pertwee, R.G., 2000. Inhibition of nitric oxide production in RAW264.7 macrophages by cannabinoids and palmitoylethanolamide. *Eur. J. Pharmacol.* 401, 121–130. doi:S0014-2999(00)00437-4 [pii]
- Saban, D.R., 2012. How do ocular corticosteroids and NSAIDs work? *Contin. Med. Educ. Publ.* 1–8. doi:10.1155/2012/789623.3.

- Sardinha, J., Kelly, M.E.M., Zhou, J., Lehmann, C., 2014. Experimental cannabinoid 2 receptor-mediated immune modulation in sepsis. *Mediators Inflamm.* 2014. doi:10.1155/2014/978678
- Schatz, A.R., Lee, M., Condie, R.B., Pulaski, J.T., Kaminski, N.E., 1997. Cannabinoid receptors CB1 and CB2: a characterization of expression and adenylate cyclase modulation. *Toxicol. Appl. Pharmacol.* 142, 278–287. doi:10.1006/taap.1996.8034
- Schmole, A.C., Lundt, R., Gennequin, B., Schrage, H., Beins, E., Kramer, A., Zimmer, T., Limmer, A., Zimmer, A., Otte, D.M., 2015. Expression analysis of CB2-GFP BAC transgenic mice. *PLoS One* 10, 1–16. doi:10.1371/journal.pone.0138986
- Sexton, M., Woodruff, G., Horne, E.A., Lin, Y.H., Muccioli, G.G., Bai, M., Stern, E., Bornhop, D.J., Stella, N., 2011. NIR-mbc94, a fluorescent ligand that binds to endogenous cB2 receptors and is amenable to high-throughput screening. *Chem. Biol.* 18, 563–568. doi:10.1016/j.chembiol.2011.02.016
- Shao, Z., Yin, J., Chapman, K., Grzemska, M., Clark, L., Wang, J., Rosenbaum, D.M., 2016. High-resolution crystal structure of the human CB1 cannabinoid receptor. *Nature* 540, 602–606. doi:10.1038/nature20613
- Shmist, Y.A., Goncharov, I., Eichler, M., Shneyvays, V., Isaac, A., Vogel, Z., Shainberg, A., 2006. Delta-9-tetrahydrocannabinol protects cardiac cells from hypoxia via CB2 receptor activation and nitric oxide production. *Mol. Cell. Biochem.* 283, 75–83. doi:10.1007/s11010-006-2346-y
- Sieve, A.N., Meeks, K.D., Bodhankar, S., Lee, S., Kolls, J.K., Simecka, J.W., Berg, R.E., 2009. A novel IL-17-dependent mechanism of cross protection: Respiratory infection with mycoplasma protects against a secondary listeria infection. *Eur. J. Immunol.* 39, 426–438. doi:10.1002/eji.200838726
- Smith, J., Hart, P., Williams, K., 1998. Basic pathogenic mechanisms operating in experimental models of acute anterior uveitis. *Immunol. Cell Biol.* 76, 497–512. doi:10.1046/j.1440-1711.1998.00783.x
- Soethoudt, M., Grether, U., Fingerle, J., Grim, T.W., Fezza, F., de Petrocellis, L., Ullmer, C., Rothenhäusler, B., Perret, C., van Gils, N., Finlay, D., MacDonald, C., Chicca, A., Gens, M.D., Stuart, J., de Vries, H., Mastrangelo, N., Xia, L., Alachouzos, G., Baggelaar, M.P., Martella, A., Mock, E.D., Deng, H., Heitman, L.H., Connor, M., Di Marzo, V., Gertsch, J., Lichtman, A.H., Maccarrone, M., Pacher, P., Glass, M., van der Stelt, M., 2017. Cannabinoid CB2 receptor ligand profiling reveals biased signalling and off-target activity. *Nat. Commun.* 8, 1–14. doi:10.1038/ncomms13958
- Steffens, S., Veillard, N.R., Arnaud, C., Pelli, G., Burger, F., Staub, C., Zimmer, A., Frossard, J.-L., Mach, F., 2005. Low dose oral cannabinoid therapy reduces progression of atherosclerosis in mice. *Nature* 434, 782–786. doi:10.1038/nature03389

- Stirling, D.P., Liu, S., Kubes, P., Yong, V.W., 2009. Depletion of Ly6G/Gr-1 leukocytes after spinal cord injury in mice alters wound healing and worsens neurological outcome. *J. Neurosci.* 29, 753–764. doi:10.1523/JNEUROSCI.4918-08.2009
- Streilein, J.W., 2003. New thoughts on the immunology of corneal transplantation. *Eye* 17, 943–948. doi:10.1038/sj.eye.6700615
- Streilein, J.W., 1999. Immunoregulatory mechanisms of the eye. *Prog. Retin. Eye Res.* 18, 357–370.
- Streilein, J.W., Ohta, K., Mo, J.S., Taylor, A.W., 2002. Ocular immune privilege and the impact of intraocular inflammation. *DNA Cell Biol.* 21, 453–459. doi:10.1089/10445490260099746
- Sun, C., Forster, C., Nakamura, F., Glogauer, M., 2013. Filamin-A regulates neutrophil uropod retraction through RhoA during chemotaxis. *PLoS One* 8, 1–9. doi:10.1371/journal.pone.0079009
- Szczesniak, A., Porter, R., Toguri, J., Borowska-Fielding, J., Siwakoti, A., Lehmann, C., Kelly, M., 2017. Cannabinoid 2 receptor is a novel anti-inflammatory target in experimental proliferative vitreoretinopathy. *Neuropharmacology* 113, 627–638. doi:10.1016/j.neuropharm.2016.08.030
- Toguri, J.T., 2015. Endocannabinoid system modulation of the ocular immune response. Dalhousie University.
- Toguri, J.T., Caldwell, M., Kelly, M.E.M., 2016. Turning down the thermostat: Modulating the endocannabinoid system in ocular inflammation and pain. *Front. Pharmacol.* 7, 1–9. doi:10.3389/fphar.2016.00304
- Toguri, J.T., Lehmann, C., Laprairie, R.B., Szczesniak, a. M., Zhou, J., Denovan-Wright, E.M., Kelly, M.E.M., 2014. Anti-inflammatory effects of cannabinoid CB2 receptor activation in endotoxin-induced uveitis. *Br. J. Pharmacol.* 171, 1448–1461. doi:10.1111/bph.12545
- Toguri, J.T., Moxsom, R., Szczesniak, A.M., Zhou, J., Kelly, M.E.M., Lehmann, C., 2015. Cannabinoid 2 receptor activation reduces leukocyte adhesion and improves capillary perfusion in the iridial microvasculature during systemic inflammation. *Clin. Hemorheol. Microcirc.* 61, 237–249. doi:10.3233/CH-151996
- Tole, S., Mukovozov, I.M., Huang, Y.-W., Magalhaes, M. a O., Yan, M., Crow, M.R., Liu, G.Y., Sun, C.X., Durocher, Y., Glogauer, M., Robinson, L. a, 2009. The axonal repellent, Slit2, inhibits directional migration of circulating neutrophils. *J. Leukoc. Biol.* 86, 1403–1415. doi:10.1189/jlb.0609391
- Tschöp, J., Kasten, K.R., Nogueiras, R., Goetzman, H.S., Cave, C.M., England, L.G., Dattilo, J., Lentsch, A.B., Tschöp, M.H., Caldwell, C.C., 2009. The cannabinoid receptor 2 is critical for the host response to sepsis. *J. Immunol.* 183, 499–505. doi:10.4049/jimmunol.0900203

- van der Velden, V.H.J., 1998. Glucocorticoids: mechanisms of action and anti-inflammatory potential in asthma. *Mediators Inflamm.* 7, 229–237. doi:10.1080/09629359890910
- Vaure, C., Liu, Y., 2014. A comparative review of toll-like receptor 4 expression and functionality in different animal species. *Front. Immunol.* 5, 1–15. doi:10.3389/fimmu.2014.00316
- Vestweber, D., 2015. How leukocytes cross the vascular endothelium. *Nat. Rev. Immunol.* 15, 692–704. doi:10.1038/nri3908
- Wei, Y., Wang, X., Wang, L., 2009. Presence and regulation of cannabinoid receptors in human retinal pigment epithelial cells. *Mol. Vis.* 15, 1243–1251.
- Wootten, D., Christopoulos, A., Sexton, P.M., 2013. Emerging paradigms in GPCR allostery: implications for drug discovery. *Nat. Rev. Drug Discov.* 12, 630–644. doi:10.1038/nrd4052
- Xu, H., Cheng, C.L., Chen, M., Manivannan, A., Cabay, L., Pertwee, R.G., Coutts, A., Forrester, J. V, 2007. Anti-inflammatory property of the cannabinoid receptor-2-selective agonist JWH-133 in a rodent model of autoimmune uveoretinitis. *J. Leukoc. Biol.* 82, 532–541. doi:10.1189/jlb.0307159
- Zhou, R., Caspi, R.R., 2010. Ocular immune privilege. *F1000 Biol. Rep.* 23, 1885–1889. doi:10.1038/eye.2008.382